



UNIVERSITY *of the*
WESTERN CAPE

**Novel tricycloundecane derivatives as potential *N*-methyl-D-
aspartate receptor and calcium channel inhibitors for
neuroprotection**

BY

AYODEJI OLATUNDE EGUNLUSI
B. Pharm (UWC)

UNIVERSITY *of the*
WESTERN CAPE

**Thesis submitted in fulfilment of the requirements for the degree of
Masters in Pharmaceutical Science (Pharmaceutical Chemistry)**

**SCHOOL OF PHARMACY, UNIVERSITY OF THE WESTERN CAPE;
BELLVILLE,
SOUTH AFRICA.**

**SUPERVISOR: Dr Jacques Joubert
CO - SUPERVISOR: Prof. Sarel Malan**

April 2014

DECLARATION

I declare that my research work titled “**Novel tricycloundecane derivatives as potential *N*-methyl-D-aspartate receptor and calcium channel inhibitors for neuroprotection.**” is my own work, that it has not been submitted before for any degree or examination in any other university, and that all the sources I have used or quoted have been indicated and acknowledged by means of complete references.

Ayodeji O. Egunlusi

April, 2014.

.....

Signature



ACKNOWLEDGEMENTS

The path to achieve a proposed target, although accompanied by challenges, begins with a step towards a great ambition. The completion of my masters has been made possible by the supervision, assistance, guidance and prayer of many people who I extend my gratitude to and hereby gratefully acknowledged. Three years ago, the conversation I had with my lecturer (Dr Jacques Joubert) encouraged me to pursue a M.Sc. in pharmaceutical chemistry. Firstly, I will like to thank God for his mercy and guidance throughout the program.

To my supervisors, Dr Jacques Joubert and Prof. Sarel Malan, I extend my endless gratitude for your devoted time and effort in this work. Your enormous care from time to time was deeply appreciated. Your self-belief was undeniably a great motivation. To the School of Pharmacy, University of the Western Cape, Bellville, Prof. Nadine Butler, Prof. Angeni Bheekie, Prof. Peter Eagles, Prof. James Syce, Mrs Erika Kapp, Mr Yunus Kippie, and all the members of staff, I thank you for creating a friendly working environment throughout my studies. I say a big thank to Ms Audrey Ramplin (senior technical officer) for her timely response in getting reagents and chemicals used in this study as it added speed in completing my research. With a gracious heart, I will like to thank Dr Kenekwue Obikeze for creating time out of his busy schedule to review some of my chapters. Special thanks go to the family of Dr & Mrs Oluwaseun Fadipe, Dr Segun Akinyemi, Ms Adeola Adeleye, Mr Toyin Ayodele, Ms Modupe Abaniwonda, Ms Mary Mbiyi, Ms Amilomo Nwaneri, Mr Rajan Sharma and my fellow post graduate students for contributing to the success of this study.

I am grateful to the National Research Foundation (South Africa) for their financial support in this research. Lastly, appreciation to my parents (Dr & Mrs Mathew Egunlusi) and my siblings, Mr Busuyi Egunlusi, Ms Oluwatosin Egunlusi, Ms Abimbola Egunlusi, Mr Oluwapelumi Akinwumi and Ms Oluwafunmilayo Egunlusi for their love and continuous support and encouragement.

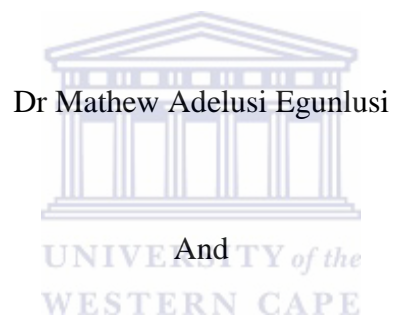
DEDICATION

This project is dedicated to

The

Almighty God,

My Parents



Mrs Oluwafunmilola Veronica Egunlusi

Novel tricycloundecane derivatives as potential *N*-methyl-D-aspartate receptor and calcium channel inhibitors for neuroprotection

Ayodeji O. Egunlusi

Key words:

Neurodegenerative disorders

Tricycloundecane

N-methyl-D-aspartate receptor

Voltage-gated calcium channel

Oxidative stress

Synaptoneuroosomes

Excitotoxicity

Apoptosis

Necrosis

Polycyclic cage

Neuroprotective agents

Fura-2 AM



ABBREVIATIONS

AD = Alzheimer's disease	PD = Parkinson's disease
ALS = Amyotrophic lateral sclerosis	HD = Huntington's disease
VGCC = Voltage-gated calcium channels	NMDA = <i>N</i> -methyl-D-aspartate
PCP = Phencyclidine	MK-801 = Dizolcipine
MS = Mass spectrometry	IR = Infrared
NMR = Nuclear magnetic resonance	UV = Ultra-violet
SN = Substantia nigra	CNS = Central nervous system
PCD = Programmed cell death	ROS = Reactive oxygen species
RNS = Reactive nitrogen species	ASIC = Acid sensing ion channel
PARP = Poly ADP ribose polymerase	A β = β -Amyloid
GABA = Gamma amino butyric acid	EAA = Excitatory amino acid
IMM = Inner mitochondrial membrane	Bcl-2 = B-cell lymphoma 2
OMM = Outer mitochondrial membrane	NO = Nitric oxide
eNOS = Endothelial nitric oxide synthases	Bax = Bcl-2-associated X
iNOS = Inducible nitric oxide synthases	JNK = c-Jun <i>N</i> -terminal kinase
nNOS = Neuronal nitric oxide synthases	ATP = Adenosine triphosphate
mGluR = Metabotropic glutamate receptor	CDI = Ca ²⁺ -dependent inactivation
MAPK = Mitogen-activated protein kinase	PI3K = Phosphatidylinositol-3-kinase
InsP ₃ = Inositol-1,4,5-trisphosphate	MEF2C = Myocyte enhancer factor 2C
PTP = Permeability transition pore	PI3K = Phosphatidylinositol-3-kinase
iGluR = ionotropic glutamate receptor	Bcl-xL = B-cell lymphoma extra large
VDI = Voltage-dependent inactivation	THF = Tetrahydrofuran
MP = Melting point	
AMPA = Alpha-amino-3-hydroxy-5-methyl-4-isoxazole-propionic acid	
PtdIns-4,5-P ₂ = Phosphatidylinositol-4,5-bisphosphate	

°C = Degree Celsius	g = Grams	mmol = Millimoles
W = Watt	ml = Millilitres	% = Percentage
Psi = Pounds per square inch	cm ⁻¹ = Per centimetre	g/mol = Gram per mole
MHz = Megahertz	ppm = Part per million	Hz = Hertz
mg = Milligrams	μ M = Micromolar	

ABSTRACT

Neurodegenerative disorders are debilitating conditions characterised by progressive dysfunction and death of neuronal cells by means of apoptosis, necrosis or autophagic degeneration. These conditions include, amongst others: Parkinson's disease (PD), Alzheimer's disease (AD), Amyotrophic lateral sclerosis (ALS), and Huntington's disease (HD). Amidst the proposed mechanisms of neurodegeneration, the effects of excitotoxicity *via* glutamate receptor stimulation on neuronal cells are prominent. Excessive extracellular glutamate and/or membrane depolarisation activates *N*-methyl-D-aspartate (NMDA) receptors and voltage-gated calcium channels (VGCC). These activations result in increased intracellular calcium ions and calcium overload that subsequently lead to neuronal cell death. Phencyclidine (PCP) and dizolcipine (MK-801) have proven to noncompetitively block NMDA receptors and in this process slow down the degenerative cascade, but are marked by undesirable side effects. Uncompetitive blockers such as memantine and amantadine proved to be neuroprotective with fewer side effects and are approved for clinical use against neurodegenerative disorders. This has led to the development of structurally related polycyclic molecules such as NPG1-01, a closed polycyclic cage, which exhibit neuroprotective properties through NMDA receptor and VGCC inhibitions with lower side effect profile.

Tricycloundecane derivatives which are open cage or rearranged polycyclic cage moieties have also been synthesised, but their potential medicinal use have not been explored. This study focused on the synthesis of a series of novel tricycloundecane derivatives and evaluation of these compounds for neuroprotection using the fluorescent ratiometric calcium assay that indicates the ability of the test compounds to inhibit NMDA receptors and VGCC. The cycloaddition reaction between *p*-benzoquinone and monomerised dicyclopentadiene yielded tricycloundeca-4,9-diene-3,6-dione which was used as the base structure and further derivatised. These derivatives were conjugated with benzylamine to form a series of imines and amines. A total of 10 compounds were synthesised for evaluation of inhibition of calcium influx through NMDA receptor channels and voltage-gated calcium channels. The structures were confirmed using NMR, IR and MS. On the proton NMR, the characteristic AB-quartet system was observed in the region of 1-2 ppm for all the

compounds and the aromatic moiety was observed between 6.5-7.5 ppm for the novel polycyclic amines. These, with other functional groups, were used to confirm the individual structures.

In the NMDA receptor inhibition assay, MK-801, memantine and NGP1-01 were used as reference compounds and all showed statistically significant ($p < 0.05$) NMDA receptor inhibitory activity of 97.47%, 57.90% and 57.20% respectively at a 100 μM concentration. Significant inhibition were observed for compound **2** (78.00%) and **3** (96.07%). The highest inhibitory activity ($p < 0.05$) was observed with compound **7**, which exceeded the inhibitory activity of MK-801 in this assay. In the VGCC inhibition assay, nimodipine, amantadine and NGP1-01 were used as the reference compounds. Nimodipine and NGP1-01 showed statistical significant VGCC inhibition of 90.19% and 25.63% respectively at a 100 μM concentration. Compound **6** (34.03%), **7** (38.07%) and **10** (40.33%) showed statistically significant ($p < 0.05$) VGCC inhibitory activity compared to NGP1-01 (25.63%). These compounds (**2, 3, 6, 7** and **10**) demonstrated potential ability to attenuate calcium influx through NMDA receptor and/or VGCC. Thus, potential mono- or dual-functional neuroprotective activities including inhibition of NMDA receptors and/or voltage-gated calcium channels were observed for these compounds.

The potential NMDA receptor and/or VGCC inhibitory activities of the tricycloundecane derivatives (**2, 3, 6, 7**, and **10**) were demonstrated in this study. However, the true potential benefit as neuroprotective agents and safety in patients is yet to be established. The compounds could serve as lead structures for the development of novel neuroprotective drugs.

TABLE OF CONTENTS

DECLARATION	ii
ACKNOWLEDGEMENTS	iii
DEDICATION	iv
KEYWORDS	v
ABBREVIATIONS	vi
ABSTRACT	vii - viii
TABLE OF CONTENTS	ix - xi
LIST OF FIGURES	xi - xii
LIST OF TABLES	xii
LIST OF SCHEMES	xii

CHAPTER ONE (Introduction)	1 - 8
1.1: Background	1
1.2: Rational and aim of this study	6
1.3: Conclusion	8
CHAPTER TWO (Literature review)	9 - 37
2.1: Neurodegeneration	9
2.1.1: Neurodegenerative disorders	9
2.1.2: Occurrence, incidence, and prevalence of neurodegenerative disorders	9
2.1.3: Cost implications	10
2.1.4: Treatment of neurodegenerative disorders	11
2.2: Mechanism of neurodegeneration	11
2.2.1: Forms of neuronal death	11
2.2.1.1: Apoptosis	11
2.2.1.2: Necrosis	13
2.2.2: Oxidative stress in neurodegeneration	14
2.2.3: Excitotoxicity in neurodegeneration	15
2.3: NMDA receptors	22
2.3.1: Introduction	22

2.3.2: Structure of iGlu receptor	23
2.3.3: Structure and functions of the NMDA receptor	24
2.3.4: NMDA receptor binding sites	25
2.3.5: NMDA receptor inhibition	25
2.4: Neuronal voltage-gated calcium channels	28
2.4.1: Introduction	28
2.4.2: Structure of VGCC	28
2.4.3: Structure and functions of VGCC	30
2.4.4: Neuronal VGCC inhibition	32
2.5: Polycyclic derivatives	34
2.5.1: Introduction	34
2.5.2: Structure-activity relationship of polycyclic derivatives	35
2.5.3: Pentacycloundecylamine-NMDA receptor interaction	36
2.5.4: Tricycloundecane derivatives	36
2.6: Conclusion	36
CHAPTER THREE (Synthesis)	38 - 52
3.1: General	38
3.2: Standard experimental procedures	39
3.2.1: Reagents and chemicals	39
3.2.2: Instrumentation	39
3.2.3: Chromatographic techniques	39
3.3: Synthetic procedures	40
3.3.1: Tricyclo[6.2.1.0 ^{2,7}]undeca-4,9-diene-3,6-dione	40
3.3.2: Tricyclo[6.2.1.0 ^{2,7}]undec-9-ene-3,6-dione	41
3.3.3: 6-hydroxytricyclo[6.2.1.0 ^{2,7}]undec-9-en-3-one	42
3.3.4: 10-bromine-6, 9-epoxytricyclo[6.2.1.0 ^{2,7}]undecan-3-one	43
3.3.5: 3-(benzylimino)tricyclo[6.2.1.0 ^{2,7}]undeca-4,9-dien-6-one	44
3.3.6: 3-(benzylamino)tricyclo[6.2.1.0 ^{2,7}]undeca-4,9-dien-6-one	46
3.3.7: 3-(benzylimino)tricyclo[6.2.1.0 ^{2,7}]undec-9-en-6-one	47
3.3.8: 3-(benzylamino)tricyclo[6.2.1.0 ^{2,7}]undec-9-en-6-one	48
3.3.9: 10-(benzylamino)-6, 9-epoxytricyclo[6.2.1.0 ^{2,7}]undecan-3-one	49
3.3.10: 10-(benzylamino)-6, 9-epoxytricyclo[6.2.1.0 ^{2,7}]undecan-3-ol	50
3.4: Conclusion	51

CHAPTER FOUR (Biological evaluation)	53 - 63
4.1: Introduction	53
4.2: Imaging experiment using Fura-2 AM	54
4.2.1: Materials	54
4.2.2: Animals	54
4.2.3: Preparation of synaptoneurosomes	54
4.2.4: General methods	54
4.2.5: General procedure for loading Fura-2 AM and incubating test compounds	55
4.2.6: NMDA/glycine-mediated NMDA receptor stimulation	55
4.2.7: KCl-mediated VGCC depolarisation	56
4.2.8: Statistical analysis	56
4.3: Results and discussion	57
4.3.1: NMDA receptor calcium flux inhibition	57
4.3.2: VGCC calcium flux inhibition	60
4.4: Conclusion	63
CHAPTER FIVE (Conclusion)	64 - 68
5.1: General	64
5.2: Chemistry	64
5.3: Biological activity	66
5.4: Conclusion and further recommendations.....	67

LIST OF FIGURES

Figure 1.1: Schematic representation of excitotoxic effects on cells	2
Figure 1.2: Schematic illustration of indirect excitotoxicity in low buffered cell	3
Figure 1.3: Chemical structures of PCP, MK-801, ketamine and polycyclic derived molecules with neuroprotective effects	4
Figure 1.4: Compounds synthesised and evaluated in this study	6
Figure 2.1: Schematic illustration of an apoptotic event	12
Figure 2.2: Direct and indirect toxicity hypothesis associated with CNS disorders	15
Figure 2.3: Interaction of Ca ²⁺ and mitochondria in ALS as a local disruptive feedback mechanism	16

Figure 2.4: Cartoon of possible points along the corticostriatal pathway where dysfunction may contribute to excitotoxicity	18
Figure 2.5: Mechanisms of NO-mediated neurotoxicity	20
Figure 2.6: Topology of a single NMDA receptor subunit	23
Figure 2.7: Chemical structures of phencyclidine, ketamine and dizolcipine	26
Figure 2.8: Chemical structures of memantine, dextromethorphan, remacemide, aptiganel and amantadine	26
Figure 2.9: Scheme of the hypothesis explaining how the fast unblocking kinetics of memantine allows this strongly voltage-dependent compound to differentiate between the physiological and pathological activation of NMDA receptors	27
Figure 2.10: Subunit composition of VGCC complex	29
Figure 2.11: Subunit structure of Ca ²⁺ channels	30
Figure 2.12: Chemical structures of neuronal Voltage calcium channel blockers	33
Figure 2.13: Chemical structure of NGP1-01	34
Figure 3.1: Successfully synthesised compounds for biological evaluation	52
Figure 4.1: Synergy™ Mx Monochromator-based fluorescent Microplate Reader	53
Figure 4.2: Screening of test compounds (100 μM, n = 9) for inhibition of NMDA-mediated calcium flux in murine synaptoneurosomes	57
Figure 4.3: Screening of test compounds (100 μM, n = 9) for inhibition of VGCC-mediated calcium flux in murine synaptoneurosomes	62
Figure 5.1: Structures of tricycloundecane derivatives (1-10)	65

LIST OF TABLES

Table 2.1: Prevalence (per 1000 people) and incidence (per 100000 persons-years) rates of neurodegenerative disorders	10
Table 4.1: Calcium influx inhibition (NMDA receptor) by tested compounds	58
Table 4.2: Calcium influx inhibition (VGCC) by tested compounds	61

SCHEMES

Scheme 1.1: Synthesis of tricycloundeca-4,9-diene-3,6-dione and Cookson's diketone cage	5
Scheme 3.1: Synthetic route of tricycloundecane derivatives (1-10) and their respective yields	38

REFERENCES

69 - 86

APPENDIX

87 - 104

Appendix 1: Infrared, mass and nuclear magnetic resonance spectra87



CHAPTER ONE

Introduction

1.1: Background

Neurodegeneration is a process characterised by progressive loss of neuronal cells in the central nervous system. These cells undergo a cascade of events, enzymatic and non-enzymatic, that results in the death of neuronal cells and is the cause of various neurological disorders. These disorders, amidst others include; Parkinson's disease (PD), Alzheimer's disease (AD), amyotrophic lateral sclerosis (ALS) and Huntington's disease (HD). The part of the brain affected differs in each disorder which is evident by their distinct symptoms (Farooqui & Farooqui, 2009; Galpern & Cudkowicz, 2007; Grosskreutz *et al.*, 2010; Landrigan *et al.*, 2005; Lee & Kim, 2006; Mayeux, 2003). The incidence of these disorders has increased in recent years and has led to a high demand in health care and social services causing a major burden to modern society (Fratiglioni & Qiu, 2009).

Unfortunately, current drugs only offer symptomatic relief. Patients show improvement initially due to blunting of symptoms, but later deteriorate. This is evident in patients who are withdrawn from treatment as they perform no better than the placebo group soon after withdrawal (Geldenhuys *et al.*, 2007). Although this approach does not halt the degenerative process, it is beneficial as increased life expectancy is observed in patients with no comorbidity. However, the overall cost, financial and human, reduces the quality of life.

Countless studies have proposed distinct or overlapping factors, genetic and environmental, and molecular mechanisms that contributes to the pathogenesis of neurodegenerative disorders. Of these studies, none could establish a definite mechanism. However, it is generally believed that for each distinct neurodegenerative disorder, selectively vulnerable neuronal populations undergo cell death, which is either necrotic or apoptotic in nature, as a consequence of potentially interrelated processes. These processes include but are not limited to oxidative stress, excitotoxicity (Leist & Nicotera, 1998), RNA metabolism, mitochondria dysfunction (Moreira *et al.*, 2012), and protein aggregation and propagation (Celsi *et al.*, 2009; Mehta *et al.*, 2013). Despite the vast knowledge and ongoing refinement in these basic insights, the pathogenesis of neurodegenerative disorders is still fragmented and poorly defined (Qureshi & Mehler, 2013).

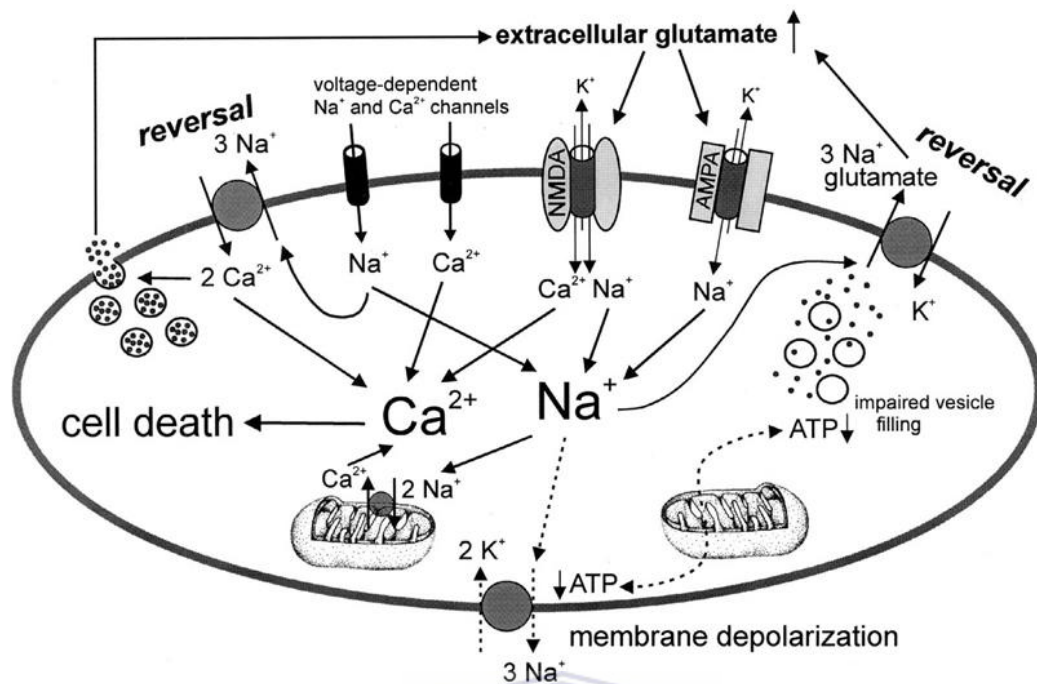


Figure 1.1: Schematic representation of excitotoxic effects on cells.

Amongst the established mechanisms of neurodegeneration, excitotoxic effects *via* glutamate receptor stimulation and calcium channel activation on neuronal cells are more prominent. These effects can either be primary or secondary. In primary or direct excitotoxicity, excessive extracellular glutamate over-activates *N*-methyl-D-aspartate (NMDA) receptors to cause calcium influx and subsequently intracellular calcium overload (Lipton, 2007). Sensitive voltage-gated calcium channel (VGCC) activation also contributes to the calcium overload. This disruption in calcium homeostasis activates enzymes and generates free radicals that lead to cell death (figure 1.1). In secondary or indirect excitotoxicity, cell death results from normal glutamate receptor stimulation of a weakened postsynaptic neuron. An example of a weak postsynaptic neuron is one with low ATP production due to mitochondrial dysfunction. As a result, the ATP produced is incapable of producing energy required for normal physiological processes. The neuron becomes damaged and eventually dies. Indirect excitotoxicity can also occur in low-buffered cells. Anti-apoptotic proteins such as B-cell lymphoma 2 (Bcl-2) or B-cell lymphoma extra large (Bcl-xL) facilitate the storage of intercellular calcium in the endoplasmic reticulum, thereby reducing mitochondrial loading and protecting neuronal cells from apoptotic death. Pathological conditions that enhances the activity of pro-apoptotic proteins

such as Bcl-2-associated X (Bax) or increases anti-apoptotic protein loss may antagonize this buffer-effect and promote apoptosis (Celsi *et al.*, 2009; Ferdek *et al.*, 2012; Bonneau *et al.*, 2013; figure 1.2). In both forms of excitotoxicity, glutamatergic neurotransmission and calcium influx plays a crucial role in cell death (Fan and Raymond, 2007; Gardoni & Di Luca, 2006; Haddad, 2005; Lau and Tymianski, 2010; Van Damme *et al.*, 2003; Van Den Bosch *et al.*, 2006). Therefore minimising calcium entry into neuronal cells without interfering with normal neuronal calcium homeostasis is vital in ameliorating neurological diseases.

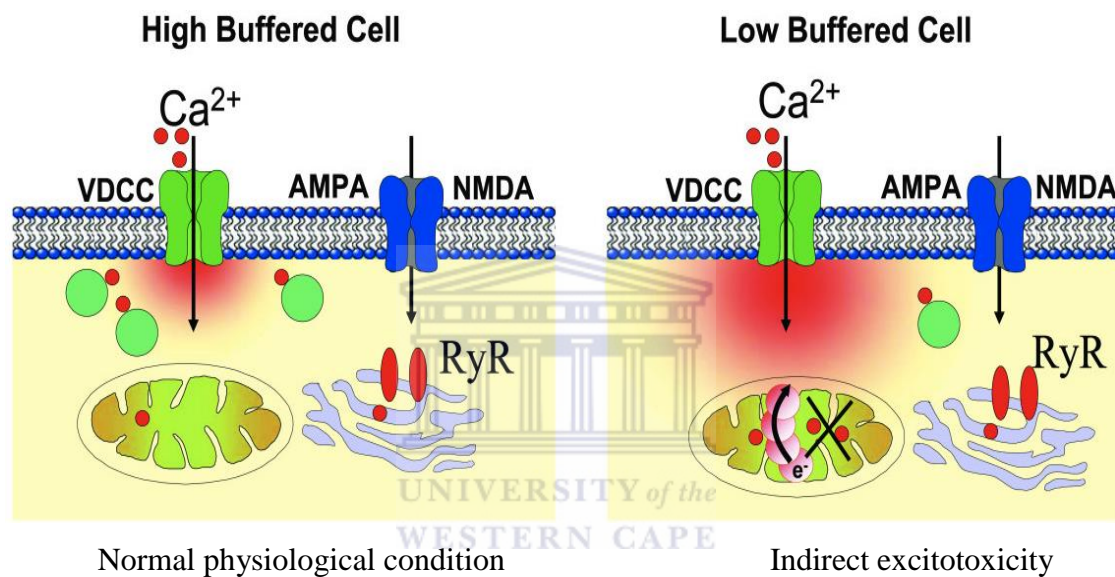


Figure 1.2: Schematic illustration of indirect excitotoxicity in low buffered cell (Taken from Wikispaces, 20 June 2013).

It is proposed that antagonising NMDA receptors and blocking calcium channels in neuronal cells will be of therapeutic value by halting or reducing excitotoxicity, an essential process in neurodegeneration. Although this therapeutic strategy is effective in preventing glutamate-mediated neurotoxicity, a competitive antagonist will halt NMDA receptor activities which are essential for normal physiological transmission in the brain (Chen & Lipton, 2006). Competitive NMDA receptor antagonist such as midafotel and selfotel have been developed but discontinued because of their dose-related psychotomimetic side effects (Sonkusare *et al.*, 2005; Loscher & Schmidt, 2006). Uncompetitive antagonism, also known as open-channel blockers, is a more appealing strategy for therapeutic intervention during excessive NMDA receptor activation as this action of blockade requires prior activation of the receptor (Chen & Lipton, 2006). Some of these uncompetitive

NMDA receptor antagonists have shown effectiveness in many experimental animal models of neurodegenerative diseases and moved into clinical trials. However, the initial enthusiasm for this approach has diminished as these drugs exhibit significant adverse effect at therapeutic doses (Gardoni & Di Luca, 2006). Phencyclidine (PCP), ketamine and dizolcipine (MK-801) (figure 1.3) have shown to uncompetitively block NMDA receptors to reduce or halt the degenerative process, but are marked by undesirable side effects such as psychotomimetic effects and impaired motor functions (Kiss *et al.*, 2005). This is attributed to the high affinity of these compounds for the NMDA receptors. Therefore, drugs with low adverse effect profiles that still retain neuroprotective activity by inhibiting NMDA receptors will be advantageous in the treatment of these neurodegenerative disorders.

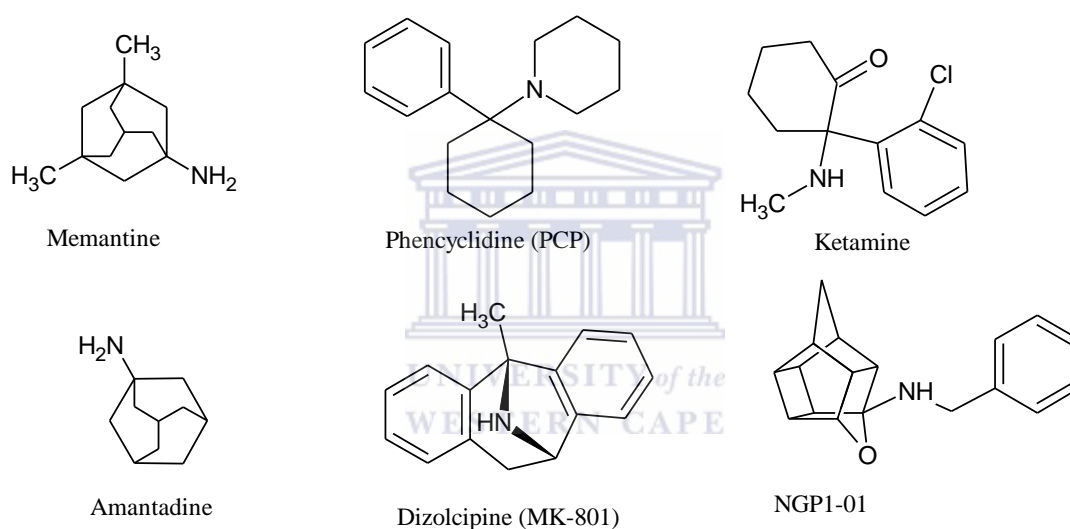
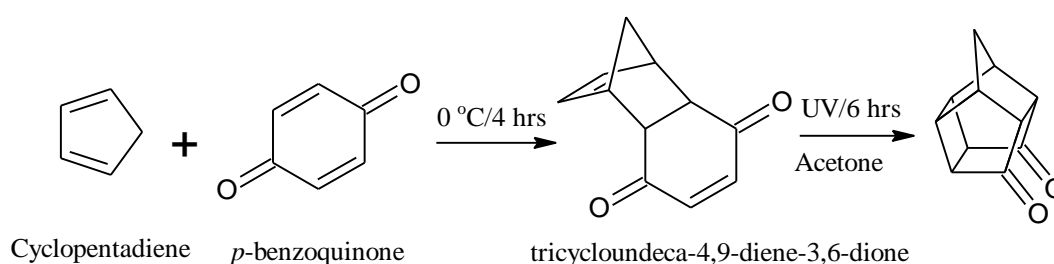


Figure 1.3: Chemical structures of PCP, MK-801, ketamine and polycyclic derived molecules with neuroprotective effects.

Although polycyclic cage derivatives such as memantine, amantadine and NGP1-01 (figure 1.3) have been of interest to chemists for more than 50 years, it is only recently that the medicinal potential thereof has been explored (Ito *et al.*, 2007). This interest has led to the development of numerous cage derivatives with established and potential therapeutic effects. These compounds and derivatives thereof have shown to inhibit NMDA receptors and/or calcium channels and are thus candidates for neuroprotection. These polycyclic compounds are uncompetitive NMDA receptor inhibitors with established neuroprotective properties and a low side effect profile is observed. These properties make them a highly promising group for the development of new drugs. An example is memantine (figure 1.3), a derivative of amantadine. Unlike ketamine, memantine is clinically well tolerated owing to its low

affinity on NMDA receptors. It is believed to block excitotoxic effect while allowing normal glutamatergic transmission. Memantine mainly modulates NMDA receptors to prevent pathological overactivation of this receptor. It has been shown in various studies that memantine only block excessive NMDA receptor activity without disrupting normal neuronal activity (Lipton, 2004). This offers protection to neurons by preventing or slowing down cell death. Derivatives of memantine are under scrutiny and could exhibit a higher potency than memantine with greater neuroprotective properties (Lipton, 2004; Johnson & Kotermanski, 2006; Wenk, 2007). Several pentacycloundecylamine derivatives have been developed and reported in literature to have neuroprotective properties. In addition to their neuroprotective abilities, they are also useful moieties to conjugate to existing structures or molecules, currently on the market or under development, for the purpose of improving their pharmacokinetic and pharmacodynamic profiles (Van der Schyf & Geldenhuys, 2009). Polycyclic cages such NGP1-01, a closed cage molecule (figure 1.3), exhibits L-type voltage-gated calcium channel blockage and NMDA receptor inhibition. NGP1-01 was also shown to be more potent than other polycyclic cages, such as the adamantanes, due to its characteristic dual inhibitory mechanism in attenuating calcium entry. This distinct characteristic gives NGP1-01 an advantage over other potential neuroprotective compounds as a drug candidate in prophylaxis and effective treatment of acute and chronic neurodegenerative disorders (Van der Schyf & Youdim, 2009). Numerous derivatives of this cage molecule have been synthesized and have shown considerable NMDA receptor and calcium channel inhibitory properties (Malan *et al.*, 2000; Geldenhuys *et al.*, 2004; Mdzinarishvili *et al.*, 2005)



Scheme 1.1: Synthesis of tricycloundeca-4,9-diene-3,6-dione and Cookson's diketone cage (Diels & Alder, 1928; Cookson *et al.*, 1964).

Tricycloundecane (scheme 1.1), an open cage polycyclic molecule, derivatives have also been extensively synthesised but its use in medicinal chemistry has not been explored (Geldenhuys *et al.*, 2011). A series of novel tricycloundecyl amine and imine

phenyl derivatives which are structurally similar to NGP1-01 (figure 1.4) will be developed and evaluated in this study for their neuroprotective properties. These novel derivatives are structurally similar to NGP1-01 and MK-801, and provide the possibility to develop another group of cage derivatives with potential NMDA receptor and VGCC inhibitory activities. Since these compounds are expected to have similar structure-activity relationships as NGP1-01, we envision that comparable or improved neuroprotective effects will be observed.

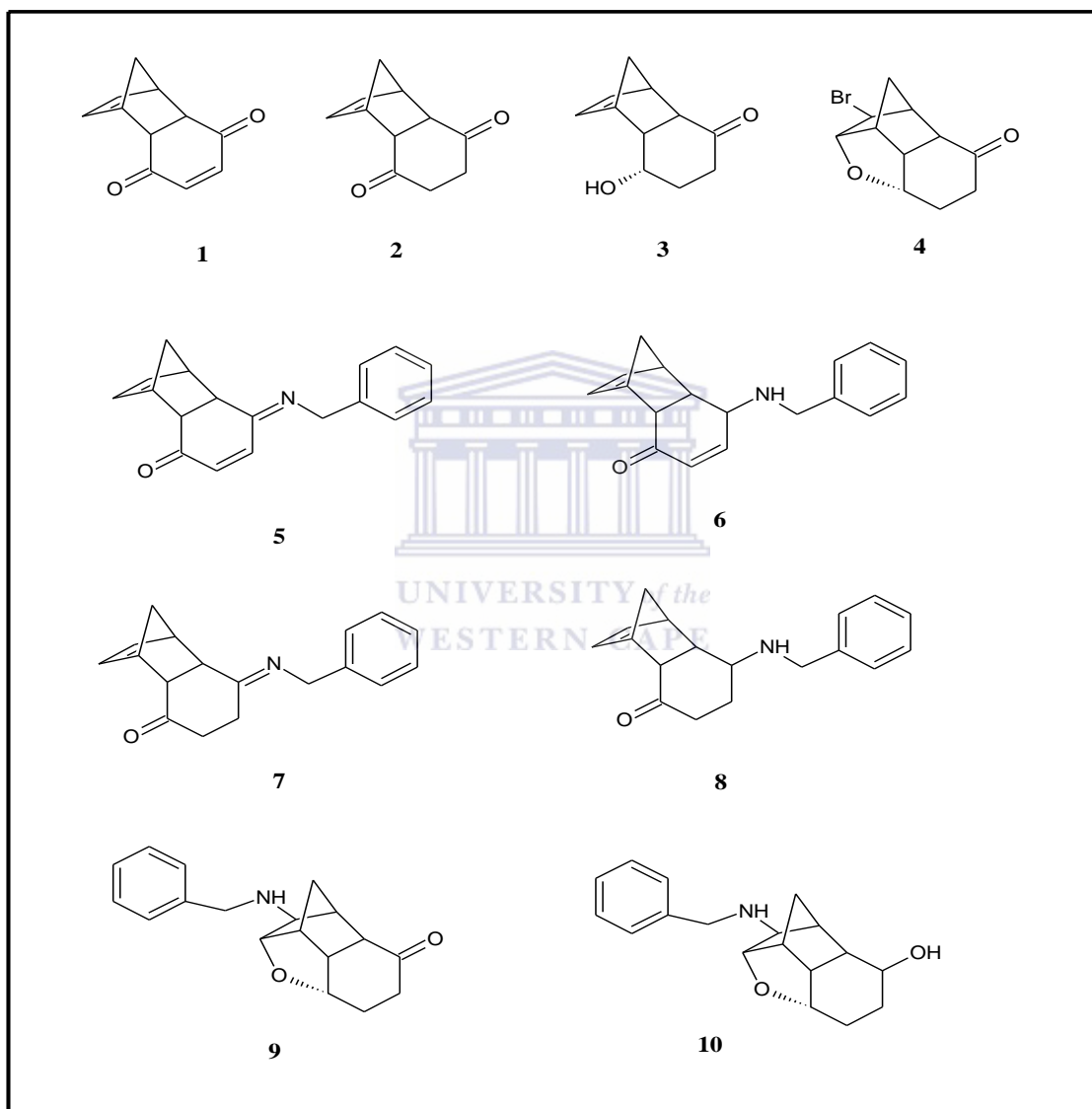


Figure 1.4: Compounds synthesised and evaluated in this study.

1.2: Rational and aim of this study

The NMDA receptors and VGCC have been recognised as the two major targets responsible for calcium overload in glutamate-mediated neurotoxicity (Mdzinarishvili *et al.*, 2005). The increased intracellular calcium mediated by these channels subsequently result in neuronal cell death. With this in mind, we direct our

research focus to slowing down the neurodegenerative processes by targeting these major pathways. Maintaining calcium homeostasis by inhibiting these channels while ensuring normal glutamatergic transmission is essential in the neuronal recovery process or neuroprotection (Grobler *et al.*, 2006). Uncompetitive NMDA receptor inhibitors (PCP, MK-801, ketamine and some polycyclic cage derivatives) and VGCC inhibitors (Nimodipine and NGP1-01) are known to reduce calcium influx mediated by excitotoxicity. This offers protection to neuronal cells. However, some of these compounds disrupt physiological processes and cause psychotomimetic side effects due to their high affinity for the NMDA receptors. Polycyclic cages such as memantine and NGP1-01 have demonstrated significant neuroprotective activities with low side effect profiles by inhibiting one or both pathways. The low side effects profile is attributed to their moderate affinity at the NMDA receptor binding site (Sonkusare *et al.*, 2005).

The vital role of these major pathways in calcium overload and the desire to diversify lead structures which inhibit these pathways justified the rationale for synthesising a series of novel tricycloundecane compounds that target these channels in order to maintain calcium homeostasis in neuronal cells.

Because NMDA receptor and VGCC inhibitions had been shown to be useful in the treatment of neurodegenerative diseases, this aim of this study was to design and synthesise tricycloundecane derivatives, structurally similar to NGP1-01 and MK-801, and evaluating these novel polycyclic cages as VGCC and NMDA receptor inhibitors. Once a final series of compounds were identified, they were synthesised, purified using conventional laboratory techniques and elucidated using infrared (IR) spectrometry, mass spectrometry (MS) and nuclear magnetic resonance (NMR) spectrometry.

The synthesised compounds were evaluated by measuring calcium influx through NMDA receptors and voltage-gated calcium channels into synaptoneurosomes using NMDA/glycine and KCl as stimulants, respectively. The fluorescent ratiometric indicator, Fura-2 AM and Synergy™ Mx Monochromator-based Microplate Reader was used to evaluate the influence of test compounds on calcium influx after stimulant-induced depolarisation. All test compounds were screened at a 100 μ M concentration. This study identified the potential NMDA and VGCC inhibitory activity of the tricycloundecane series.

1.3: Conclusion

The disruption in calcium homeostasis mediated by excitotoxicity plays a major role in the neurodegenerative process. Drugs available in the market only offer symptomatic relief without halting the degenerative process. Maintaining calcium homeostasis through NMDA receptor and VGCC inhibitions is beneficial. We envision that the synthesised compounds will inhibit the NMDA receptor and VGCC, and exhibit a low side effect profile. This would add to the list of lead structures with potential neuroprotection properties and aid in the development of effective neuroprotective drugs.



CHAPTER TWO

Literature review

2.1: Neurodegeneration

2.1.1: Neurodegenerative disorders

Neurodegenerative disorders are debilitating diseases characterised by progressive dysfunction and death of neuronal cells (Jellinger, 2007). The cells affected either become necrotic or apoptotic, the two main forms of death in neurodegenerative disorders (Connor & Dragunow, 1998), although autophagic degeneration, an uncommon form of cell death, is also a possibility (Waldmeier, 2003; Puyal *et al.*, 2013). These forms differ morphologically and biochemically (Martin *et al.*, 1998). These disorders, amongst others, include; Parkinson's disease (PD), Alzheimer's disease (AD), amyotrophic lateral sclerosis (ALS) (Bains & Shaw, 1997), and Huntington's disease (HD) (Caraci *et al.*, 2012; Connor & Dragunow, 1998; Galpern & Cudkowicz, 2007; Gilgun-Sherki *et al.*, 2001; Marambaud *et al.*, 2009; Nicholls & Budd, 1998; Parsons *et al.*, 1999; Walker, 2007). This group of diseases has more to do with advancing age, environmental cues and/or dysfunctional immune system and less with host genetics (Kabanov & Gendelman, 2007). Each disease affects different parts of the brain of susceptible individuals and presents with distinct devastating symptoms that greatly reduce the patient's quality of life. The dopaminergic neurons in the substantia nigra (SN) pars compacta of the brain are depleted in PD and deterioration of cortical neurons is a characteristic of AD (Landrigan *et al.* 2005). Pyramidal neurons in the motor cortex and associated corticospinal tracts are degenerated in ALS. Lower neurons in the brainstem nuclei and anterior horn of the spinal cord are also degenerated (Mayeux, 2003), which result into progressive muscle weakness, atrophy, and spasticity (Galpern & Cudkowicz, 2007; Grosskreutz *et al.*, 2010). Neurons mainly in the striatum and other basal ganglia structures are lost in HD (Lee & Kim, 2006; Farooqui & Farooqui, 2009). These critical areas in the central nervous system (CNS) are responsible for coordination and cognitive functions. Defects in these vital areas have mental, social and physical implications that negatively influence the individual's active life.

2.1.2: Occurrence, incidence, and prevalence of neurodegenerative disorders

PD and AD are the most common neurodegenerative disorders (Calon & Cole, 2007), and occur mainly in the elderly. The onset and peak of symptoms of these

diseases occur in the sixth decade of life (Landrigan *et al.*, 2005; Barlow *et al.*, 2007), with early occurrence suggesting the involvement of genetic and/or environmental factors and poor prognosis (Schmechel *et al.*, 2006). Although risk increases with age, it is not a normal senescence. The duration of illness before death for PD and AD is between 2-20 years and 9 years respectively. In PD, higher incidence is noted in men than in women (Mayeux, 2003; Wooten *et al.*, 2004). Relative to AD and PD, ALS and HD are rare, but fatal with no effective treatment (Mayeux, 2003). These disorders can manifest at anytime between infancy and senescence with significant increase in rate with age (Lee & Kim, 2006; Fratiglioni & Qiu, 2009; Mayeux, 2003). In ALS, the duration of illness from the onset of signs and symptoms, most times subtle, is 3 to 5 years (Bains & Shaw., 1997; Di matteo *et al.*, 2007; Galpern & Cudkowicz, 2007). The prevalence and incidence rate of the aforementioned neurodegenerative disorders are outlined in table 2.1 (Farooqui & Farooqui, 2009). Not only are these disorders (AD, PD, HD and ALS) similar in their degenerative mechanism but also in risk factors (old age and positive family history). Onset is often subtle (Farooqui & Farooqui, 2009, Eriksen *et al.*, 2008).

Table 2.1: Prevalence (per 1000 people) and incidence (per 100000 persons-years) rates of neurodegenerative disorders (Fratiglioni & Qiu, 2009).

Neurodegenerative disorders	Ages range (in years)	Prevalence per 1000 people	Incidence per 100000 person-year
Amyotrophic lateral sclerosis	All ages	0.06	1.5-20
Huntington's disease	All ages	0.04 -0.10	0
Parkinson's disease	≥ 65	10- 20	100 – 180
Alzheimer's disease	≥ 65	40 - 80	1200 - 3000

2.1.3: Cost implications

The costs of managing neurodegenerative diseases have increased over the years (Landrigan *et al.*, 2005). This is due to the rapid increase in the number of individuals suffering from these disorders which has led to high demand for health care and social services (Fratiglioni & Qiu, 2009). In addition to the financial cost is the human cost of distress, sadness and despair, and reduction in overall quality of life

(Landrigan *et al.*, 2005), thus a costly burden on modern society (Eriksen *et al.*, 2008).

2.1.4: Treatment of neurodegenerative disorders

Most registered drugs available in the market only offer symptomatic relief without reducing or halting the degenerative process. At the onset of a symptomatic treatment, metrics of benefit initially show significant improvement compared to placebo but ultimately, a parallel rate of decline is seen with untreated patients. Typically then, patients withdrawn from treatment would perform no better than the placebo group soon after withdrawal, even though they initially benefited due to the blunting of symptoms. The effect derived from symptomatic treatment is beneficial but palliative. In stark contrast, disease-modifying agents would either arrest or slow the progression of the disease, resulting in an attenuated velocity of decline that diverges significantly from the placebo (Kennedy, 2007; Geldenhuys *et al.*, 2011).

2.2: Mechanism of neurodegeneration

As pointed out earlier, neurodegenerative disorders share a common form or mechanism of degeneration or neuronal damage. The etiopathology of these disorders is extremely complex and heterogeneous (Geldenhuys *et al.*, 2011). Genetic and environmental factors are the main initiators of the neurodegenerative process. Neuronal cells prone to degeneration either become apoptotic or necrotic depending on the extent of insult (Le Feuvre *et al.*, 2002) and in some cases, these forms of death may overlap as an apoptotic cell may eventually become necrotic.

2.2.1: Forms of neuronal death

2.2.1.1: Apoptosis

Apoptosis is an energy-dependent programmed cell death characterised by a cascade of enzymatic action with non-traumatic phagocytic clearance, that is, phagocytosis without inducing inflammatory response (Raffray & Cohen, 1997; Love, 2003). Apoptosis is the most common form of neuronal cell death, however its involvement in normal aging remains controversial (Krantic *et al.*, 2005). Apoptosis or programmed cell death (PCD) plays a major role in the normal growth and differentiation of organ systems in vertebrates and invertebrates. This PCD is responsible for matching neuronal populations to target size, and it is thought to be largely controlled by a limiting supply of target-derived trophic factors, but is also controlled by afferent stimulation (Martin *et al.*, 1998). Two main pathways (intrinsic and extrinsic) lead to apoptotic neuronal cell death. The intrinsic pathway involves

mitochondrial damage due to reactive oxygen species (ROS) and reactive nitrogen species (RNS), increased Ca^{2+} influx leading to excitotoxicity, hypoxia and UV exposure. This leads to cytochrome c release into the cytosol, with the subsequent formation of the apoptosome and the activation of effector caspases. The extrinsic pathway involves binding of a specific ligand to apoptotic initiating receptors of the tumour necrosis factor family, which induces activation of effector caspases (Artal-Sanz & Tavernarakis, 2005; Waldmeier, 2003).

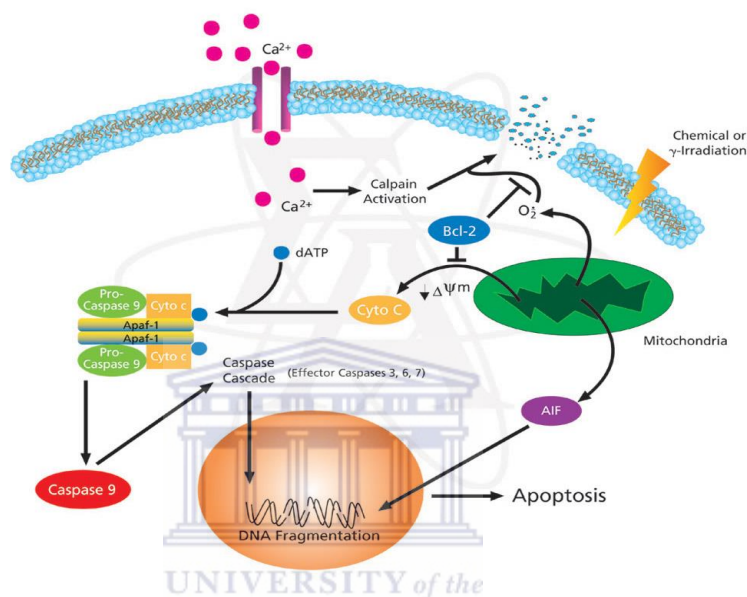


Figure 2.1: Schematic illustration of an apoptotic event (Taken from Sigma-Aldrich, 24 June 2012).

Toxic agents such as detrimental free radicals, drugs and toxic chemicals interact with the cell (figure 2.1). These interactions lead to the formation of lesions on the cell surfaces. The cells sense the damage and initiate the repair process in non-apoptotic cells. In apoptotic cells, the damage exceeds the repair capability of the cell leading to activation of caspases, products of proteolytic cleavage of procaspases (proenzymes), directly involved in apoptosis (Raffray & Cohen, 1997). These caspases are divided into two broad groups which are initiator caspases and effector caspases. The initiator caspases interact with the dead domains of other transmembranes and intracellular proteins involved in apoptosis initiation; *via* these interactions, a range of pro-apoptotic stimuli is transduced into proteolytic activity. At this stage, the cells have reached ‘a point of no return’. Activation of the apoptotic-effector system, involving effector caspases, results in death of the cells. The effector caspases involved in the cleavage of cellular substrates that are directly responsible for most morphological and biochemical changes evolve in apoptosis. The substrates

inactivated by caspases include cytoskeletal proteins such as actin, α -fodrin, and gelsolin; structural nuclear protein such as lamins; DNA repair proteins such as DNA-dependent protein kinase, and poly (ADP-ribose) polymerase (PARP); the anti-apoptotic protein Bcl-2 and Bcl-x_L; and the inhibitor of caspase-activated DNase. The enzymatic cleavage of inhibitors of caspase-activated DNase leads to the release of caspase-activated DNase, an enzyme that causes apoptotic cleavage of nuclear DNA. Although caspases is the main mediator for apoptosis, others include apoptotic inducing factor, a flavoprotein confined to the mitochondrial intermembrane space, endonucleases, and transglutaminase (Love, 2003). Apoptosis is more involved in scattered discrete cells with a lower injury level capable of initiating apoptotic response in comparison to necroses (Raffray & Cohen, 1997).

2.2.1.2: Necrosis

Necrosis, a relatively unordered process (Yanamadala & Friedlander, 2009), is the passive killing of a cell (Jellinger, 2007). In contrast to apoptosis, cells involved in necrosis are usually in large numbers or confluent volume and undergo extensive inflammatory response. Severe, sudden or high degree of injury results from detrimental agents and target cell interaction. This causes irreversible damage leading to homeostatic failure, 'point of no return'. At this point, the cell loses its function and uncontrolled degradable enzymatic action leads to lysis and reactive inflammation (Raffray & Cohen, 1997).

Cell death by necrosis exhibits rapid cell swelling and subsequent rupture of the plasma membrane, due to an inflammatory response, that usually induces substantial secondary cell damage in the surrounding tissues (Jellinger, 2007). Although the molecular mechanism that brings about necrotic death is not fully elucidated, experimental evidence indicates that necrosis of adult neurons is mediated by an increase in intracellular Ca²⁺ and is independent of caspases. Instead cytosolic calpains and spilled lysosomal cathepsins are the major players in necrotic neuronal death.

Energy depletion is a potent trigger for necrosis. Acidification, a consequence of oxygen depletion, also plays an important role in necrotic neuronal death. Acidosis activates Ca²⁺-permeable acid sensing ion channels (ASIC) resulting in glutamate receptor-independent neuronal injury due to Ca²⁺ toxicity (Artal-Sanz & Tavernarakis, 2005).

2.2.2: Oxidative stress in neurodegeneration

Oxidative stress, a major cause of neurotoxicity, arises as a result of an imbalance in the production of detrimental free radicals and natural antioxidants, enzymatic and non-enzymatic, leading to oxidative damage to the cell and its constituents (Gilgun-Sherki *et al.*, 2001; Crouch *et al.*, 2008; Gonsette, 2008). The brain as a vital organ, although small in size, has a disproportionately high level of oxygen consumption mainly due to its high energy (ATP) demand. The centre for ATP production is the mitochondrial electron transport chain known as the powerhouse or engine of the cell (Sas *et al.*, 2007; Crouch *et al.*, 2008). This mitochondrial electron transport chain and its enzyme complexes form ROS, mostly *via* inhibition of one or more enzyme complexes leading to ineffective transfer of electrons to oxygen during oxidative ATP production (Crouch *et al.*, 2008). The ROS include superoxide anion ($O_2^{\cdot-}$), hydrogen peroxide (H_2O_2), hydroperoxy radicals ($^{\cdot}OOH$), Hydroxy radical ($^{\cdot}OH$), Nitric oxide (NO^{\cdot}), and peroxynitrate ($ONOO^{\cdot}$) (Raffray & Cohen, 1997; Gilgun-Sherki *et al.*, 2001; Gonsette, 2008). Reactive species such as $^{\cdot}OH$, $O_2^{\cdot-}$, $^{\cdot}OOH$ and NO^{\cdot} are free radicals while H_2O_2 and $ONOO^{\cdot}$ are molecules capable of generating free radicals through various chemical reactions (Gilgun-Sherki, 2001). β -Amyloid ($A\beta$) interaction with copper ions can also generate ROS. $A\beta$ has the ability to reduce Cu (II) to Cu (I) to produce H_2O_2 as a by-product (Crouch *et al.*, 2008). ROS are capable producing multiple of potentially lethal cellular effects, including ATP depletion, calcium influx elevation, and oxidation of glutathione, NADH, lipids, and macromolecular thiol, all of which contributes to the degeneration process (Raffray & Cohen, 1997). Cerebrovascular disorders are also capable of generating nitrogen and oxygen free radicals *via* a complex cascade of metabolic events (Qureshi *et al.*, 2004).

Under physiological conditions, the ROS are counterbalanced by both natural enzymatic and non-enzymatic antioxidants (Gilgun-Sherki *et al.*, 2001; Lobo *et al.*, 2010). At low levels, ROS function as signalling intermediates for the modulation of fundamental cellular activities such as growth and adaption responses (Farooqui & Farooqui, 2009). In pathological conditions such as inflammation or age-related neurodegeneration, high level of ROS are produced which overwhelm natural antioxidant defence, leading to oxidative stress (Gilgun-Sherki *et al.*, 2001; Farooqui & Farooqui, 2009). ROS oxidise important cellular component such as lipids, protein and DNA to cause cellular damage (Ricciarelli *et al.*, 2007) and eventually cell death

mainly by apoptosis (Gilgun-Sherki *et al.*, 2001). Oxidative molecular damage to DNA and proteins increase exponentially with age (Calabrese *et al.*, 2001) mainly due to a progressive decline in the ability of the human body to combat environmental stress and to successfully repair DNA fault (Sas *et al.*, 2007).

2.2.3: Excitotoxicity in neurodegeneration

Neurons are excitable cells designed to have sophisticated membrane ion channels and their excitatory neurotransmitter receptor systems are inherently sensitive to cation overload and oxidative damage caused by ROS (Raffray & Cohen, 1997). Excitotoxicity is a process which involves over activation of excitatory neurotransmitter receptors accompanied by decreased inhibitory processes mediated by gamma amino butyric acid (GABA) and glycine (Gonsette, 2008) and finally leads to neuronal cell death. This is either by rapid necrosis or delayed apoptosis depending on the severity of the insult, extent of energy recovery (Kaul & Lipton, 2000) or glutamate exposure to its receptors.

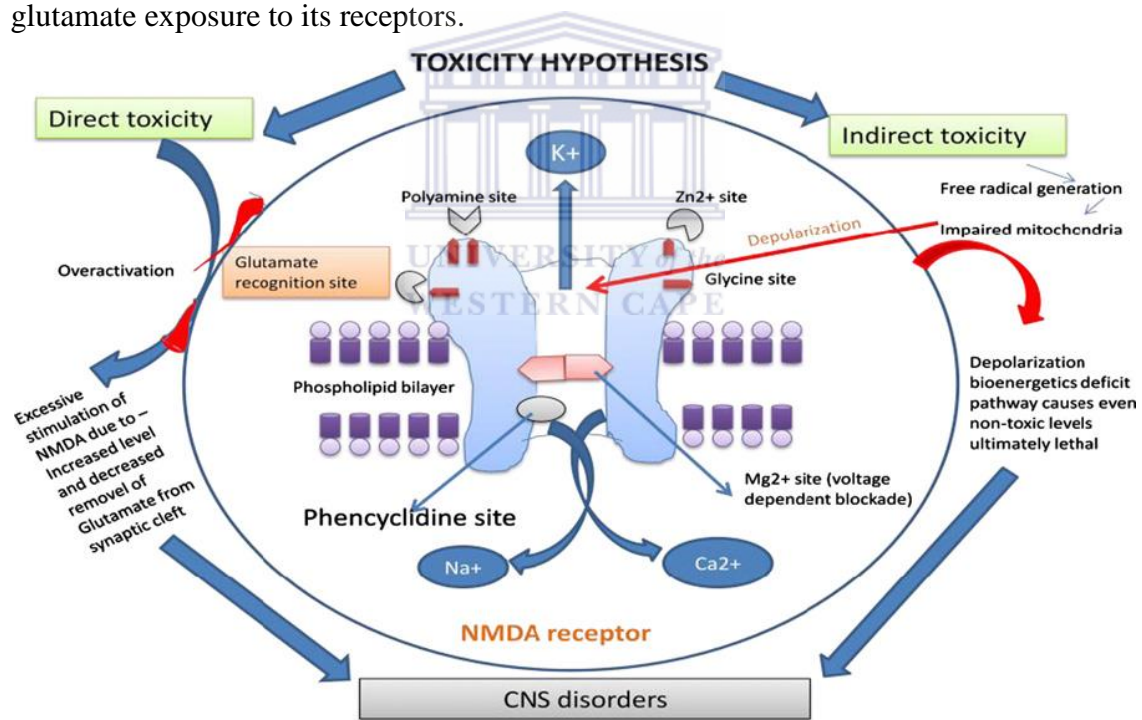


Figure 2.2: Direct and indirect toxicity hypothesis associated with CNS disorders.

Diagram shows the interaction between the direct and indirect toxicity hypothesis in the etiology of various neurodegenerative disorders. Focusing on the common NMDA bridge between the two hypothesis which results in excitotoxic damage to brain. In direct toxicity, there is a overactivation of NMDA due to continuous stimulating response under pathological conditions whereas in indirect toxicity there is an impairment of mitochondrial function which results in the cascade of excitotoxic pathways leading to various neurodegenerative disorders (Mehta *et al.*, 2013).

Excitotoxic neuronal death can be direct or through indirect pathways (figure 2.2). Direct excitotoxicity is the result of excessive stimulation of NMDA receptors that was initially proposed as a causative factor in the pathogenesis of neurodegenerative disorders. In ‘indirect excitotoxic hypothesis’, depolarisation by bioenergetics deficit causes even the non-toxic levels of glutamate ultimately to become lethal (Mehta *et al.*, 2013).

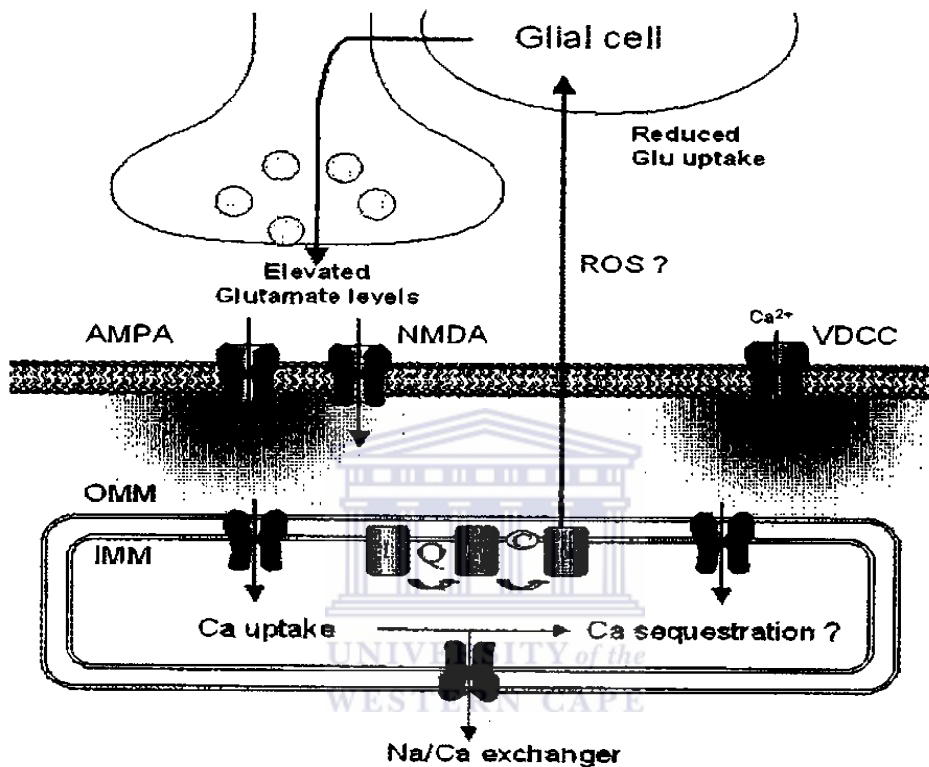


Figure 2.3: Interaction of Ca^{2+} and mitochondria in ALS as a local disruptive feedback mechanism. Several research reports indicate an impairment of the mitochondrial respiratory chain in ALS (complex I – complex IV), which has multiple implications for Ca^{2+} regulation in motor neurons. First, impairment of complex VI presumably increase ROS production, which leads to reduced glutamate uptake in neighbouring glia cells, elevated glutamate levels in synaptic cleft and increased calcium influx through Ca^{2+} -permeable glutamate receptor channels. Second, disturbed mitochondria affect cytosolic calcium regulation by a reduction of mitochondrial Ca^{2+} uptake/sequestration and an impaired function of Na/Ca exchanger in the inner mitochondrial membrane. Taken together, these disturbances might form a local feedback mechanism that contributes to motor neuron degeneration in ALS (Grosskreutz *et al.*, 2010).

Normally glutamate, the principal excitatory neurotransmitter in mammalian CNS, (Doble, 1999; Hogg *et al.*, 2005; Barber *et al.*, 2006; Betzen *et al.*, 2009) and related compounds are stored within intracellular compartments with extracellular

glutamate retrieved *via* plasma membrane transporters. Other excitatory neurotransmitters include quinolinic, ibotenic, kainic, quisqualic and domoic acids. Astrocytes also take up glutamate from the extracellular spaces *via* excitatory amino acids (EAA) transporters and convert it to glutamine *via* ATP dependent mechanisms. In turn, neurons take up glutamine release by astrocytes from extracellular spaces and convert it back to glutamate *via* glutaminase (Gonsette, 2008). This ensures extracellular levels are precisely controlled, keeping it at physiological concentration. Figure 2.3 illustrates the processes involved in the release, uptake, and metabolism of glutamic acid and glutamine by glutamatergic nerve terminals and glial cells (astrocytes) at a central synapse (Doble, 1999).

In cases of anoxia (Doble, 1999), CNS trauma, stroke, epilepsy and certain neurodegenerative diseases, increased concentrations of extracellular glutamate are caused either by excessive vesicular release (Stone & Addae, 2002), transporter reversal, disruption of cellular uptake, astrocyte dysfunction, or liberation of glutamate following necrotic cell lysis, which further results in the over-activation of local ionotropic glutamate receptors (iGluR) (Greenwood & Connolly, 2007). Astrocytes also serve as the major homeostatic regulator, buffers for excess neurotransmitters, neurotrophic factor secretors (Block & Hong, 2005), and as storage site for manganese in the brain but increased accumulation may alter release of glutamate and elicit excitotoxicity (Milatovic *et al.*, 2009). They become activated in response to immunologic challenges or brain injuries to prevent neuronal death. However, activated astrocytes become hypertrophic, exhibit increased production of glial fibrillary acidic protein, and form glial scars, which hinder axonal regeneration (Block & Hong, 2005). Na^+/K^+ pump failure caused by cellular ATP depletion also has a depolarising effect on neurones resulting in excess release and accumulation of glutamate (figure 2.3; Le Feuvre *et al.*, 2002).

The iGluRs activated are NMDA, kainate and alpha-amino-3-hydroxy-5-methyl-4-isoxazole-propionic acid (AMPA; Wollmuth & Sobolevsky, 2004; Mayer, 2011). Although they share a common endogenous ligand, they show numerous pharmacological, biochemical and modulatory differences (Wollmuth & Sobolevsky, 2004). The AMPA receptors are permeable to Na^+ and K^+ ; and also permeable to Ca^{2+} unless the receptor contains a GluR_2 subunit that in most cases is absent (Aarts & Tymianski, 2003; Marambaud *et al.*, 2009; Grosskreutz *et al.*, 2010). The NMDA receptors are highly permeable to Ca^{2+} and Na^+ . Thus, over-activation of these

receptors results in excessive influx of Ca^{2+} and Na^+ leading to Ca^{2+} overload (delayed phase) and osmotic swelling (early phase) of the neuronal cellular bodies and dendrite spines respectively (Aarts & Tymianski, 2003). The osmotic component is potentially reversible if the stimulus is removed as the osmotic swelling will be prevented. Thus it is the calcium-dependent part of the excitotoxic cascade that appears to be essential for the initiators of excitotoxicity (Doble, 1999). The delayed Ca^{2+} -dependent phase has been the target of pharmacological interventions aimed at protecting neurons against glutamate-induced excitotoxicity by preventing either Ca^{2+} influx or its intracellular release (Abdel-Hamid & Balmbridge, 1997). Voltage sensitive calcium channels are also activated to increase intracellular Ca^{2+} upon glutamate stimulation (Crews *et al.*, 1998). However, Ca^{2+} overloading from this channel during KCl-depolarisation is much less excitotoxic (Nicholls & Budd, 1998). Nicholls and Budd suggested that initial Ca^{2+} entry (Ca^{2+} loading) in polarised cells may be more critical than the absolute amount of accumulated (Ca^{2+}) in triggering excitotoxicity. Cell death does not depend on this initial Ca^{2+} rise, but rather invariably follows a delayed massive accumulation of Ca^{2+} , occurring a few hours after the toxic challenge and representing a no-return transition into the death process (Celsi *et al.*, 2009). Although Ca^{2+} plays a key role in the pathology underlying neurodegeneration, it is not the sole mechanism mediating neuronal cell death (Choi *et al.*, 1988; Grobler *et al.*, 2006).

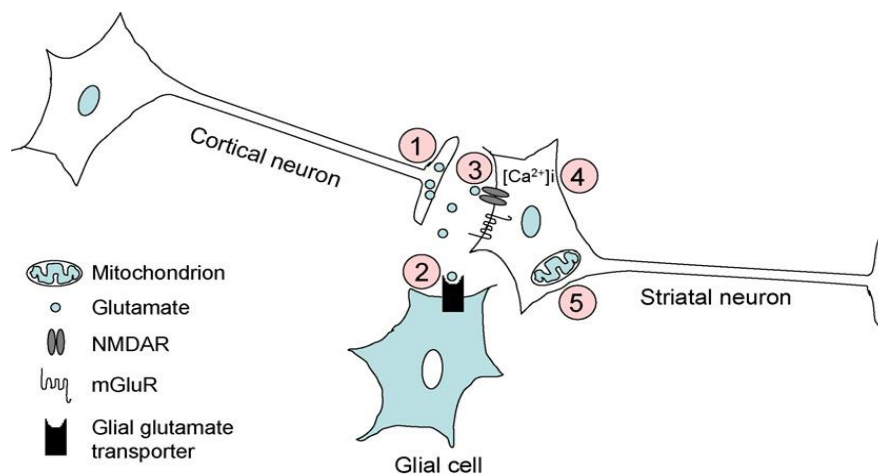


Figure 2.4: Cartoon of possible points along the corticostriatal pathway where dysfunction may contribute to excitotoxicity. Excitotoxic neuronal death may result from a combination of: (1) increased glutamate release from cortical afferent; (2) reduced uptake of glutamate by glia; (3) hypersensitivity augmentation of mGluR signalling; (4) altered intracellular calcium homeostasis; and/or (5) mitochondrial dysfunction (Fan & Raymond, 2007).

Normally, the mitochondria possess the ability to sequester large quantities of intracellular Ca^{2+} within their matrices whenever local cytoplasmic free concentrations rise above the critical point, particularly in severe cellular dysfunction (Celsi *et al.*, 2009; Nicholls & Budd, 1998; Greenwood & Connolly, 2007). However, massive Ca^{2+} loading of the mitochondrial matrix activates the permeability transition pore (PTP) in the inner mitochondrial membrane (Greenwood & Connolly; 2007; Marambaud *et al.*, 2009) thus exceeding the capacity of Ca^{2+} regulatory mechanism (Aarts & Tymianski, 2003). Activation of PTP and sodium ion influx leads to complete depolarization and collapse of mitochondrial membrane potential ($\Delta\Psi_m$) (figure 2.1) accompanied by ATP hydrolysis (Kaul & Lipton, 2000), generation of ROS, rupture of the outer mitochondrial membranes, and the release of the accumulated matrix Ca^{2+} (Greenwood & Connolly, 2007). ATP depletion (Nicholls & Budd, 1998), ROS, and excessive intracellular Ca^{2+} accumulation activate the chain of events leading to channelopathy, calcium overload, mitochondriopathy, proteolytic enzyme production and activation of pathways leading to cell death (figure 2.4; Gonsette, 2008; Calabrese *et al.*, 2001). Disturbance of Ca^{2+} homeostasis can also be caused by inflammation and $\text{A}\beta$ -induced mitochondrial dysfunction, particularly Alzheimer disease, leading to apoptosis or necrosis (Witte *et al.*, 2010).

Krantic *et al.* (2005) reviewed the involvement of MPTP in excitotoxicity. It was indicated that MPP^+ blocks complex I of the mitochondrial respiratory chain, consequently inhibiting oxidative phosphorylation and leading to decrease in intracellular ATP levels. These events are directly involved in neuronal depolarization, release of glutamate and over-stimulation of NMDA receptors (Krantic *et al.*, 2005). Importantly, excessive Ca^{2+} influx also activates the stress-related p38 mitogen-activated protein kinase (p38 MAPK)/myocyte enhancer factor 2C (MEF2C transcription factor) pathway and c-Jun *N*-terminal kinase (JNK) pathways in cerebrocortical or hippocampal neurons. Activation of these pathways has been implicated in neuronal apoptosis (Kaul & Lipton, 2000).

It has been suggested that in contrast to what is observed with NMDA receptor agonists, administration of AMPA/kainate receptor agonists into the CNS can lead to an apoptotic rather than a necrotic form of cell death *in vivo*. This would be compatible with the idea that AMPA/kainate receptor-mediated excitotoxicity involves sustained, low-level insult (Doble, 1999). Glutamate stimulation of NMDA

receptors also initiate endothelial barrier dysfunction, a phenomenon termed ‘endothelial excitotoxicity’ (Betzen *et al.*, 2009).

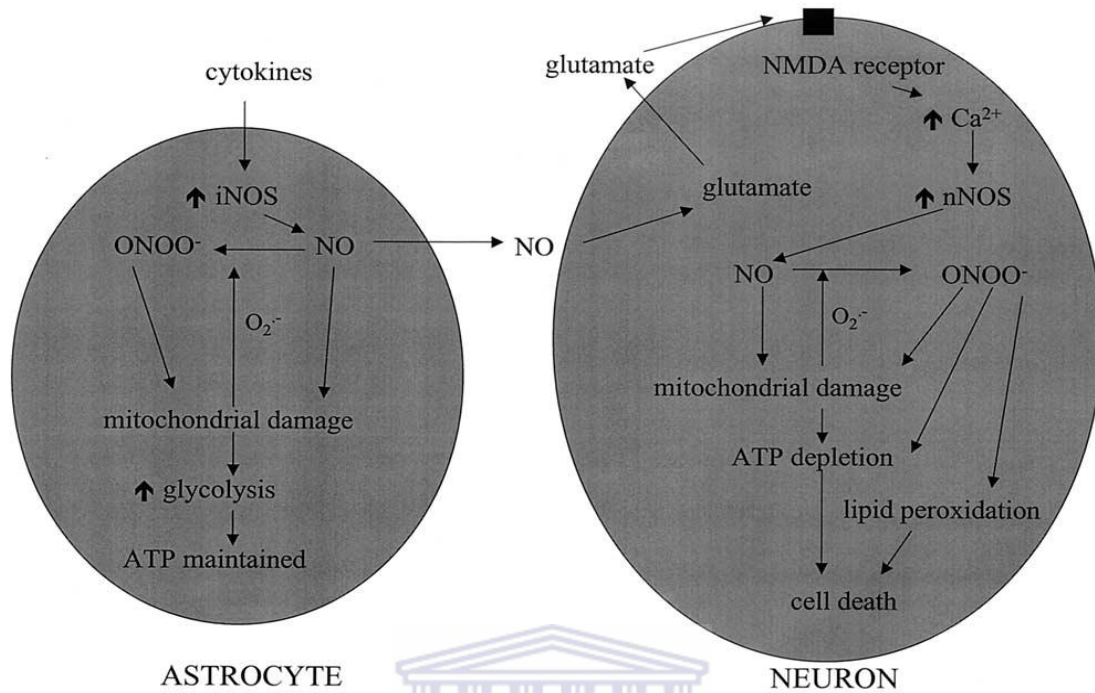


Figure 2.5: Mechanisms of NO-mediated neurotoxicity. Exposure of astrocytes to cytokines leads to the induction of iNOS, generation of NO, and mitochondrial respiratory chain damage. Superoxide radicals generated by the respiratory chain further react with NO, forming ONOO⁻ and causing more mitochondrial damage. Despite this mitochondrial damage, astrocytic ATP levels are maintained by switching to glycolysis. Diffusion of NO into neighbouring neurons causes neuronal glutamate release, which then activates NMDA-type glutamate receptors, either on the same or neighbouring neurons. Activation of the neuronal NMDA receptor triggers Ca²⁺ influx and activation of nNOS. The subsequent generation of NO/ONOO⁻ initiates neuronal mitochondrial damage, lipid peroxidation, and ATP depletion. Since neurons are unable to increase glycolysis to maintain their energy demands, cell death may ultimately occur (Stewart & Heales, 2003).

Nitric oxide (NO) is generated following activation of three isoforms of NO synthases (NOS); the endothelial (eNOS), neuronal (nNOS) and inducible (iNOS). These isoforms differ from each other in terms of intracellular localization, activation properties and sensitivity to regulation by protein interactions and second messenger molecules. Neuronal NO synthase is constitutively expressed in neurons and astrocytes and associated more often with physiological actions of NO, while iNOS is induced by proinflammatory conditions in microglia, astrocytes and neurons, and mediates generation of NO in pathophysiological conditions (De Palma *et al.*, 2008). Upregulation of iNOS can produce large amount of NO (Witte *et al.*, 2010). The role

of eNOS in the nervous system has been studied only to a limited extent (De Palma *et al.*, 2008).

NO can induce physiological response like vasodilatation, but massive influx of Ca^{2+} , upon activation of excitotoxic stimulus, can over-activate neuronal nitric oxide synthase leading to excessive production of NO. The NO produced is capable of combining with free radicals generated from the mitochondria to form highly toxic peroxynitrite that contribute (by lipid peroxidation, protein nitration and DNA damages) to neuronal cell death (Chung & David, 2010). Exposure of neurons to NO can cause neuronal glutamate release which in turn stimulates NMDA receptors thus enhancing excitotoxicity. Glial-derived NO is also capable of eliciting neuronal glutamate release hence stimulating further formation of reactive nitrogen species to cause neuronal death (figure 2.5; Stewart & Heales, 2003).

Activation of metabotropic glutamate receptors (mGluR), anchored to the NMDA Receptors *via* a chain of scaffold proteins i.e. receptors coupled to G protein (Rodriguez *et al.*, 2000), can either modulate neurodegeneration or neuroprotection. mGlu 1a and 5 can stimulate intracellular Ca^{2+} release *via* hydrolysis of phosphatidylinositol-4,5-bisphosphate (PtdIns-4,5-P_2), a substance that ensure the formation of inositol-1,4,5-trisphosphate (InsP_3), and activate the phosphatidylinositol-3-kinase (PI3K) pathway. This is known to support neuronal survival by inhibiting glycogen synthase kinase-3 β and other mechanism, only if the C-terminus domain is intact. In conditions where elevated intracellular Ca^{2+} level cause a calpain-mediated cleavage of the C-terminus portion of the mGlu1a receptor, the PI3K pathway is prevented but leaves its ability to stimulate PtdIns-4,5-P_2 hydrolysis intact (Pellegrini-Giampietro *et al.*, 1999; Caraci *et al.*, 2012). This may cause an imbalance in favour of the neurotoxic signal which results in neuronal death. In contrast to mGlu1 and mGlu5 agonists, mGlu1 and mGlu5 antagonists or negative allosteric modulators are consistently neuroprotective, by enhancing GABA release, independently of the nature of insult (Bordi & Ugolini, 1999; Nicoletti *et al.*, 1999; Pellegrini-Giampietro *et al.*, 1999; Caraci *et al.*, 2012). mGlu2 and mGlu3 receptor activation have also shown neuroprotective activity. They reduce neuronal excitability by activating different K^+ channel and negatively regulate glutamate release (Di Liberto *et al.*, 2010; Caraci *et al.*, 2012).

Interestingly, glial-mGlu3 (mGlu3 in astrocytes) receptors are neuroprotective. They also regulate the production of neurotrophic factor, to stimulate neuronal

regeneration (Caraci *et al.*, 2012). Neurotrophic factors play a vital role in the neuroprotection of specific neuronal population by suppressing the expression of 'suicide genes' which, when activated are involved in the induction of the apoptotic processes (Connor & Dragunow, 1998). Other mGluRs which include: mGlu4, mGlu7, and mGlu8 are presynaptically localized and behave as autoreceptors inhibiting glutamate release. Metabotropic glutamate receptors involvement in excitotoxicity is still a 'hot topic' that warrant further investigation (Caraci *et al.*, 2012).

Although both ionotropic and metabotropic glutamate receptors are involved in excitotoxicity, ionotropic glutamate receptors pose greater danger as its stimulation triggers neurodegeneration with little or no hope of neuronal survival.

2.3: NMDA receptors

2.3.1: Introduction

Ionotropic glutamate receptors mediate the fast response to the major excitatory neurotransmitter in human central nervous system and play an essential role in its development and function. Many neurological disorders such as epilepsy or chronic neurodegenerative conditions, as well as stroke, can be linked to iGluRs (Stawski *et al.*, 2010; Jensen *et al.*, 2011). Glutamate-induced excitotoxicity in aging or pathological conditions play a central role in acute and chronic neurodegenerative disorders and is a fundamental target in neuroprotective strategies (Gascon *et al.* 2008). Although mGluR and iGluR are both stimulated in glutamate-induced excitotoxicity, iGluRs effects are more detrimental. This is due to the neuroprotective properties of mGluRs. Notwithstanding, they potentiate iGluR functions, downregulating K⁺ channel and upregulating non-selective cation channel, and inhibit GABA receptor activity to enhance neuronal excitability (Aarts & Tymianski, 2003). Among the iGluRs, NMDA receptor stimulation produces the major effect. NMDA receptors have several unique pharmacological and biophysical features, including the requirement for simultaneous binding of the co-agonist glycine and glutamate for activation (Monaghan *et al.*, 2012), slow deactivation, voltage-dependent Mg²⁺ block, and high permeability to Ca²⁺, that distinguish them for other iGluRs (Chen & Roche, 2007; Hedegaard *et al.*, 2012).

Under most physiological conditions or at resting membrane potentials, NMDA receptors are blocked by magnesium ions, a voltage-dependent process, that prevent them from being activated by glutamic acid, but the blockage is relieved

either by AMPA- or kainate-mediated depolarisation, or pathological conditions. This contributes to excitotoxicity (Dobles, 1999; Stone & Addae, 2002).

2.3.2: Structure of iGlu receptor

The iGluR subunits contain three transmembrane domains (M1, M3 and M4) and a re-entrant membrane loop (M2) on the cytoplasmic side that lines the inner channel pores and defines the distinct ion selectivity of the ion channel. The large, extracellular amino-terminal domain of each subunit includes a necessary component of the glutamate recognition site (S1) and customises selective receptor modulation *via* several mechanisms including redox modulation of interdomain disulfide linkages or affinity to allosteric modulators such as extracellular protons, Zn^{2+} and polyamines. The M3-M4 loop includes a second required component of the glutamate recognition site (S2) and RNA splice variants that affect receptor desensitisation. The intracellular carboxyl terminus is involved in signal transduction, receptor anchoring and contains phosphorylation sites that modulate receptor activity (figure 2.6). Each subunit is a glycosylated, membrane-inserted polypeptide with an approximate length of 900 amino acids (Bigge, 1999; Tichelaar *et al.*, 2004; Mandolesi *et al.*, 2009).

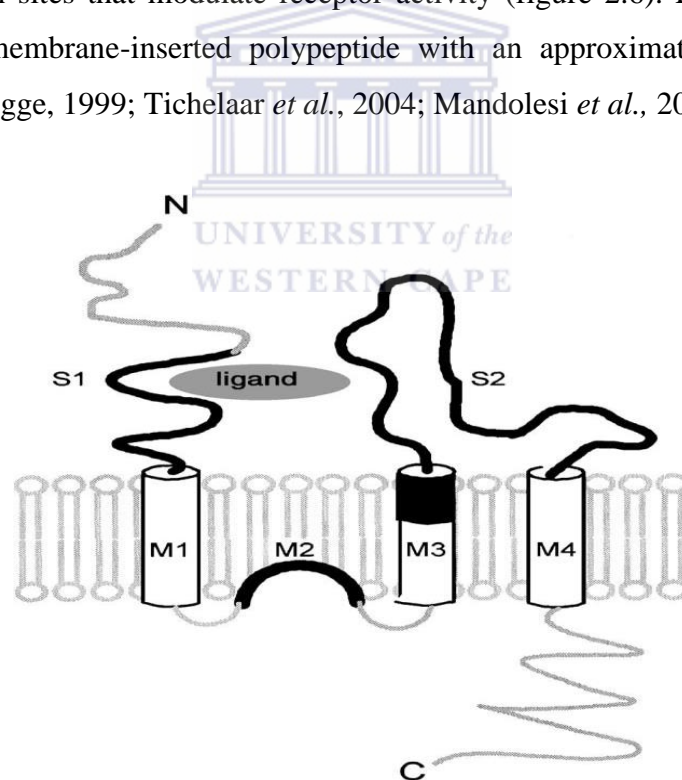


Figure 2.6: Topology of a single NMDA receptor subunit. N is the extracellular N-terminal; M1, M3, and M4 the three transmembrane regions; M2 the reentrant P-loop; and C the intracellular C-terminal. M1–M4 are spread out for clarity; their relative positions are unknown. S1 and S2 form the ligand binding site. The external portion of M3, indicated by black, may be involved in channel gating. Four subunits are thought to comprise a functional NMDA receptors (Bigge, 1999; Qian & Johnson, 2002).

2.3.3: Structure and functions of the NMDA receptor

NMDA receptors are grouped into three identified subunits that include: NR1 subunit, four distinct NR2 subunits (A-D) (Hogg *et al.*, 2005), and two NR3 subunits (A and B) (Cull-Candy *et al.*, 1998; Aarts & Tymianski, 2003; Mayer, 2005; Losi *et al.*, 2006; Chen & Roche, 2007; Li & Han, 2008; Monaghan *et al.*, 2012). The NMDA receptor is structurally made up of a large extracellular amino-terminal domain (N terminus) that contributes to ligand binding, four membrane domains (three true transmembrane segments and a re-entrant pore loop (Chen & Roche, 2007) and an intracellular carboxyl-terminal regulatory domain (figure 2.11; O'Brien *et al.*, 1998; Hogg *et al.*, 2005). The N terminus binds to agonists, antagonists, and modulators such as Zinc, protons, polyamines, which can finally control the opening of the ion channel or modulate ion channel function and desensitization behaviour (Qiu *et al.*, 2011). The NR2 subunits of the NMDA receptors are much larger (> 1300 amino acid residues) because of an extended intracellular carboxyl terminus containing phosphorylation sites that regulate receptor function and level of activation. The NR1 is obligatory for channel activity of NMDA receptors, whereas the NR2 subunit confers specificity of functions (Bigge, 1999). The pharmacology of the channel is mainly determined by the type of NR2 subunits and by alternative splicing of NR1 subunits (Losi *et al.*, 2006). NR2 subunits also confer distinct physiological and biochemical properties to the NMDA receptor complex. The various NR2-containing receptors differ in their single channel conductance, open probability, the ability to desensitize, decay rate, sensitivity to L-glutamate and glycine, and the ability to bind to various intracellular signalling proteins (Monaghan *et al.*, 2012).

The binding sites for glycine and glutamate are subunit NR1 and NR2 respectively (Qian & Johnson, 2002; Chen & Roche, 2007; Hedegaard *et al.*, 2012). However, glycine can act on glycine binding sites at synaptic NR2A and NR2B containing NMDA receptors to enhance NMDA receptor functions (Li & Han, 2008).

Of the previously mentioned iGluR families, activated by glutamate, the NMDA receptor family has received special attention. This is due to its distinct role in regulation of synaptic plasticity- long-term potentiation, long-term depression, and experience-dependent synaptic refinement (Costa *et al.*, 2012). In addition, its role is critical in neurological and psychiatric disorders (Monaghan *et al.*, 2012).

2.3.4: NMDA receptor binding sites

The overall fold of the ligand-binding domains of iGluR families (AMPA, kainite and NMDA receptors) are nearly identical. They possess key amino acid side chains that interact with ligand α -amino and α -carboxyl groups. What differs are the amino acids that interact with the glutamate γ -carboxyl groups or, in the case of NR1 subunits, prevent the binding of glutamate. In the agonist-bound complex of all iGluRs, the ligand is buried in the interior of the protein but the volume of the ligand-binding cavity varies substantially (Mayer, 2005). The S1 and S2 adjacent to M1 and the M3-M4 loop respectively form a bi-lobed glutamate binding pocket that is in dynamic equilibrium between open and closed gate. Short segments linking the recognition site to the transmembrane domains play a central role in the gating of NMDA receptor channel and glutamate binding induces conformational changes that create mechanical tension in M1 that activate the channel (figure 2.6).

Glutamate binds to NR2 subunits and glycine binds to a homologous site on NR1 and NR3 subunits, to cause the opening of the receptor's $\text{Na}^+/\text{K}^+/\text{Ca}^{2+}$ -permeable ion channel. It is the influx of Ca^{2+} ions through this channel that initiates many of the actions of the NMDA receptors (Monaghan *et al.*, 2012).

2.3.5: NMDA receptor inhibition

NMDA receptor antagonism may have therapeutic application. This has led to the study and development of several NMDA antagonists with diverse mechanisms of action with a hope to treat disorders such as stroke, hypoxic injury, pain and neurodegeneration (Monaghan *et al.*, 2012). Despite high expectations, the results from clinical studies of NMDA receptor antagonists have been largely disappointing (Costa *et al.*, 2012). Antagonists that functionally inhibit NMDA receptors *via* either the binding site on the regulatory N-terminal domain (Monaghan *et al.*, 2012), PCP site located inside the channel (open channel block) (Geldenhuys *et al.*, 2007), the primary transmitter binding site (competitive) or the strychnine-insensitive glycine site (glycine_B) (Parsons *et al.*, 1999; Kiss *et al.*, 2005; Monaghan *et al.*, 2012) show inadequate selectivity among different subtypes of NMDA receptors and have been plagued by unacceptable side effects such as psychotomimetic effects and impaired motor function (Kiss *et al.*, 2005). Compounds like PCP, ketamine and MK-801 (figure 2.7) produce these undesirable side effects owing to high affinity for NMDA receptors (Doble, 1999; Monaghan *et al.*, 2012). These compounds are uncompetitive antagonists of NMDA receptors and are highly potent (Doble, 1999). MK-801 for

example, slows the blocking rate and allows significant Ca^{2+} influx such that very high concentrations of MK-801 are required to completely block NMDA triggered Ca^{2+} responses, producing long-lasting, maximal blockade of the channel (Black *et al.*, 1996). As a result, only few compounds targeting these receptors have been converted from pre-clinically active compounds into drugs for human use.

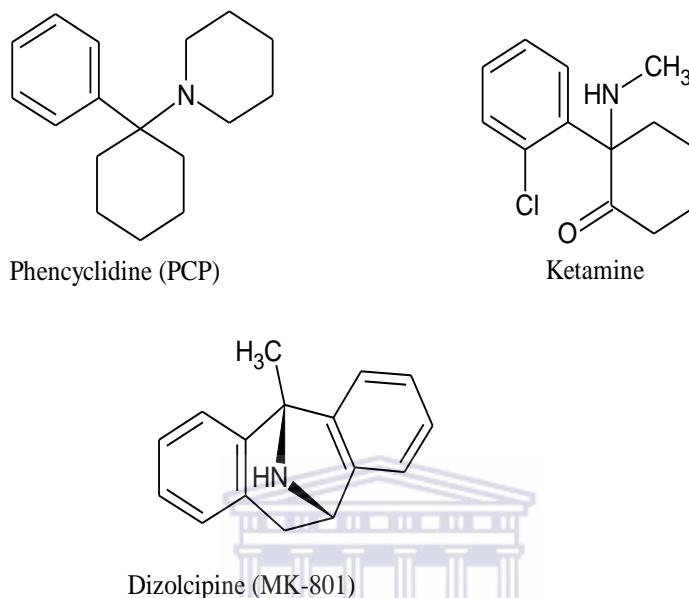


Figure 2.7: Chemical structures of phencyclidine, ketamine and dizolcipine.

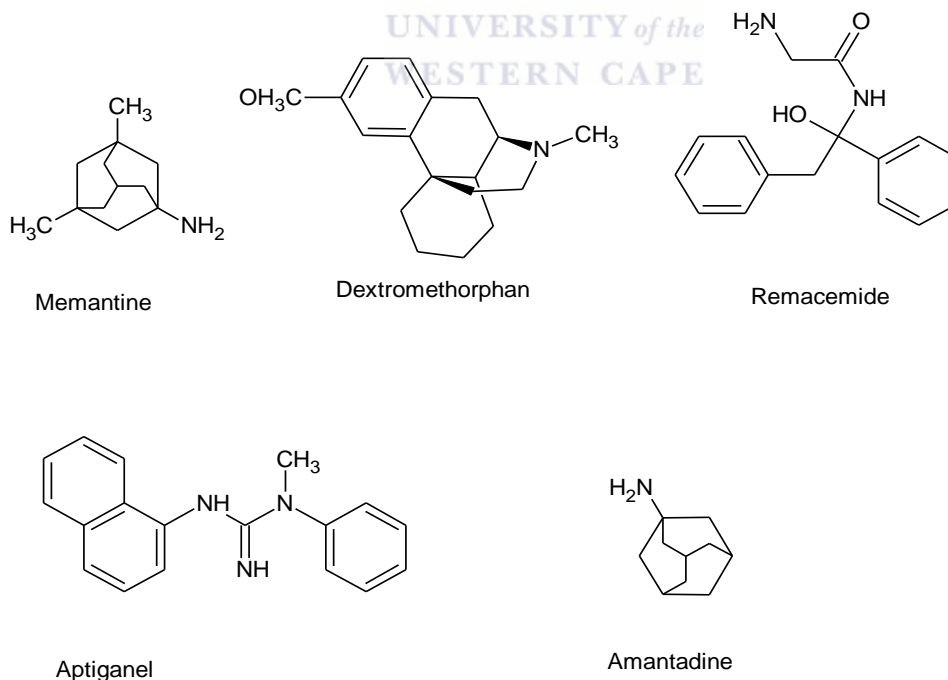


Figure 2.8: Chemical structures of memantine, dextromethorphan, remacemide, aptiganel and amantadine.

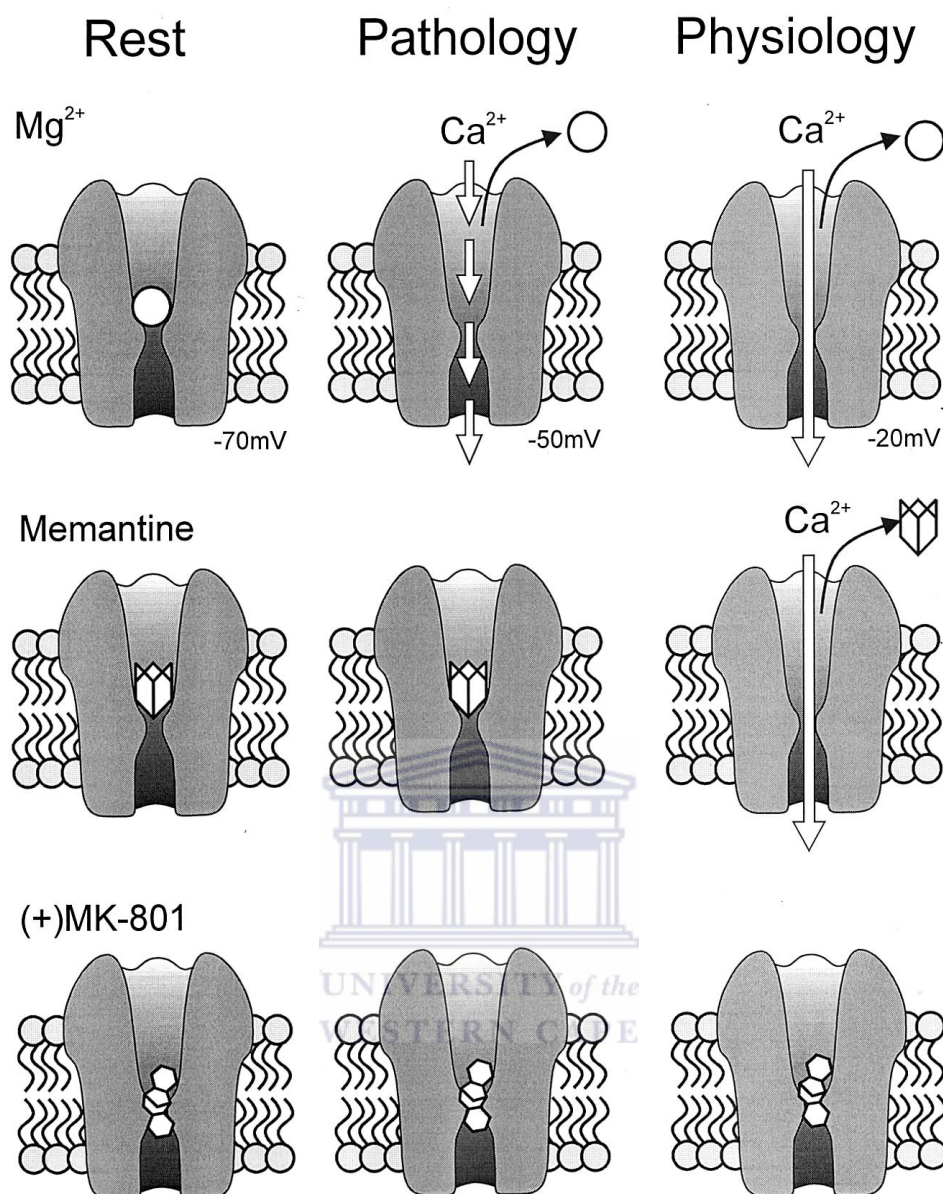


Figure 2.9: Scheme of the hypothesis explaining how the fast unblocking kinetics of memantine allows this strongly voltage-dependent compound to differentiate between the physiological and pathological activation of NMDA receptors (Parsons *et al.*; 1999).

Low-affinity un-competitive antagonists and allosteric modulators of NMDA receptors have demonstrated improved safety profiles compared to competitive antagonists, which have failed in clinical trials due to their narrow therapeutic window (Hedegaard *et al.*, 2012). These clinically-tolerated NMDA receptor channel blockers include: memantine, dextromethorphan, remacemide, aptiganel and amantadine (figure 2.8; Monaghan *et al.*, 2012; Doble, 1999). The reduce toxicity or safety profile is probably due to faster rates of unblocking (memantine; figure 2.9) and equilibrium block (Black *et al.*, 1996). These compounds produce shorter-acting channel block with lower potency (Doble, 1999).

2.4: Neuronal voltage-gated calcium channels

2.4.1: Introduction

In the central nervous system, calcium influx through VGCC mediates a range of cytoplasmic processes, including vesicular release of neurotransmitters, intracellular signalling pathways, gene expression, synaptic plasticity, and regulation of neuronal excitability (Snutch *et al.*, 2001; McDonough, 2007; Christel & Lee, 2012; Morton *et al.*, 2013). The electric potential across cellular membranes is controlled by a gradient of ions produced by membrane pumps, buffering molecules and the activity of the ion channels themselves, either in response to the electrical gradient (voltage sensing ion channels) or inter- and intra-cellular chemical messengers (ligand-gated ion channels). Voltage-gated calcium channels respond to neuronal membrane depolarisation by opening and allowing conductance of the calcium ions down the gradient of voltage across the membrane to activate various physiological functions (Hurley & Dexter, 2012). In addition to their normal physiological function, Ca²⁺ channels are also implicated in a number of neurological disorders such as neuropathic pain, epilepsy, Parkinson's disease, Alzheimer's disease and other neurodegenerative disorders (Snutch *et al.*, 2001; Solntseva *et al.*, 2007; Hurley & Dexter, 2012). Under these pathological conditions, there is elevation of intracellular calcium due to slower or longer-lasting increase of Ca²⁺ entry via VGCCs that results in calcium overload. The overload disrupts Ca²⁺ signalling, alters neuronal excitability and neurotransmitter release, and can cause cell death (Bailey *et al.*, 2013). This contributes to neuronal degeneration in many neurodegenerative disorders. Therefore, the blockage of VGCC is a desirable pharmaceutical property for neurodegenerative disorder therapy (Solntseva *et al.*, 2007).

2.4.2: Structure of VGCC

The neuronal VGCC are subdivided into four different types that include the L, N, P/Q and R (Triggle, 1999; Hurley & Dexter, 2012). These are high-voltage-activated channels that can be distinguished by their unique pharmacological, kinetic, and voltage-dependent gating characteristics (Triggle, 1999; Snutch, 2009). They are multi-subunit complexes (Christel & Lee, 2012) that comprised of a pore-forming α_1 subunit and auxiliary β , α_2 , γ , and δ subunits (Fontaine *et al.*, 1997; Arikath & Campbell, 2003; Wong *et al.*, 2006; Conte Camerino *et al.*, 2007; Morton *et al.*, 2013). Each subunit consists of amino and carboxyl termini (Buraei & Yang, 2013).

The entire complex appears to be roughly cylindrical, with dimensions of approximately 9 nm wide by 20 nm high (figure 2.10; Snutch, 2009).

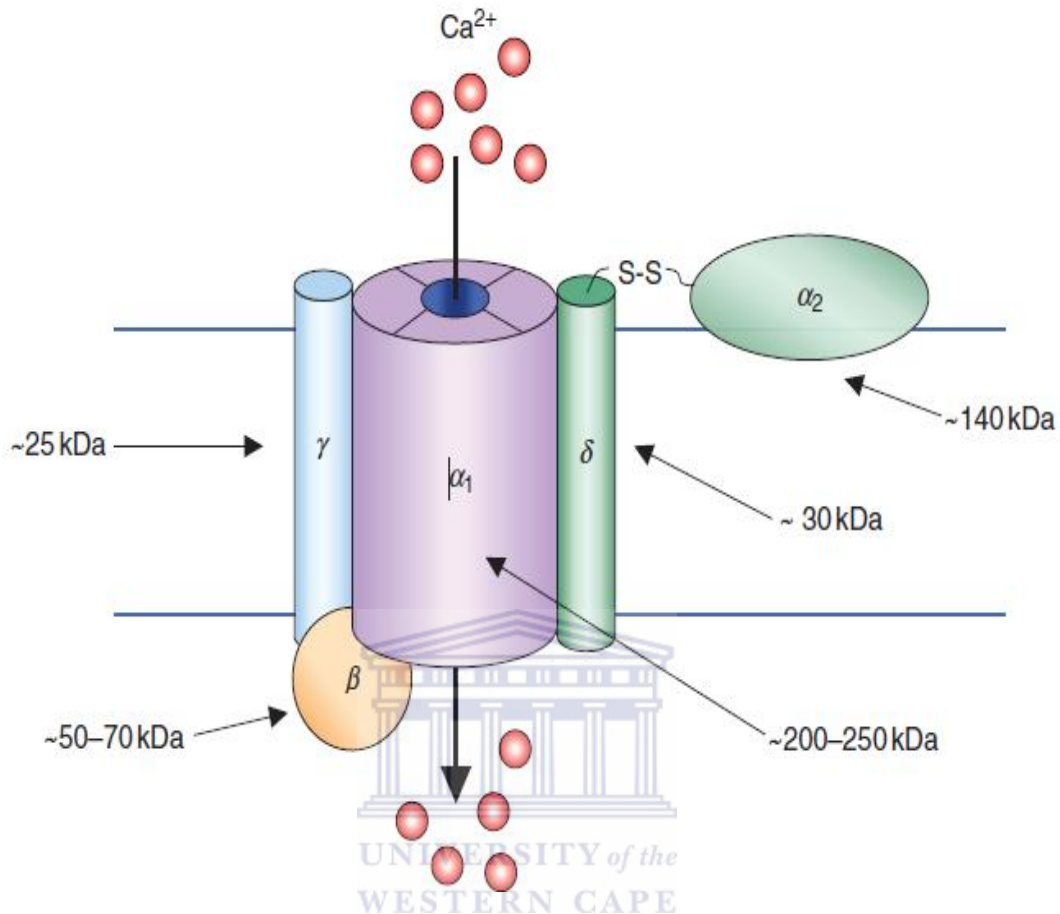


Figure 2.10: Subunit composition of VGCC complex (Snutch, 2009).

The α_1 subunit complexed with one or more auxiliary β determines the main gating and permeation properties (McDonough, 2007), whereas the other subunits modulate various properties of the α_1 subunits (Snutch *et al.*, 2001; Snutch, 2009). The pore-forming α_1 subunit is a single peptide chain consisting of a fourfold internal repeat; each repeat has six membrane-spanning domains (1-6) with substantial α -helical character. Primary sequence of the four internal repeats is homologous but non-identical (McDonough, 2007). The intracellular β subunit has α -helices but no transmembrane segments, while the γ subunit is a glycoprotein with four transmembrane segments. The cloned α_2 subunit has many glycosylation sites and several hydrophobic sequences, but biosynthesis studies indicate that it is an extracellular, extrinsic membrane protein, attached to the membrane through disulfide linkage to the δ subunit. The δ subunit is encoded by the tertiary end of the coding sequence of the same gene as the α_2 subunit, and the mature forms of these two

subunits are produced by posttranslational proteolytic processing and disulfide linkage (figure 2.11; Catterall, 2010).

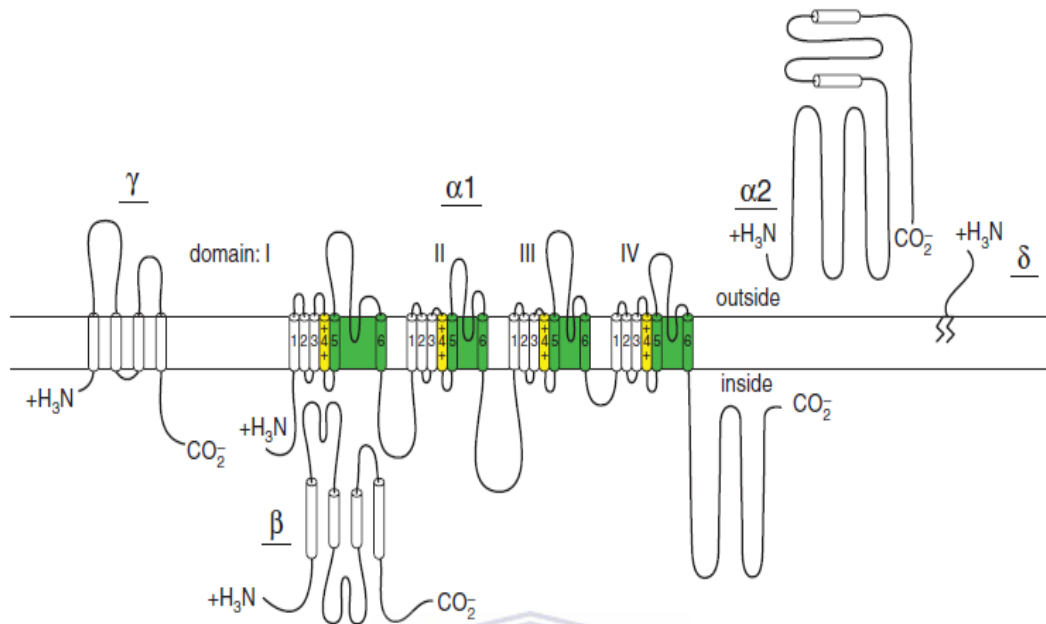


Figure 2.11: Subunit structure of Ca^{2+} channels.

The subunit composition and structure of Ca^{2+} channels purified from skeletal muscle are illustrated. The model is update description of the subunit structure of skeletal muscle Ca^{2+} channels. This model also fits most biochemical and molecular biological results for neuronal Ca^{2+} channels (Catterall, 2011).

2.4.3: Structure and functions of VGCC

VGCC expression is widespread throughout the brain, but each subtype has a unique distribution. The neuronal VGCC L-subtypes are found on cell bodies, proximal dendrites of projection neurons and some interneurons in cerebral cortex, hippocampus, cerebellum and spinal cord and they are responsible primarily for excitation-contraction coupling, synaptic plasticity and neurotransmitter release. The N, P/Q and R subtype are predominantly associated with presynaptic terminal, and they play a role in regulating neurotransmitter release. They are also present on the cell body and dendrites of neurons, where they regulate depolarisation (Hurley & Dexter, 2012).

The α_1 subunit contains the essential elements for ion permeation, gating, and pharmacology (He *et al.*, 2007). The α_1 subunit defines the calcium channel subtype and contains all the molecular machinery to produce a functional channel, such as p-loops that permit ion permeation and selectivity, voltage sensors that allow the channel to respond to membrane depolarisation, and intrinsic inactivation machinery

(Jarvis & Zamponi, 2007). It is a large hydrophobic protein with 24 transmembrane regions distributed over four domains and forms the voltage sensor and the pore of the channel to allow Ca^{2+} influx into the cell in a voltage-dependent manner (figure 2.11; Arikath *et al.*, 2002).

The α_2 and δ subunits, linked by disulphide bridges, form a single functional subunit ($\alpha_2\delta$) that enhances the activity of α_1 . A topological analysis support a model for the protein in which α_2 is entirely extracellular and δ has a single transmembrane region with a very short intracellular portion, which serves to anchor the protein in the plasma membrane. Although δ is the portion of the protein that is anchored in the membrane, it is α_2 that interacts with the α_1 subunit (figure 2.10). Of the four genetically distinct $\alpha_2\delta$ subunits ($\alpha_2\delta-1$ - $\alpha_2\delta-4$) described in the literature, only three subunits ($\alpha_2\delta-1$ - $\alpha_2\delta-3$) are expressed in the brain (Arikath & Campbell, 2003; Davies *et al.*, 2007). The co-expression of $\alpha_2\delta-1$ allows an enhancement in the membrane trafficking of α_1 , associated with an increase in the number of ligand binding sites. This subunit also causes an increase in current amplitude, faster activation and inactivation kinetics and a hyperpolarising shift in the voltage dependence of activation. The $\alpha_2\delta-2$ subunit only appears to increase the current amplitude. The co-expression of $\alpha_2\delta-3$ subunit with β subunit causes increase in current density, voltage dependent activation and steady state inactivation (Arikath & Campbell, 2003).

The β subunits are cytosolic proteins that switch its localisation from cytosolic to membrane-bound in the presence of α_1 subunits. Without the co-expression, α_1 subunits show little and no surface expression and produce very small or no currents. Besides enhancing channel surface expression, they regulate channel gating and enhance channel activation and inactivation. All β subunits facilitates channel opening by shifting the voltage dependence of channel activation by $\sim 10-15$ mV to more hyperpolarised voltages. This is reflected as an increase in the open probability at the single channel level, with β_{2a} producing the most dramatic increase in channel open probability. They also often speed channel activation. Calcium channel inactivation occurs in a voltage- and Ca^{2+} -dependent manner (VDI and CDI, respectively). This process is modulated by β subunits in three ways: (1) they shift the voltage dependence of inactivation to more hyperpolarised voltage $\sim 10-20$ mV, which enhances VDI and CDI. (2) Except for β_{2a} , they promote calcium channels' (N, P/Q

and R) 'closed state' inactivation. (3) They generally accelerate inactivation kinetics, but β_{2a} and β_{2e} , decelerate inactivation kinetics (Buraei & Yang, 2013).

The expression of γ subunits show wide tissue distribution, but the γ_1 subunit expression is restricted to skeletal muscle. The γ subunits in the brain produce effects that include inhibitory effect, activation/inactivation kinetics, trafficking of AMPA receptor and reduction of recurrent amplitude (Arikath & Campbell, 2003).

2.4.4: Neuronal VGCC inhibition

Activation of VGCC mediates calcium-dependent processes that play important roles in regulating various neuronal physiological functions (Takahashi & Ogura, 1983). However, disruption in calcium signalling as a result of pathological elevations of intracellular calcium concentration can occur and lead to the inappropriate activation of normally dormant (or low level) calcium-dependent processes, which in turn, result in metabolic disturbances and eventually neurodegeneration (Grobler *et al.*, 2006). The ideal drug targets should focus on reducing intracellular calcium ion from overload to normal physiological level. This prevents neuronal cell death caused by excitotoxicity. VGCC are such target, since they not only mediate calcium influx in response to membrane depolarisation, but are also crucial in the release of neurotransmitters like glutamate, an excitatory neurotransmitter (Varming *et al.*, 1996). Thus, agents that modulate voltage-gated calcium channels are of interest in the treatment of conditions associated with neurodegeneration. Such agents are mainly neuronal VGCC blockers that exhibit neuroprotective properties (Scott *et al.*, 2012). 2-amino-1-(2,5-dimethoxyphenyl)-5-Trifluoromethyl benzimidazole (NS-649) is a non-selective neuronal VGCC blocker that protects cultured neurons from degeneration caused by energy depletion. VGCC blockers such as ziconotide (Wang *et al.*, 2000; Snutch *et al.*, 2001), A-686085, A-1048400, NP118809, NP078585 (Zamponi *et al.*, 2009), TROX-1, Z123212 (Hildebrand *et al.*, 2011), and TTA-P2 (figure 2.12; Choe *et al.*, 2011) have been described to block neuronal VGCC without significant cardiovascular or CNS side-effects. These compounds have shown to effectively produce antinociceptive effect (Scott *et al.*, 2012). Although these antinociceptive agents have not been reported in the literature as neuroprotective agents, mechanism of action suggests the possibility of potential neuroprotective activities. Dihydropyridine and polycyclic cage compounds such as nimodipine and NGP1-01 have shown to reduce excitotoxicity by blocking VGCC. This offers protection to neuronal cells susceptible to calcium

overload. Amlodipine and azelnidipine, dihydropyridine derivatives, are VGCC blockers that prevent intracellular calcium accumulation and protect neuronal cells (Lukic-Panin *et al.*, 2007). This strongly suggests that drugs acting as antagonists, selective or non-selective, on voltage-gated calcium channels may function as neuroprotective agents in disorders associated with excitotoxicity (Lockman *et al.*, 2012).

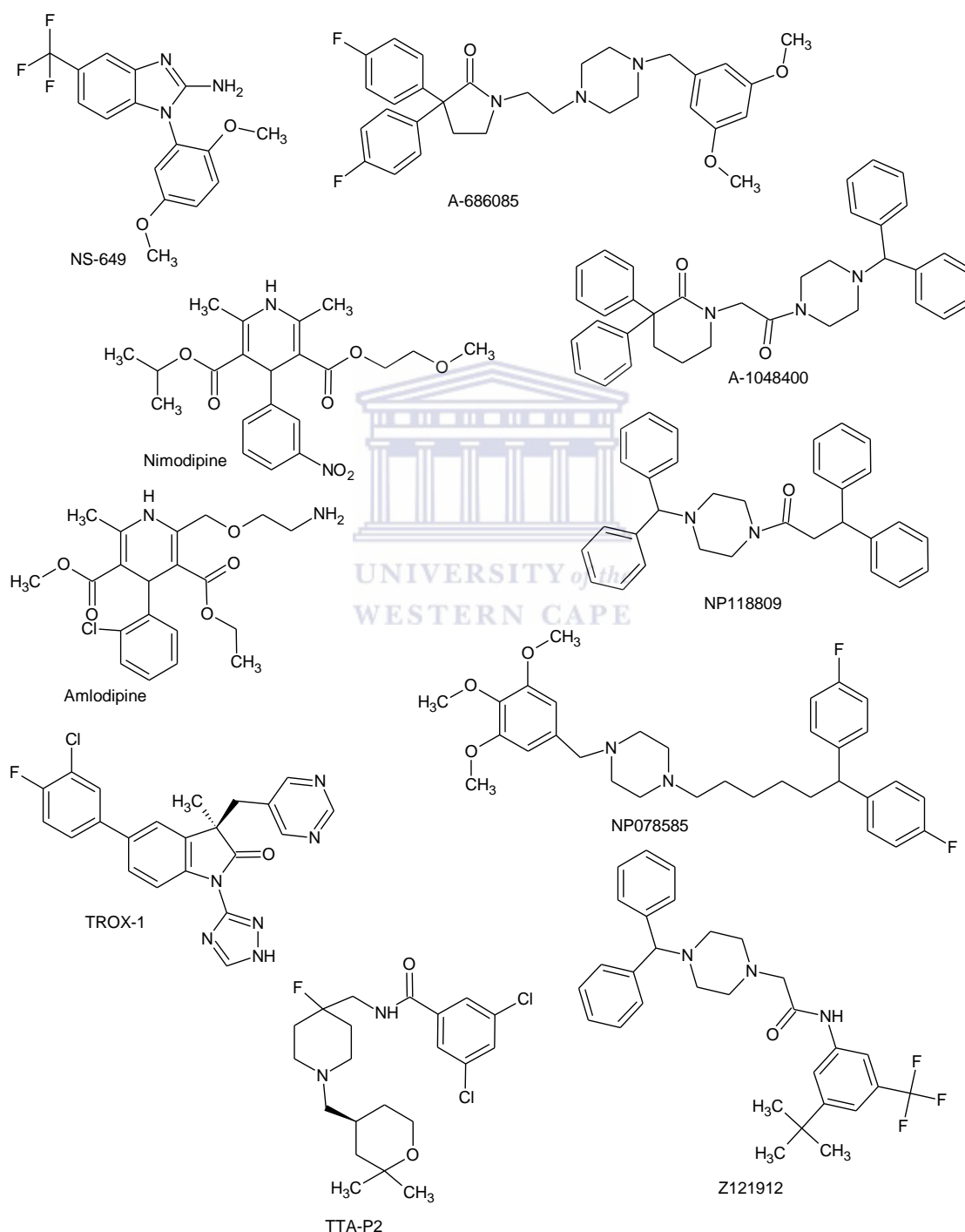


Figure 2.12: Chemical structures of voltage calcium channel blockers.

2.5: Polycyclic derivatives

2.5.1: Introduction

The polycyclic cage structure has been of interest to chemists for more than 50 years, but only recently has the medicinal possibilities of these cage compounds been explored (Geldenhuys *et al.*, 2009). They are an interesting and highly promising group of compounds that are receiving intense scrutiny as potential chemical scaffolds for the development of new drugs (Geldenhuys *et al.*, 2007). The uncompetitive NMDA receptor blockers, memantine and amantadine, are polycyclic cage-like compounds with established neuroprotective properties. Although the biological activities of these compounds were found serendipitously, it has led to considerable interest in the development and studies of several cage-like rigid polycyclic molecules. The structural peculiarities of these cage-like molecules may not only enable them to interact with biological receptors and/or trap smaller chemical species in their interior, but also minimise metabolic degradation (Ito *et al.*, 2007).

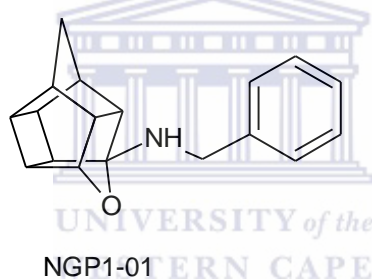


Figure 2.13: Chemical structure of NGP1-01.

Pentacycloundecane derivatives such as pentacycloundecylamine (NGP1-01; figure 2.13), a polycyclic amine, is one of the cage-like rigid polycyclic molecules that exhibit *L*-type voltage-gated calcium channel (VGCC) block (Geldenhuys *et al.*, 2004; Joubert *et al.*, 2011) and potent uncompetitive NMDA receptor channel inhibition (Hao *et al.*, 2008). It is also referred to as a multifunctional ion-channel blocker (Mdzinarishvili *et al.*, 2005; Van Der Schyf & Geldenhuys, 2009). These dual inhibitions attenuate the calcium entry pathway, thus preventing neuronal damage (Mdzinarishvili *et al.*, 2005; Youdim, 2010). In an experiment performed by Van Der Schyf and Geldenhuys on a mouse brain, it was proven that NGP1-01 is more potent when compared with memantine. In addition to its neuroprotection properties, it can cause PQ-interval prolongation and increased antioventricular conduction in the heart, therefore, may have use in treating heart arrhythmias (Van Der Schyf &

Geldenhuys, 2009). This compound also exhibits favourable distribution to the brain and therefore penetrates the blood-brain barrier readily (Prins *et al.*, 2009).

Biological activity are attributed to the pentacycloundecylamines, thus suggesting possible neuroprotective abilities through modulation of voltage activated sodium, potassium and Ca^{2+} channels, as well as interaction with NMDA receptor operated channels. Studies evaluating the biological activity of these compounds indicate actions that include amongst others, neuroprotective activity, selectivity, and high affinity for the sigma receptor binding site (Grobler *et al.*, 2006).

Amine-triquinane derivatives, the product of thermal ring-opening of the pentacycloundecane cage skeleton and especially the benzylamine derivatives thereof has been suggested to interact with both the voltage-gated calcium channels and the NMDA receptor. This suggestion was based on their ability to completely suppress the action potential in guinea pig papillary muscle, and displace [^3H]-MK-801 with an IC_{50} value of 1.9 μM when a series of amine-triquinane derivatives were screened against [^3H]-MK-801 binding in murine synaptoneurosomes (Van Der Schyf & Geldenhuys, 2009).

2.5.2: Structure-activity relationship of polycyclic derivatives

The basic pharmacophoric requirement for NMDA receptor antagonists (PCP, MK-801 and polyamines) includes: a hydrophobic moiety which is the lipophilic area, an aromatic ring apparently required for high affinity to the receptor, and a basic nitrogen atom (protonated amine) that forms a hydrogen bond with the receptor (Leeson *et al.*, 1990; Kroemer *et al.*, 1998). Pentacycloundecylamines such as NGP1-01 possesses all of these characteristics. The structure-activity relationships for pentacycloundecylamine appear to be determined primarily by geometric factors or steric constraints, with a small influence of electronic effects (Geldenhuys *et al.*, 2007; Van Der Schyf & Geldenhuys, 2009).

Geldenhuys *et al.* (2007) pointed out in their study that the polycyclic cage amine seems to be the most important pharmacophoric element contained within the pentacycloundecane-amine structure required to interact with the NMDA receptor. The phenyl ring adds to the NMDA receptor interaction and thus increased antagonism. Substitution on the phenyl ring lowers its potency. It could be that the moiety is too bulky for the proposed 'phenyl pocket' with steric hindrance causing attenuated affinity and therefore reduced NMDA antagonism. However, this proposed steric interaction seems to be more tolerant toward substitution on the meta position

than the para position. The number of atoms between the amino and phenyl rings appears to play an important role in its activity. An increase in chain length from methyl to ethyl reduces NMDA receptor inhibition (Geldenhuys *et al.*, 2007) probably due to increased steric and electronic interaction. However, an increase in chain length increase calcium channel (*L*-type) inhibition probably due to a deeper immersion into the calcium channel that might result in a stronger interaction with the putative binding site (Joubert *et al.*, 2011). Electron donating methoxy moieties increase activity while electron withdrawing nitro moieties reduces the calcium channel inhibition (Geldenhuys *et al.*, 2004). The donation of electrons makes the phenyl ring more lipophilic and would increase affinity for an aromatic π - π or hydrophobic interaction. Increase in cage size diminishes activity but an improvement may occur if there is increase in hydrophobicity (Geldenhuys *et al.*, 2007).

2.5.3: Pentacycloundecylamine-NMDA receptor interaction

Interestingly, the binding of pentacycloundecylamines, such as NGP1-01, to the NMDA receptor is not to the PCP binding site. It was suggested that the phenyl ring undergoes a π - π type aromatic interaction with an aromatic amino acid located at the entrance of the NMDA receptor channel. Such an interaction would allow the molecules to be 'anchored' in such a way that the cage can descend into the channel lumen to a depth allowed by the 'spacer' between the nitrogen and the phenyl ring (Geldenhuys *et al.*, 2007; Joubert *et al.*, 2011).

2.5.4: Tricycloundecane derivatives

Tricyclo[6.2.1.0^{2,7}]-undeca-4,9-dien-3,6-dione is an intermediate compound formed during the synthesis of pentacycloundecane (Scheme 1.1). Although this structure and its derivatives have been extensively synthesised, its use in medicinal chemistry has not been explored in depth (Ito *et al.*, 2007). In this study, its derivatives with expected similar structure-activity relationships and NMDA receptor interaction as the pentacycloundecylamine, will be synthesized and evaluated for NMDA receptor and Ca²⁺ channel inhibition.

2.6: Conclusion

Neurodegenerative disorders are increasingly leading to morbidity and mortality in our society. The treatment of these disorders possesses perplexing challenges (Geldenhuys *et al.*, 2011) that not only lie in difficult diagnoses, but also in design and development of drugs which may halt the degeneration process (Emard *et al.*, 1995). Pathways to neurodegeneration are numerous and include amidst other;

extensive cascades of enzymatic events, cerebrovascular accidents, mutation in certain genes and excitotoxicity. Understanding these pathways has resulted in development of various compounds with potential neuroprotective activities. Although differences exist among these disorders, excitotoxicity is a common mechanism to all. Having highlighted the role of excitotoxicity, halting or reducing the degenerative process through blocking excitotoxicity would be a major breakthrough in the treatment of these disorders. Although numerous compounds have been developed, they have yet to reach clinical trials owing to their low safety profile. The vast majority of approved drugs for neurodegenerative disorders only offer symptomatic relieve to increase life expectancy of affected individual.

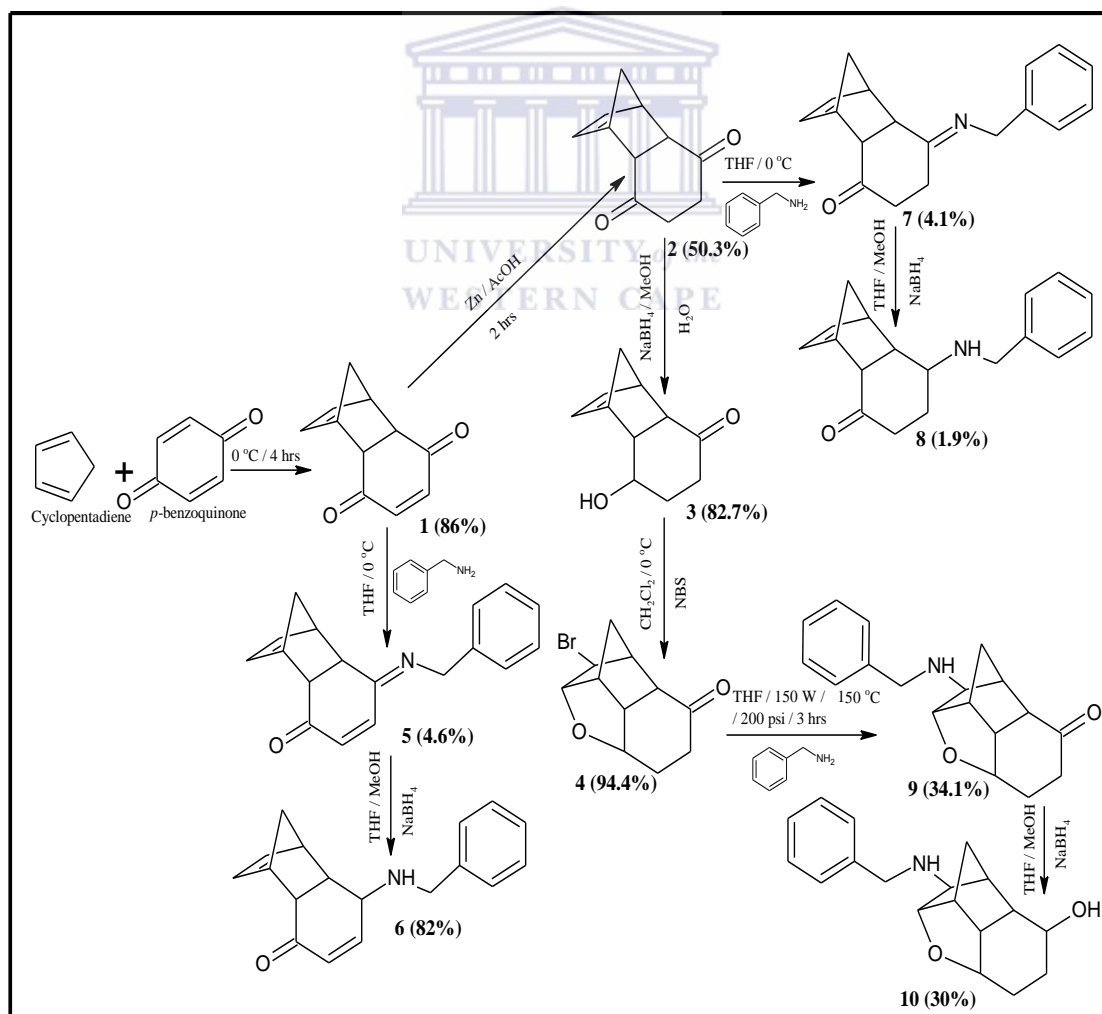


CHAPTER THREE

Synthesis

3.1: General

The synthesis of the proposed series of compounds evaluated for NMDA receptor and calcium channel inhibition involved several experimental procedures and methods. Cycloaddition reaction between *p*-benzoquinone and monomerised dicyclopentadiene yielded tricycloundeca-4,9-diene-3,6-dione (**1**) which was used as the lead structure for all further synthesis (**2-10**). This compound (**1**) was further derivatised to yield a comprehensive series of compounds (**1-10**; Scheme 3.1). The compounds were synthesised to evaluate the effect of the open cage (**1, 2, 3, 5, 6, 7, 8**) moiety, rearranged cage (**4, 9, 10**) moiety, C=C (**1** vs **2**) and C=O (**2** vs **3** and **9** vs **10**) bond reductions, and tertiary (**5, 7**) and secondary (**6, 8, 9, 10**) amines on biological activity.



Scheme 3.1: Synthetic route of tricycloundecane derivatives (**1-10**) and their respective yields.

3.2: Standard experimental procedures

3.2.1: Reagents and chemicals

Unless otherwise specified, reagents used in the synthesis were obtained from Merck (St Louis, MO, USA) and Sigma-Aldrich® (UK) and used without further purification. Solvents used for reactions and chromatography were purchased from various commercial sources and dried using standard methods.

3.2.2: Instrumentation

Infrared (IR) absorption spectrophotometer: Infrared spectra were obtained on a Perkin Elmer Spectrum 400 spectrometer, fitted with a diamond attenuated total reflectance (ATR) attachment.

Mass spectrometry (MS): Mass spectra were obtained on waters API Q-ToF Ultima mass spectrometer at 70 eV and 100 °C. All HR-ESI samples were introduced by a heated probe and perfluorokerosene was used as a reference standard.

Melting point (MP) determination: Melting points were determined using a Stuart SMP-300 melting point apparatus and capillary tubes. The melting points are uncorrected.

Nuclear magnetic resonance (NMR) spectroscopy: ¹H and ¹³C spectra were obtained at 200 MHz and 50 MHz respectively on a Varian Gemini 200 NMR spectrometer. Tetramethylsilane (TMS) was used as internal standard, with deuterated chloroform (CDCl₃) as solvent. All chemical shifts are reported in parts per million using the internal standard ($\delta = 0$) and the CDCl₃ peaks as reference. The following abbreviations are used to indicate the multiplicity of respective signals: s-singlet; bs-broad singlet; d-doublet; dd-doublet of doublets; t-triplet; and m-multiplet.

Microwave synthesis system: Microwave synthesis was performed using a CEM Discover™ focused closed vessel microwave synthesis system.

3.2.3: Chromatographic techniques

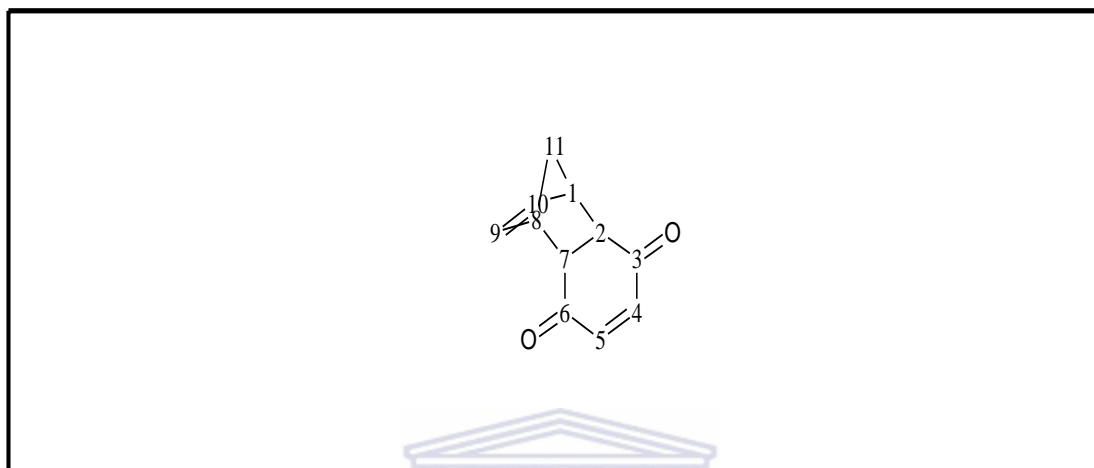
The mobile phases used for thin layer chromatography (TLC) and column chromatography were prepared on a volume-to-volume (v/v) basis using the prism model described by Nyiredy *et al.* (1985).

Thin layer chromatography (TLC): The progress of all chemical reactions was monitored using thin layer chromatographic methods which also aided the isolation processes. Visualisation of thin layer chromatography was achieved using UV light at 254 nm and 366 nm, iodine vapour and ninhydrin (1.5%).

Column chromatography: Separation and purification of mixtures were performed using a standard glass column that is 50 cm in length with an inner diameter of 2.5 cm. The stationary phase used was mesh 70-230 (63-200 μm) silica gel with mobile phases as indicated in section 3.3 for each compound.

3.3: Synthetic procedures

3.3.1: Tricyclo[6.2.1.0^{2,7}]undeca-4,9-diene-3,6-dione (1)



Synthetic method: To a solution of *p*-benzoquinone (10.0 g, 92.5 mmol) in 100 ml benzene, a mixture of 100 ml hexane:ethyl acetate (5:1) was added and cooled to 0 °C. Monomerised cyclopentadiene (12.24 g, 185.2 mmol), in stoichiometric quantities, was slowly added to the resulting mixture and stirred for 4 hours. The solvents were removed *in vacuo* rendering the crude product as yellow crystals which was further purified by recrystallisation using hexane as the solvent to form compound **1** as pure yellow crystals (yield: 14.0 g, 86%).

PHYSICAL DATA:

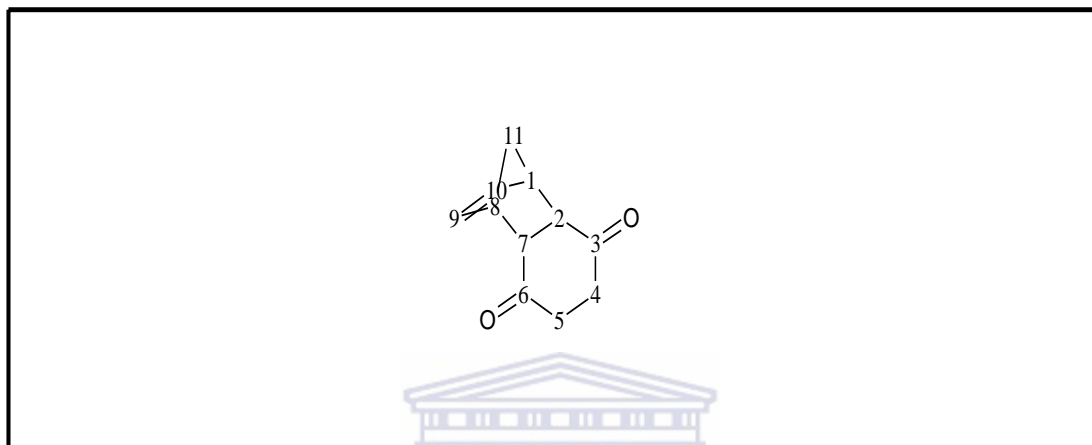
C₁₁H₁₀O₂; MW: 174.2 g/mol; **Mp.:** 69-73 °C, Literature: 71-75 °C (Ito *et al*, 2007); **IR (ATR; cm⁻¹):** 2987, 1660, 1604, 1281, 1055, 726 cm⁻¹; **¹³C-NMR (50 MHz, CDCl₃) δ (ppm):** 199.4 (C-3/6), 142.0 (C-4/5), 135.2 (C-9/10), 49.5 (C-2/7), 48.7 (C-11), 48.3 (C-1/8); **¹H-NMR (200 MHz, CDCl₃) δ (ppm):** 6.38 (d, *J* = 1.8 Hz, 2H, H-4/5), 5.86 (t, *J* = 3.6/1.8 Hz, 2H, H-9/10), 3.33-3.36 (m, 2H, H-1/8), 2.98-3.15 (m, 2H, H-2/7), 1.32-1.36 (AB-q, 2H, *J* = 8.8/5.2/1.8 Hz, H-11).

STRUCTURE ELUCIDATION:

In the infrared spectrum, the C=O bond was present as a sharp peak at 1660 cm⁻¹ while the C=C vibration was present at 1604 cm⁻¹. In the ¹H NMR spectrum, the doublet and triplet signals found downfield was assigned to H-4/5 (6.38 ppm) and H-9/10 (5.86 ppm) respectively and the AB-quartet of the bridge at C-11 (1.32-1.36

ppm) was identified to confirm the structure of **1**. The AB-quartet system has coupling constants of 1.8, 5.2 and 8.8 Hz. The ^{13}C NMR spectrum presented resonance of the C=O at 199.4 ppm and C=C at 135.2-142.0 ppm and were detected downfield while the saturated and unsaturated carbons were identified upfield (48.3-49.5 ppm). The physical data conformed to the literature and confirmed the formation of an *endo* adduct (Ito *et al.*, 2007; Salles *et al.*, 2012).

3.3.2: Tricyclo[6.2.1.0^{2,7}]undec-9-ene-3,6-dione (**2**)



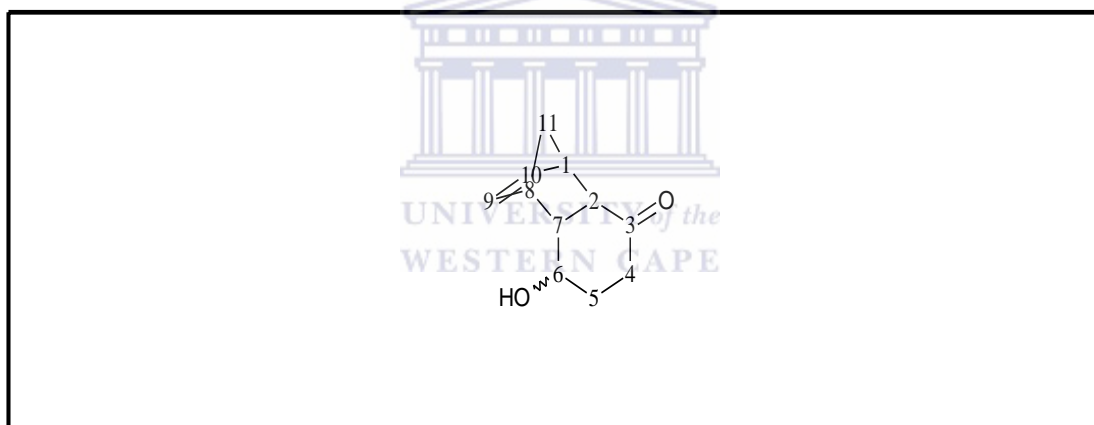
Synthetic method: Powdered zinc (6.00 g, 91.7 mmol) was added to a solution of compound **1** (4.0 g, 23.0 mmol) in 100 ml of glacial acetic acid. The resulting mixture was sonicated for 2 hours. After 2 hours, the mixture was filtered and the residue washed with CH_2Cl_2 (10 ml). The combined filtrates were added to brine (50 ml) and shaken vigorously. The layers were separated, and the aqueous layer was extracted with CH_2Cl_2 (2 x 50 ml). The combined organic layers were washed with water (50 ml), a saturated aqueous NaHCO_3 solution (100 ml) and again with water (50 ml). The organic layer was dried using anhydrous MgSO_4 , filtered and concentrated under reduced pressure. The yellow oil formed was purified by silica gel column chromatography using hexane:ethyl acetate (3:1) as the eluent rendering the pure product as a yellow oil (yield: 3.02 g, 50.3%).

PHYSICAL DATA:

$\text{C}_{11}\text{H}_{12}\text{O}_2$; MW: 176.2 g/mol; IR (ATR; cm^{-1}): 2973, 1660, 1254, 1155, 1055, 725 cm^{-1} ; ^{13}C -NMR (50 MHz, CDCl_3) δ (ppm): 209.6 (C-3/6), 136.6 (C-9/10), 51.8 (C-2/7), 48.7 (C-11), 47.4 (C-1/8), 37.9 (C-4/5); ^1H -NMR (200 MHz, CDCl_3) δ (ppm): 6.15 (t, $J = 3.4/1.6$ Hz, 2H, H-9/10), 3.43 (t, $J = 3.2/1.4$ Hz, 2H, H-1/8), 3.19 (m, 2H, H-2/7), 2.19-2.70 (m, 4H, H-4/5), 1.43-1.48 (AB-q, $J = 10.8/6.8/2$ Hz, 2H, H-11).

STRUCTURE ELUCIDATION:

The spectra of compound **2** is similar to compound **1** except for the selective reduction of C=C bond at C-4/5. Upfield shifts were identified in both the ^1H and ^{13}C NMR spectra. In the IR spectrum, the signal at 1604 cm^{-1} assigned to C=C, which was present in compound **1**, was absent in the spectra of compound **2**, confirming the reduction of C=C at C-4/5. In the ^1H NMR spectrum, the multiplet assigned to H-4/5 was present at 2.19-2.70 ppm, the triplet assigned to H-9/10 was identified downfield (6.15 ppm), and the AB-quartet system of the bridge was identified at 1.43-1.48 ppm. In the ^{13}C NMR spectrum, the spectrum was similar to compound **1** except for the ^{13}C for C-4/5 which had shifted more upfield (37.9 ppm). The C=O and C=C peaks were identified at 209.6 ppm and 136.6 ppm, respectively. The physical data conformed to the literature (Ito *et al.*, 2007; Salles *et al.*, 2012).

3.3.3: 6-hydroxytricyclo[6.2.1.0^{2,7}]undec-9-en-3-one (3)

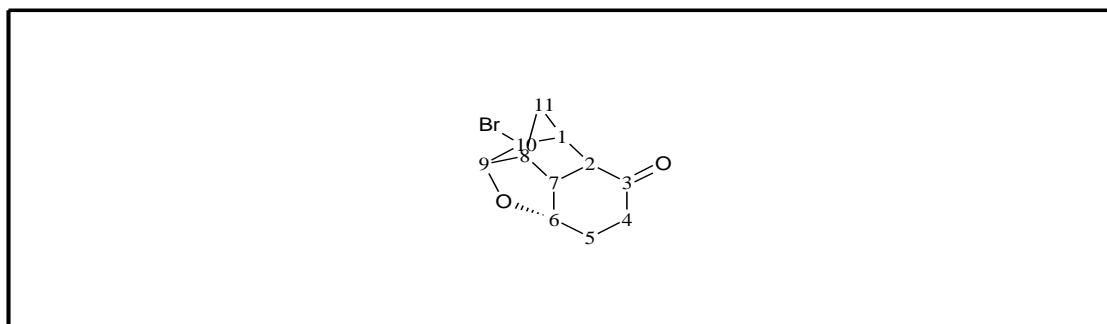
Synthetic method: A solution of compound **2** (0.61 g, 3.5 mmol) in a mixture of MeOH (12 ml) and H₂O (2 ml) was cooled to 0 °C using an external ice-water bath. NaBH₄ (0.045 g, 4.5 mmol) was added to the cooled mixture and allowed to warm to room temperature for 1 hour and then stirred continuously at room temperature for 2 hours. Glacial acetic acid (0.1 ml) was added, followed by the addition of ice-water (10 ml). The resulting mixture was extracted with CH₂Cl₂ (2 x 30 ml). The combined organic layers were washed with water (30 ml), dried over anhydrous MgSO₄, and filtered. The filtrate was concentrated under reduced pressure to afford the crude product as a yellow oil. The product was purified *via* silica gel column chromatography using hexane:ethyl acetate (3:2) as the eluent, yielding the desired compound as pale yellow oil (yield: 0.50 g, 82.7%)

PHYSICAL DATA:

C₁₁H₁₄O₂; MW: 178.2 g/mol; **IR (ATR; cm⁻¹):** 3404, 2937, 1686, 1331, 1033, 739 cm⁻¹; **¹³C-NMR (50 MHz, CDCl₃) δ (ppm):** 212.9 (C-3), 137.4 (C-10), 134.6 (C-9), 67.7 (C-6), 51.5 (C-2), 50.1 (C-11), 46.2 (C-1), 45.5 (C-7), 45.2 (C-8), 35.6 (C-4), 28.0 (C-5). **¹H-NMR (200 MHz, CDCl₃) δ (ppm):** 5.01 (d, *J* = 1.2 Hz, H-9), 4.13 (t, *J* = 7.0/3.4Hz, 1H, H-10), 3.11 (m, 1H, H-6), 2.89 (s, 1H, H-O), 2.62-2.76 (m, 2H, H-1/8), 1.99-2.19 (m, 2H, H-2/7), 1.58-1.71 (m, 4H, H-4/5), 1.11-1.29 (AB-q, *J* = 35.8/19/8.4/1.8 Hz, 2H, H-11).

STRUCTURE ELUCIDATION:

In confirming the structure of compound **3**, the hydroxyl group attached to C-6 was identified despite the distinct spectral similarities with compound **2**. The IR spectrum showed a broad peak present at 3404 cm⁻¹ which was identified as the OH functional group. A multiplet peak was observed at 3.11 ppm and a singlet at 2.89 ppm which were assigned as the peaks of H-6 and O-H respectively on the ¹H NMR spectrum. The doublet, with a coupling constant of 1.2 Hz, present downfield (5.01 ppm), was identified as the peak for H-9. The H-10 peak was identified downfield as a triplet (4.15-4.12 ppm) with coupling constants of 7.0 and 3.4 Hz. The AB-quartet system of the bridge was also identified downfield at 1.11-1.29 ppm. In the ¹³C NMR spectrum, the carbon of C-6 shifted to 67.7 ppm as expected as a result of the reduction. The peaks of C-3 (212.9 ppm), C-10 (137.4 ppm) and C-9 (134.6 ppm) were identified and assigned in the ¹³C NMR spectra. The presence of these peaks (C-3, C-9 and C-10) indicate that only the carbonyl moiety at C-6 was reduced while the double bond and carbonyl moiety of C-9/10 and C-3 respectively, were intact. The physical data of compound **3** conformed to the literature (Ito *et al.*, 2007; Salles *et al.*, 2012).

3.3.4: 2-bromine-3, 6-epoxytricyclo[6.2.1.0^{2,7}]undecan-9-one (4)

Synthetic method: To a solution of compound **3** (0.56 g, 3.16 mmol) in CH₂Cl₂ (20 ml) cooled to 0 °C *via* an external ice-water bath, *N*-bromosuccinimide (0.84 g, 4.74 mmol) was added and stirred for 2 hours. The resulting mixture was concentrated *in vacuo* and purified *via* silica gel column chromatography using hexane:ethyl acetate (1:4) as eluent, yielding the pure compound as a yellow powder (yield: 0.53 g, 94.4%).

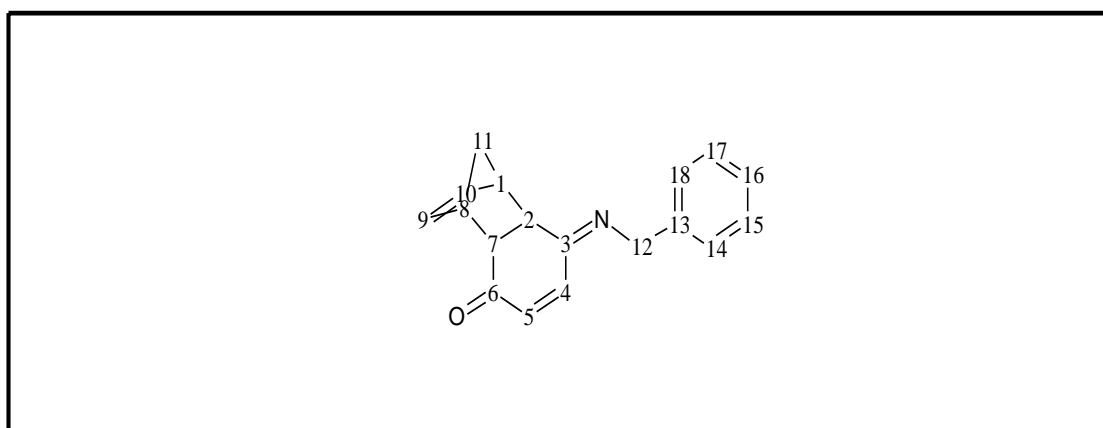
PHYSICAL DATA:

C₁₁H₁₃BrO₂; MW: 257.1 g/mol; Mp.: 72-75 °C; IR (ATR; cm⁻¹): 3681, 1695, 1411, 1033, 1184, 711 cm⁻¹; ¹³C-NMR (50 MHz, CDCl₃) δ (ppm): 203.7 (C-3), 87.5 (C-9), 75.1 (C-6), 54.8 (C-10), 48.7 (C-2), 48.5 (C-8), 47.8 (C-1), 45.1 (C-7), 42.5 (C-4), 38.4 (C-11), 34.8 (C-5). ¹H-NMR (200 MHz, CDCl₃) δ (ppm): 4.28-4.35 (m, *J* = 7.4/3.8 Hz, 2H, H-6/9), 4.02 (d, *J* = 3.2 Hz, 1H, H-10), 3.56 (m, 1H, H-2), 3.07-3.14 (dd, *J* = 10.2/4.4 Hz, 1H, H-8), 2.61-2.84 (m, 3H, H-1/4), 2.24-2.37 (m, 1H, H-7), 1.99-2.12 (m, 2H, H-5), 1.06-1.56 (m, 2H, H-11).

STRUCTURE ELUCIDATION:

Several characteristic functional moieties such as the epoxy between C-9 and C-6, the carbonyl at C-3 and the bromo functional group at C-10 were used to identify the structure. In the infrared spectrum, the carbonyl group is present at 1695 cm⁻¹, the bromo group present at 3681 cm⁻¹, and the epoxy group is present at 1184 cm⁻¹. The epoxy group connected to C-9 deshielded the carbon resulting in downfield shift on both the ¹³C (87.5 ppm) and ¹H (4.28 ppm) NMR spectra. The physical data conformed to the literature (Ito *et al.*, 2007; Salles *et al.*, 2012).

3.3.5: 3-(benzylimino)tricyclo[6.2.1.0^{2,7}]undeca-4,9-dien-6-one (5)



Synthetic method: Compound **1** (0.52 g, 3.0 mmol) was dissolved in tetrahydrofuran (THF, 10 ml). The mixture was cooled to 0 °C *via* an external ice-

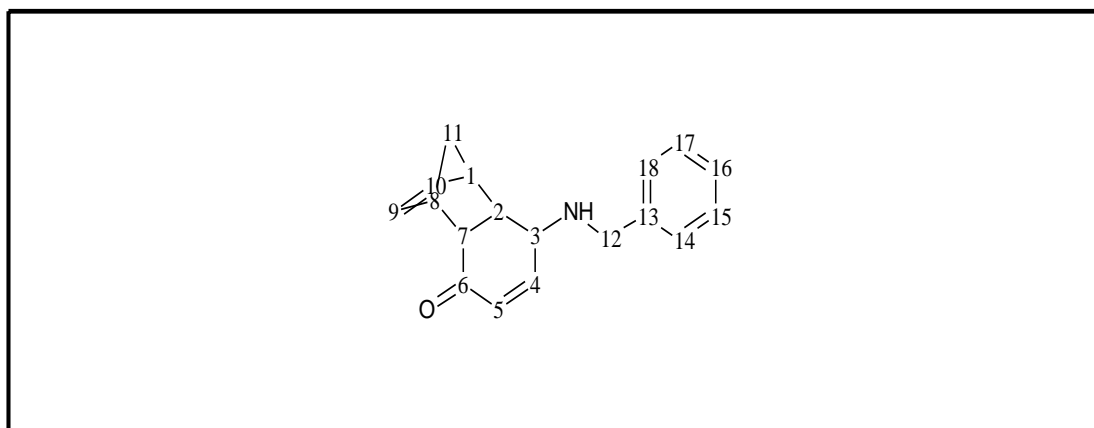
water bath while being stirred. To the cooled mixture, an equal molar amount of benzylamine (0.32 g, 0.33 ml) was added drop-wise over a period of 10 min. The mixture was stirred for 1 hour and the concentrated *in vacuo* to afford a dark oil. The oil was dissolved in dry benzene and placed under Dean-Stark conditions for 4 hours. The benzene was evaporated *in vacuo* and the product purified *via* silica gel column chromatography using dichloromethane:ethyl acetate:hexane (1:1:1) as eluent, yielding the desired compound as white crystals (yield: 36 mg, 4.6%).

PHYSICAL DATA:

C₁₈H₁₇NO; MW: 263.3 g/mol; Mp.: 115-118 °C; IR (ATR; cm⁻¹): 3242, 1677, 1580, 1247, 1033, 722 cm⁻¹; HR-ESI ([M+H]⁺, +O): Calcd. 280.1334, exp. 280.1383; ¹³C-NMR (50 MHz, CDCl₃) δ (ppm): 196.7 (C-6), 149.8 (C-3), 136.1 (C-13), 135.8 (C-4/5), 133.7 (C-9/10), 128.9 (C-14/18), 128.0 (C-15/17), 127.5 (C-16), 107.1 (C-3), 49.4 (C-12), 48.9 (C-7), 48.1 (C-11), 46.6 (C-1/8), 30.9 (C-2). ¹H-NMR (200 MHz, CDCl₃) δ (ppm): 7.12-7.33 (m, 5H, H-14/15/16/17/18), 5.90-6.07 (m, 2H, H-9/10), 5.49 (d, *J* = 6.4 Hz, 1H, H-5), 4.11(d, *J* = 5.4 Hz, 1H, H-4), 3.45 (t, *J* = 3.6/1.8 Hz, 1H, H-7), 3.04-3.21 (m, 2H, H-1/8), 1.97-2.14 (m, 3H, H-2/12), 1.46-1.51 (AB-q, *J* = 8.8/5.2/1.8 Hz, 2H, H-11).

STRUCTURE ELUCIDATION:

Characteristic functional moieties such as the C=N bond, the C=C bond of C-9/10, the carbonyl group, the benzyl moiety and the bridge at C-11 were identified to confirm this novel open cage-like molecule. In the infrared spectrum, the C=O is present as a sharp peak at 1677 cm⁻¹, the C=N is observed at 1580 cm⁻¹, and the aromatic group is present at 3242 cm⁻¹. In the ¹H NMR spectrum, the AB-quartet system of the bridge at H-11 (1.46-1.51 ppm), the protons of the aromatic group (7.12-7.33 ppm), and the multiplet of H-9/10 (5.90-6.07 ppm) were evident. The ¹³C NMR spectrum revealed aromatic peaks (127.5-128.9 ppm) and the C=N (149.8 ppm) moiety were identified. The C=C bonds of C-9/10 (133.7 ppm), C-4/5 (135.8 ppm) were identified downfield. The molecular ion from the MS confirmed a mass of 280.1334 amu.

3.3.6: 3-(benzylamino)tricyclo[6.2.1.0^{2,7}]undeca-4,9-dien-6-one (6)

Synthetic method: Compound **5** (0.1 g, 0.38 mmol) was dissolved in a mixture of MeOH (12 ml) and THF (60 ml). To this solution, NaBH₄ (0.03 g, 0.76 mmol) was added and stirred for 36 hours at room temperature. The mixture was concentrated *in vacuo* and water (50 ml) was added. The mixture was extracted with CH₂Cl₂ (3 x 25 ml). The combined organic layers were washed with water (50 ml) and dried with MgSO₄. Evaporation of the organic solvents yielded the desired compound as a brown-yellow oil (yield: 82 mg, 82%).

PHYSICAL DATA:

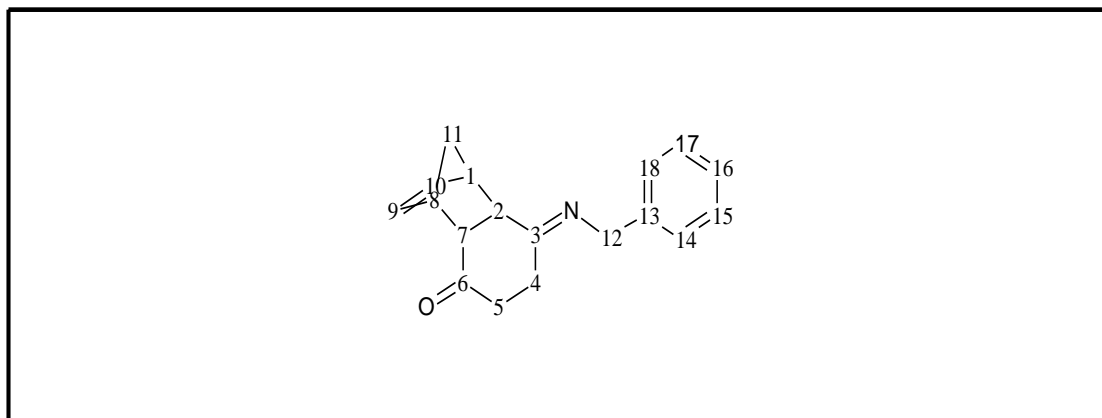
C₁₈H₁₉NO; MW: 265.3 g/mol; **IR (ATR; cm⁻¹):** 3243, 1677, 1581, 1496, 1246, 1033, 723 cm⁻¹; **HR-ESI ([M+H]⁺, +O):** Calcd. 282.1493, exp. 282.1539; **¹³C-NMR (50 MHz, CDCl₃) δ (ppm):** 207.2 (C-6), 164.1 (C-13), 137.1 (C-4), 136.4 (C-5), 133.1 (C-9/10), 128.7 (C-14/18), 127.8 (C-15/17), 127.5 (C-16), 66.0 (C-3), 49.8 (C-12), 48.6 (C-7), 46.7 (C-11), 45.5 (C-1/8), 30.9 (C-2). **¹H-NMR (200 MHz, CDCl₃) δ (ppm):** 7.22-7.29 (m, 5H, H-14/15/16/17/18), 5.74-6.15 (m, 2H, H-9/10), 5.27 (s, 1H, H-3), 4.85 (s, 1H, H-4), 4.17 (d, *J* = 8 Hz, 1H, H-5), 3.44 (d, 2H, H-12), 3.11 (s, 1H, H-8), 2.86 (t, *J* = 8.8/2.2 Hz, 2H, H-1/7), 2.10-2.23 (m, 2H, H-2 and H-N), 1.81-1.39 (m, 2H, H-11).

STRUCTURE ELUCIDATION:

Since there are structural similarities between compound **5** and **6**, it is expected that its spectra should be similar. The difference in the structures of **5** and **6** is the reduction of the imine in compound **5** to the amine in compound **6**. The amine bonds were used to identify this structure. In the infrared spectrum, the N-H is present at 1581 cm⁻¹. In the ¹H NMR spectrum, the aromatic protons (7.22-7.29 ppm), the proton of H-3 (5.27 ppm) and the proton of N-H bond (2.23 ppm) were evident. In the

^{13}C NMR spectrum, an upfield shift of C-3 (66.0 ppm) was evident. The molecular ion from the MS confirmed a mass of 282.1493 amu.

3.3.7: 3-(benzylimino)tricyclo[6.2.1.0^{2,7}]undec-9-en-6-one (7)



Synthetic method: Compound **2** (0.3 g, 1.7 mmol) was dissolved in THF (20 ml). The mixture was cooled to 0 °C with an external ice-water bath with stirring. To the cooled mixture, an equal molar amount of benzylamine was added drop-wise over a period of 10 min and it was stirred for 1 hour. The mixture was concentrated *in vacuo* to afford a brown oil. The oil was dissolved in dry benzene and placed under Dean-Stark conditions for 4 hours. The benzene was evaporated and the crude product was purified *via* silica gel column chromatography using dichloromethane:ethyl acetate:hexane (1:3:1) as eluent, yielding compound **7** as a brown oil (yield: 17 mg, 4.1%).

PHYSICAL DATA:

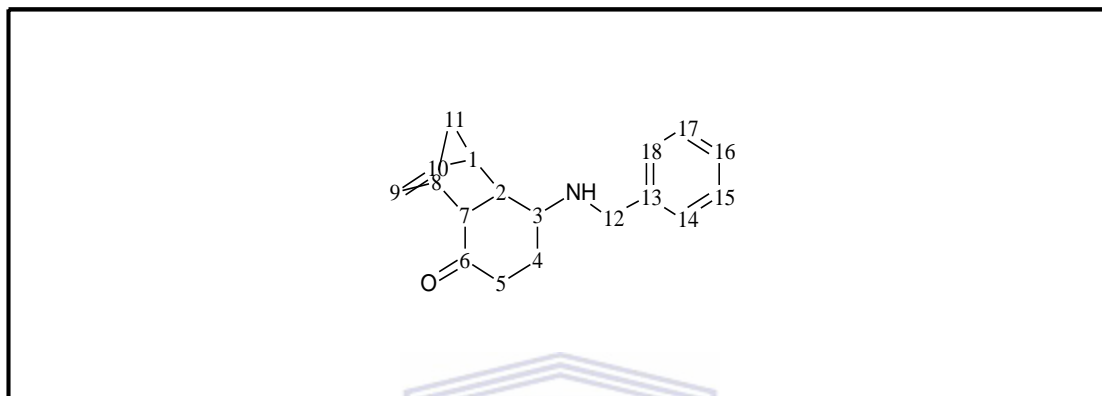
$\text{C}_{18}\text{H}_{19}\text{NO}$; MW: 265.3 g/mol; IR (ATR; cm^{-1}): 3243, 1667, 1580, 1246, 1033, 722 cm^{-1} ; HR-ESI ($[\text{M}+\text{H}]^+$, +O): Calcd. 282.1485, exp. 282.1539; ^{13}C -NMR (50 MHz, CDCl_3) δ (ppm): 206.9 (C-6), 142.4 (C-3), 137.7 (C-13), 135.8 (C-9/10), 128.8 (C-14/18), 128.2 (C-15/17), 127.7 (C-16), 50.0 (C-12), 49.4 (C-7), 48.1 (C-11), 46.7 (C-1/8), 30.8 (C-5), 28.8 (C-2), 21.2 (C-4). ^1H -NMR (200 MHz, CDCl_3) δ (ppm): 7.23-7.39 (m, 5H, H-14/15/16/17/18), 7.16 (d, $J = 0.8$ Hz, 1H, H-9), 6.94 (t, $J = 3.4/1.6$ Hz, 1H, H-10), 4.42 (d, $J = 3.4$ Hz, 2H, H-1/8), 4.09 (t, $J = 3.4/1.8$ Hz, 1H, H-7), 2.86-2.99 (m, 1H, H-2), 2.34-2.51 (m, 6H, H-4/5/12), 1.41-1.45 (AB-q, $J = 8/4.4/2.8/0.8$ Hz, 2H, H-11).

STRUCTURE ELUCIDATION:

Characteristic signals that were identified to confirm compound **7** included; the aromatic group, the C=N bond, and the carbonyl group at C-6. In the infrared

spectrum, the aromatic hydrogen is present at 3243 cm^{-1} , the C=N bond at 1580 cm^{-1} , and the carbonyl group (C=O) at 1677 cm^{-1} . In the ^1H NMR spectrum, the aromatic hydrogens (7.23-7.39 ppm) and AB-quartet system of the bridge at C-11 (1.41-1.45 ppm) were evident. In the ^{13}C NMR spectrum, the aromatic carbons (127.7-128.8 ppm) and carbonyl group (206.9 ppm) were identified. The molecular ion from the MS confirmed a mass of 282.1485 amu.

3.3.8: 3-(benzylamino)tricyclo[6.2.1.0^{2,7}]undec-9-en-6-one (8)



Synthetic method: Compound **7** (80 mg, 0.38 mmol) was dissolved in a mixture of MeOH (12 ml) and THF (60 ml). To the final solution, NaBH_4 (0.03 g, 0.76 mmol) was added and stirred for 36 hours at room temperature. The mixture was concentrated *in vacuo* and water (50 ml) was added. The mixture was extracted with CH_2Cl_2 (3 x 25 ml). The combined organic layers were sequentially washed with water (50 ml), aqueous NaHCO_3 solution (100 ml) and again with water (50 ml) and dried over MgSO_4 . The organic layer was evaporated, yielding the product as a brown oil (yield: 32 mg, 40%). The product was further purified *via* a silica gel preparative chromatography plate using dichloromethane:ethyl acetate:hexane (1:3:1) as eluent, yielding the final compound as a brown oil (yield: 1.52 mg, 1.9%).

PHYSICAL DATA:

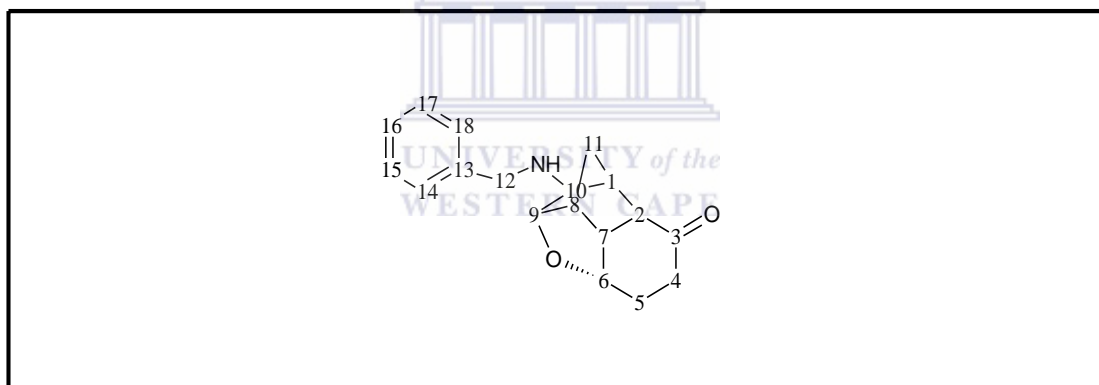
$\text{C}_{18}\text{H}_{21}\text{NO}$; MW: 267.4 g/mol; ^{13}C -NMR (50 MHz, CDCl_3) δ (ppm): 207.2 (C-6), 136.0 (C-13), 135.2 (C-9/10), 128.9 (C-14/18), 128.1 (C-15/17), 127.6 (C-16), 59.5 (C-3), 51.9 (C-12), 49.8 (C-7), 47.3 (C-11), 46.1 (C-1/8), 39.0 (C-5), 30.9 (C-2), 22.8 (C-4). ^1H -NMR (200 MHz, CDCl_3) δ (ppm): 7.22 (t, $J = 10.4/7.2$ Hz, 5H, H-14/15/16/17/18), 6.10 (s, 2H, H-9/10), 3.99-4.29 (m, 2H, H-12), 3.79 (m, 1H, H-8), 3.72 (m, 1H, H-3) 3.44 (s, 1H, H-1), 3.09-3.23 (m, 1H, H-7), 2.86-2.99 (m, 2H, H-5), 1.81-2.44 (m, 4H, H-2/4 and N-H), 1.21-1.45 (AB-q, $J = 15/7.4$ Hz, 2H, H-11). The

NMR, MS and IR spectra of purified compound **8** are not available because of a very low yield.

STRUCTURE ELUCIDATION:

The NMR spectra outlined for compound **8** were those of the crude product. Further purification resulted in low yield and thus could not be elucidated using the MS and IR. Although impure, similarities exist between compound **7** and **8**. Characteristic peaks that were used to identify this structure include; the ^{13}C and ^1H at position 3, the N-H moiety, the aromatic hydrogens and the AB-quartet system of the bridge. On the ^1H NMR spectrum, the aromatic hydrogens (7.22-7.31 ppm) and AB-quartet system of the bridge at C-11 (1.21-1.45 ppm) were evident. The hydrogens of the N-H (1.81-2.44 ppm) and H-3 (3.72 ppm) were identified upfield and downfield, respectively. In the ^{13}C NMR spectrum, the aromatic carbons (127.6-128.9 ppm) and carbonyl group (207.2 ppm) were identified. Due to the reduction of C=N bond, there was a upfield shift (59.5 ppm) of C-3 in the ^{13}C NMR spectrum.

3.3.9: 10-(benzylamino)-6, 9-epoxytricyclo[6.2.1.0^{2,7}]undecan-3-one (**9**)



Synthetic method: To a solution of compound **4** (80 mg, 0.31 mmol) in THF (5 ml), benzylamine (34 mg, 0.31 mmol) was added. The mixture was placed in a microwave reactor and reacted at 150 W, 150 °C and 200 psi for 3 hours. The mixture was concentrated *in vacuo* and purified *via* silica gel column chromatography using dichloromethane:ethyl acetate:hexane (1:1:1) as eluent, yielding compound **9** as a brown oil (yield: 30 mg, 34.1%).

PHYSICAL DATA:

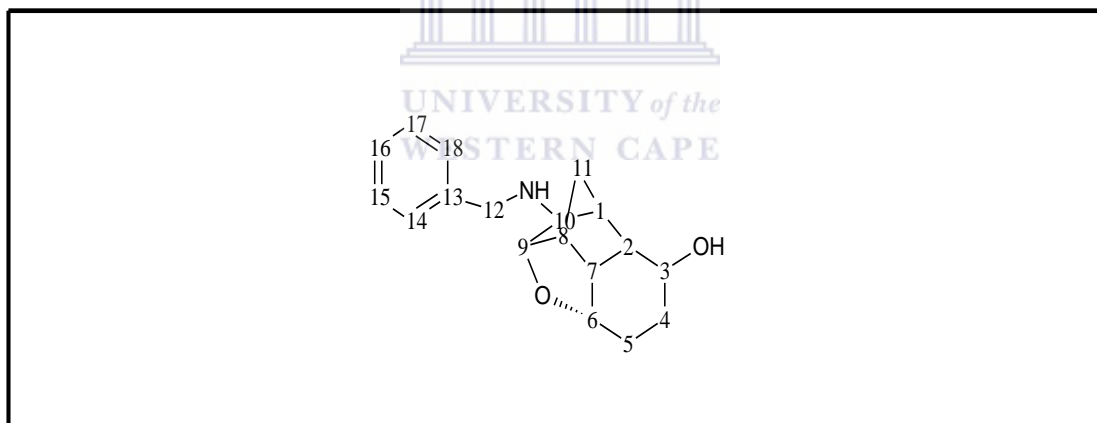
$\text{C}_{18}\text{H}_{21}\text{NO}_2$; MW: 283.4 g/mol; IR (ATR; cm^{-1}): 3366, 1691, 1405 1197, 1023, 684 cm^{-1} ; HR-ESI $[\text{M}+\text{H}]^+$: Calcd. 284.1646, exp. 284.1645; ^{13}C -NMR (50 MHz, CDCl_3) δ (ppm): 213.5 (C-3), 131.0 (C-13), 129.7 (C-14/18), 129.2 (C-15/17), 129.0 (C-16), 81.8 (C-6), 75.6 (C-9), 63.7 (C-8), 49.5 (C-7), 48.7 (C-12), 48.5 (C-2), 42.3

(C-10), 40.5 (C-4), 34.8 (C-1), 33.9 (C-5), 25.6 (C-11). $^1\text{H-NMR}$ (200 MHz, CDCl_3) δ (ppm): 7.15-7.30 (m, 5H, H-14/15/16/17/18), 4.01 (d, $J = 1.8$ Hz, 2H, H-12), 3.68 (s, 1H, H-6), 2.92 (d, $J = 5$ Hz 1H, H-9), 2.61 (m, 1H, H-10), 1.76-2.61 (m, 9H, H-1/2/4/5/7/8 and H-N), 1.21-1.45 (dt, $J = 14.0/8.8/4.0$, 2H, H-11).

STRUCTURE ELUCIDATION:

Several characteristic functional moieties such as the carbonyl group ($\text{C}=\text{O}$) at C-3, the epoxy group of C-6 and C-9, the N-H (amine bond), the bridge at C-11 and the aromatic group were used to identify this structure. On the infrared spectrum, the aromatic group is present at 3366 cm^{-1} , the $\text{C}=\text{O}$ at 1691 cm^{-1} , the N-H at 1196 cm^{-1} and the epoxy group at 1023 cm^{-1} . In the ^1H NMR spectrum, the double triplet (1.21-1.45 ppm) of the bridge at C-11, the aromatic hydrogens (7.15-7.30 ppm), the hydrogens of the epoxy group at C-6 (3.68 ppm) and C-9 (2.92 ppm) were evident. In the ^{13}C NMR spectrum, the $\text{C}=\text{O}$ (213.5 ppm) and the aromatic carbons (129.0-129.7 ppm) were identified. The molecular ion from the MS confirmed a mass of 284.1646 amu.

3.3.10: 10-(benzylamino)-6, 9-epoxytricyclo[6.2.1.0^{2,7}]undecan-3-ol (10)



Synthetic method: Compound **9** (100 mg, 0.3 mmol) was dissolved in a mixture of methanol (12 ml) and THF (60 ml). To the mixture, NaBH_4 (11 mg, 0.3 mmol) was added and stirred at room temperature for 1.5 days. The mixture was concentrated *in vacuo*, water (50 ml) was added and the solution was extracted with dichloromethane (3 x 25 ml). The combined organic layers were washed with water (50 ml) and dried with MgSO_4 . The organic layer was concentrated *in vacuo* and the product purified *via* a silica preparative chromatography plate using ethanol:ethyl acetate (1:2) as mobile phase. The product was obtained as a brown oil (yield: 30 mg, 30%).

PHYSICAL DATA:

$C_{18}H_{23}NO_2$; MW: 285.4 g/mol; IR (ATR; cm^{-1}): 3356, 1559, 1456, 1052, 700 cm^{-1} ; HR-ESI [M-H]⁺: Calcd. 284.1643, exp. 284.1645; ¹³C-NMR (50 MHz, CDCl₃) δ (ppm): 136.4 (C-13), 129.3 (C-14/18), 128.6 (C-15/17), 127.9 (C-16), 84.2 (C-6), 69.8 (C-9), 64.7 (C-3), 50.4 (C-8), 48.8 (C-7), 42.4 (C-12), 40.1 (C-10), 40.0 (C-2), 33.5 (C-1), 31.9 (C-11), 29.7 (C-5), 27.2 (C-4). ¹H-NMR (200 MHz, CDCl₃) δ (ppm): 7.48-7.59 (m, 5H, H-14/15/16/17/18), 4.07 (t, $J = 3.6/1.8$ Hz, 2H, H-12), 3.61 (s, 1H, H-O), 3.31 (s, 1H, H-3), 3.14 (s, 3H, H-6/9/10), 2.54 (d, $J = 1.6$ Hz, 1H, H-8), 2.18-2.31 (m, 1H, H-7) 1.99 (s, 2H, H-1/2), 1.85-1.92 (m, 4H, H-4/5), 1.47-1.61 (m, 2H, H-11).

STRUCTURE ELUCIDATION:

In confirming compound 10, the hydroxyl group at C-3 was identified. The C=O of compound 9 was reduced to produce the C-OH (compound 10). The infrared spectrum shows that the peaks for C=O is absent and the broad peak of C-OH is present at 3356 cm^{-1} . In the ¹H NMR spectrum, the aromatic hydrogens (7.48-7.59 ppm), the hydroxyl hydrogen (3.61 ppm) and the hydrogen at C-3 (3.31 ppm) were evident. In the ¹³C NMR spectrum, the aromatic carbons (127.9-129.3 ppm), the carbons attached to the epoxy group, and the carbon at C-3 (64.7 ppm) were identified. As expected, there was a shift to the right (upfield) in the NMR spectrum of compound 10. The molecular ion from the MS confirmed a mass of 284.1643 amu.

3.4: CONCLUSION

A total of 10 compounds were successfully synthesised. The structure and purity of all except compound 8 were confirmed with IR, MS and NMR analysis. The exception of compound 8 was due to low yield obtained during final purification. However, the NMR spectrum of the impure compound 8 was analysed for the purpose of identification. In future, a larger optimised synthetic procedure needs to be conducted in order to synthesise enough material for NMR, MS and IR analysis.

Of the 10 compounds synthesised, only compound 1 (86%), 3 (82.7%), 4 (94.4%) and 6 (82%) showed substantial yields. Low to moderate yields were observed with the remaining compounds (2, 5, 7, 8, 9, and 10). The low yields observed were due to the formation of by-products during synthesis and compound lost during purification. Optimisation of the various synthetic techniques developed in this study is required to produce final products with substantial yields.

The spectra from MS, IR and NMR were used to confirm these novel polycyclic cage-like molecules. However, spectra analyses were purely based on chemical shifts and literature assignment with the novel compounds (5-10) extrapolated from the existing compounds (1-4), thus additional NMR spectral analyses, including HSQC, HMBC, COSY, NOESY, DEPT and 2D experiments are required to adequately assign signals of synthesised compounds. Further analysis will include XRD to unequivocally confirm these novel structures.

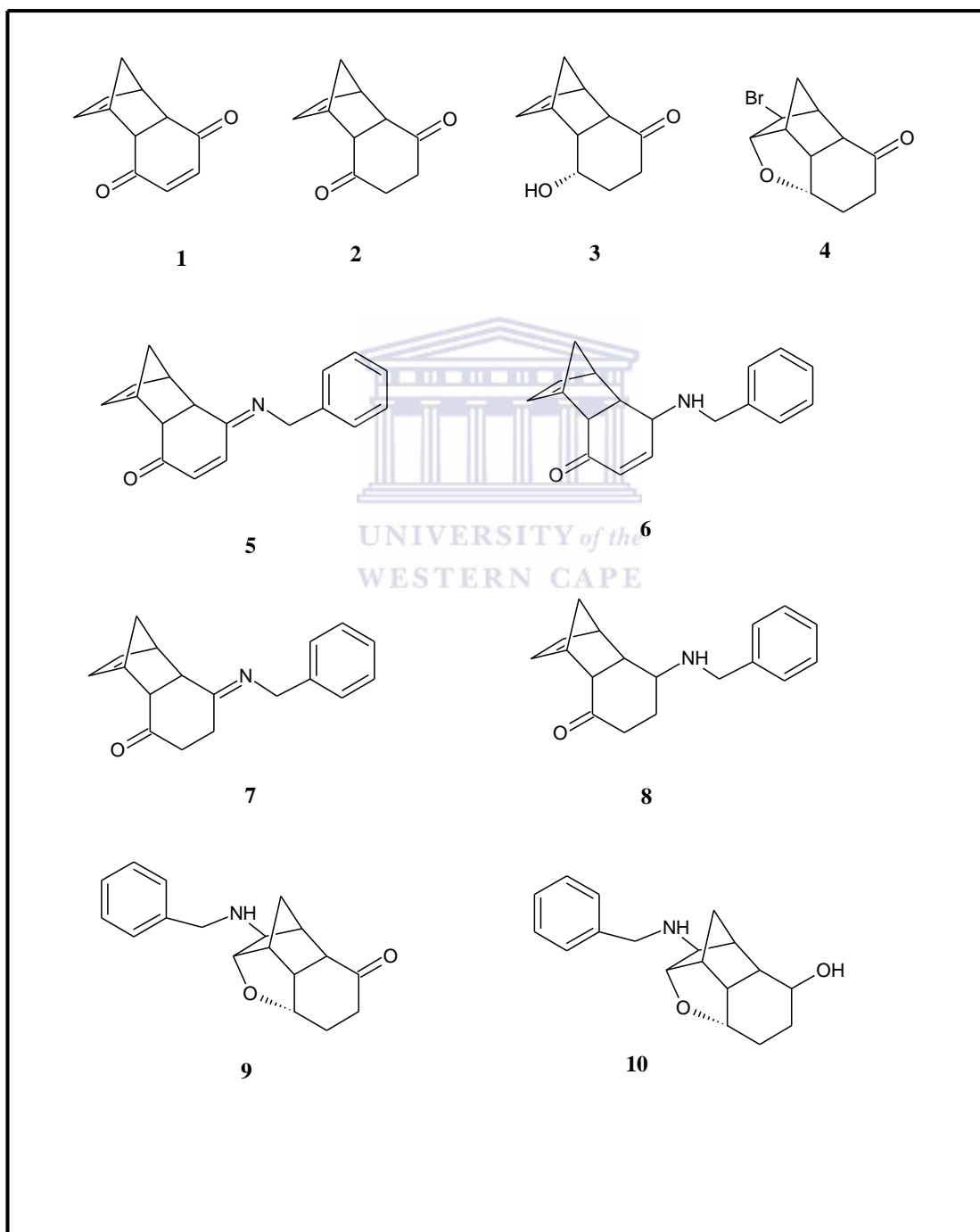


Figure 3.1: Successfully synthesised compounds for biological evaluation.

CHAPTER FOUR

Biological evaluation

4.1: Introduction

The evaluation of calcium flux through NMDA receptors and VGCC was conducted, utilising murine synaptoneurosomes. The test model was developed in our laboratory and is described in this chapter. This model uses the fluorescent ratiometric indicator, Fura-2 AM, and a Synergy™ Mx Monochromator-based fluorescent Microplate Reader (figure 4.1) with Gen 5™ data analysis software to measure relative changes in intracellular calcium levels after cell membrane depolarisation. This dual wavelength ratiometric approach detects excitation of calcium-bound and calcium-free concentrations at wavelength of 340 nm and 380 nm respectively, and emission at 510 nm. The ratio of fluorescent intensities, at the two excitations, enables the monitoring and quantification of intracellular calcium ions (Bozark *et al.*, 1990; Neher, 1995). This approach offers the advantage of internal calibration of calcium ions, and obviates the need for experimental correction for photobleaching, sample thickness variability and dye concentration (Gee *et al.*, 2000; Hu *et al.*, 2005; Kukkonen, 2009). Inevitable problems such as compartmentalisation, incomplete AM ester hydrolysis and extrusions may potential arise with the use of Fura-2 AM (Hu *et al.*, 2005). The treatment of the synthesised compounds (**1-10**) in the same manner as the control (DMSO only) and reference compounds, with known activities, is capable of producing results that indicates the relative change in calcium flux through the murine synaptoneuromes. Thus, the influence of the aforementioned problems on the results (NMDA receptor and VGCC assays) is negligible. With the described method, we envision that the potential mono-inhibition or dual inhibitions of the synthesised compounds on NMDA receptors and/or VGCC will be established. All results are expressed as percentage of the control.



Figure 4.1: Synergy™ Mx Monochromator-based fluorescent Microplate Reader.

4.2: Imaging experiment using Fura-2 AM

4.2.1: Materials

Chemicals used were of analytical grade or spectroscopy grade and were purchased from Sigma-Aldrich (UK) and Merck (St. Louis, MO, USA).

4.2.2: Animals

The study protocol employed was approved by University of the Western Cape Ethical Committee responsible for research on Experimental Animals (SRIRC 2012/06/13). The rats were sacrificed by decapitation and the brain tissue was removed and kept on ice for homogenisation. The homogenised brain tissue was used immediately.

4.2.3: Preparation of synaptoneuroosomes

Wistar rats were decapitated and the whole brain was removed after cerebral cortex dissection. The brain was homogenised in 20 ml ice-cold incubation buffer (118 mM NaCl; 4.7 mM KCl; 1.18 mM MgCl₂; 0.1 mM CaCl₂; 20 mM HEPES and 30.9 mM glucose. pH adjusted to 7.4) using a Teflon glass homogeniser (8 strokes by hand). To reduce proteolysis, the homogenate was kept on ice-cold water throughout the preparation. The tissue suspension was divided into two polycarbonate tubes and centrifuged at 1000 g (Labofuge 20 at 3300 rpm) for 5 minutes at 4 °C. The supernatant was decanted and redistributed in 2-ml aliquots, which were again centrifuged at 15000 g (Labofuge 20 at 12500 rpm) for 20 minutes. The supernatant was discarded and the pellet re-suspended in sufficient calcium-free buffer (118 mM NaCl; 4.7 mM KCl; 1.18 mM MgCl₂; 20 mM HEPES and 30.9 mM glucose. pH adjusted to 7.4) to obtain a 3 mg/ml protein concentration (protein yield is approximately 10 mg per 1 g of tissue).

4.2.4: General methods

Utilising the Synaptoneuroosomes isolated from murine brain tissue. Samples of the control (DMSO only) and the test compounds, at 100 µM, were prepared. The samples were screened using a Synergy™ Mx Monochromator-based fluorescent Microplate Reader (BioTek®, Germany) connected to Gen 5™ data analysis software. Analyses from these data were used to evaluate the influence of tested compounds on calcium flux. The methods used in preparation of murine synaptoneuroosomes and solution, and techniques, for experimental measurement of fluorescent intensities were similar to published studies (Stout & Reynolds, 1999; Geldenhuys *et al.*, 2007; Joubert *et al.*, 2011). All data analysis and calculations were performed using Prism

6.02[®] (GraphPad, Sorrento Valley, CA). Data in bar charts are expressed in % values of the control with each bar representing the mean \pm SEM. Statistical analysis was carried out using the Student Newman Keuls multiple range test. The level of significance was accepted at $p < 0.05$.

4.2.5: General procedure for loading Fura-2 AM and incubating test compounds

Experiments were carried out at 37 °C and the fluorescent intensities measured using a Synergy[™] Mx Monochromator-based Microplate Reader with Gen 5[™] analytical software. Fura-2 AM (1 mg/ml in DMSO) was added to the re-suspended tissue to make a final concentration of 5 μ M. The synaptoneurosomes were then incubated at 37 °C for 30 minutes. To prevent hydrolytic degradation of Fura-2 AM, the synaptoneurosomal-Fura-2 AM were protected from light. The incubated tissue was centrifuged at 7000 g for 5 minutes and the supernatant was discarded to remove all extracellular Fura-2 AM. The pellets were re-suspended in CaCl₂ containing buffer (118 mM NaCl; 4.7 mM KCl; 1.18 mM MgCl₂; 2 mM CaCl₂; 20 mM HEPES and 30.9 mM glucose, pH adjusted to 7.4) to obtain a final concentration of 0.6 mg/ml (protected from light). A 10 μ M stock solution of the test compounds were prepared. 2 μ l of the individual stock solutions were diluted with synaptoneurosomal-Fura-2 AM suspension (0.2 ml) in 96-well plates to give 100 μ M concentrations of the compounds. DMSO was used as the control to eliminate the possible influence of DMSO in the experiment.

4.2.6: NMDA/glycine-mediated NMDA receptor stimulation

The wavelengths selected for calcium-bound and calcium-free excitations were 340 nm and 380 nm respectively, and both emitted light as fluorescence at 510 nm. An automated fluorescent plate reader with the optics position set at the top and sensitivity set at 100 was used. The runtime was 5 minutes with 48 milliseconds intervals to obtain a total of 626 readings per run. The procedure was initiated and kept at 37 °C. At 10 seconds into the reading, 10 μ l (225 μ l/sec) of stimulation solution (0.1 mM NMDA; 0.1 mM glycine; 1.4 mM CaCl₂, pH adjusted to 7.4) was injected into each well plate, using an automated dispenser, to activate the NMDA receptor channels for the purpose of calcium influx. Calcium flux is determined by the fluorescence intensity produced through stimulation. An increase in fluorescence intensity after NMDA/glycine-induced stimulation represents 100% calcium influx as indicated by control (DMSO only). A decrease in fluorescent intensity, relative to the

control, with reference compounds and synthesised compounds indicate the inhibitory activity exhibited by test compounds. The difference in fluorescent intensity as a result of these inhibitions, after neuronal membrane depolarization, is expressed in percentage. The experiments were performed in triplicate using fresh synaptoneurosomes prepared on the same day. This was repeated three times.

4.2.7: KCl-mediated VGCC depolarisation

The wavelengths selected for calcium-bound and calcium-free excitations were 340 nm and 380 nm respectively, and both emitted light as fluorescence at 510 nm. An automated fluorescent plate reader with the optics position set at the top and sensitivity set at 100 was used. The runtime was 5 minutes with 48 milliseconds intervals to obtain a total of 626 readings per run. The procedure was initiated and kept at 37 °C. At 10 seconds into the reading, 10 µl (225 µl/sec) of KCl (140 mM) depolarisation solution (5.4 mM NaCl; 140 mM KCl; 10 mM NaHCO₃; 0.6 mM KH₂PO₄; 0.6 mM Na₂HPO₄·10H₂O; 0.9 mM MgSO₄; 1.4 mM CaCl₂; 20 mM HEPES and 5.5 mM glucose, pH adjusted to 7.4) was injected into each well plate, using an automated dispenser, to depolarise the voltage-gated calcium channels for the purpose of calcium influx activation. The KCl-induced increase in fluorescence intensity represents 100% calcium influx through depolarised membrane as indicated by the control (DMSO only). A decrease in fluorescent intensity, relative to the control, with reference and synthesised compounds indicate the inhibitory activity exhibited by test compounds. The difference in fluorescent intensity reflects the extent of inhibition, which is expressed in percentage. The experiments were performed in triplicate using fresh synaptoneurosomes prepared on the same day. This was repeated three times.

4.2.8: Statistical analysis

All data analysis, graphs and calculation were performed using the Prism 6.02[®] (GraphPad, Sorrento Valley, CA). Data in bar charts are expressed in % values of the control with each bar representing the mean ± SEM. Statistical analysis was carried out using the Student Newman Keuls multiple range test. The level of significance was accepted at $p < 0.05$. Bonferroni's multiple comparison, one way analysis of variance ANOVA was performed on selected data to indicate significant differences between test compounds ($p < 0.05$ was considered to be a statistically significant difference).

4.3: Results and discussion

4.3.1: NMDA receptor calcium flux inhibition

In this NMDA receptor inhibition study, the relative change in calcium flux, as indicated by change in fluorescence intensity, through synaptoneuromes after NMDA/glycine-induced receptor stimulation was used to evaluate the NMDA receptor inhibition of the reference compounds (memantine, MK-801 and NGP1-01) and tricycloundecane derivatives (**1-10**). The ratiometric fluorescent indicator, Fura-2 AM, was used to monitor these changes. The results, average inhibition of three experiments on different murine synaptoneurosomes (table 4.1), represent the inhibitory effects, at 100 μ M, and were relative to the control. The control (DMSO only) represented 100% calcium flux (figure 4.2). The reference compounds were MK-801, NGP1-01 and memantine.

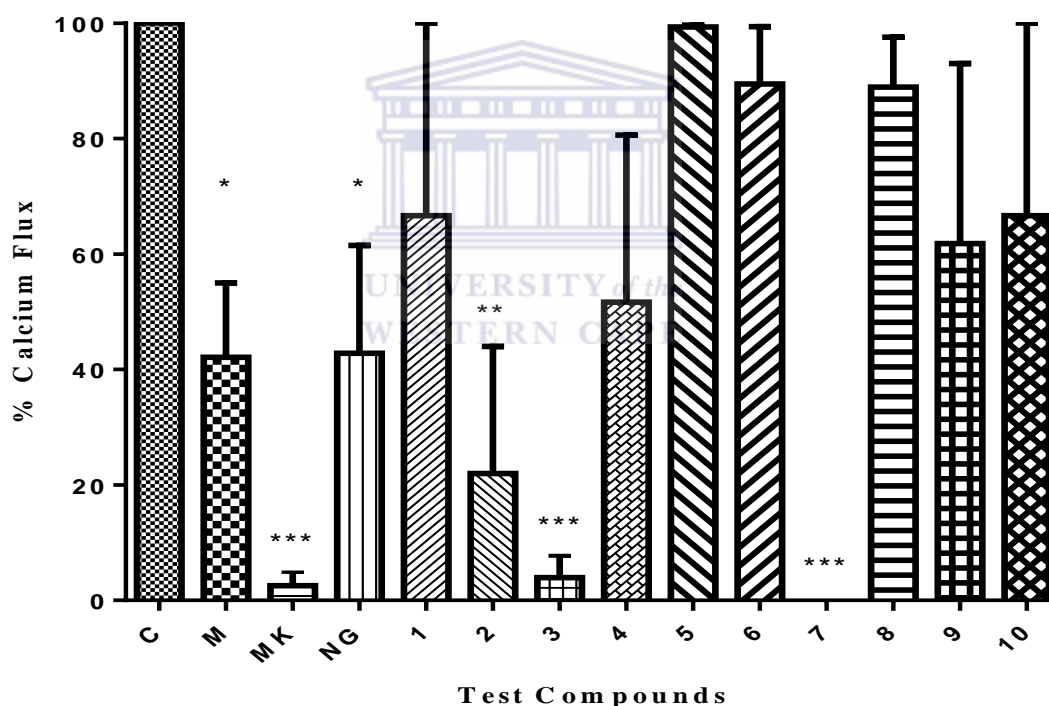
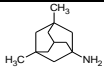
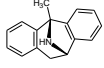
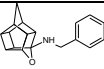
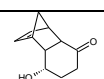
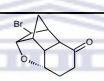
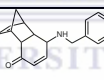
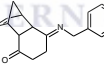


Figure 4.2: Screening of test compounds (100 μ M, n = 9) for inhibition of NMDA-mediated calcium flux in murine synaptoneurosomes. Each bar denotes mean percentage of control values \pm SEM. Abbreviations are: Control (C), memantine (M), MK-801 (MK) and NGP1-01 (NG). Statistical analysis was performed on raw data. The asterisks indicate significance of inhibitory effect of test compounds [(*) $p < 0.1$. (**) $p < 0.05$. (***) $p < 0.001$] when compared to the control (100%).

Table 4.1: Calcium influx inhibition (NMDA receptor) by tested compounds.

Compound	Structure	Calcium flux inhibition (100 μM) (%)
^ε Control		0
Memantine		57.90 [*]
MK-801		97.47 ^{***}
NGP1-01		57.20 [*]
1		33.33
2		78.00 ^{**}
3		96.07 ^{***}
4		48.33
5		0.33
6		10.53
7		100.00 ^{***}
8		11.10
9		38.20
10		33.33

^εControl = DMSO only **p* < 0.1 ***p* < 0.05 ****p* < 0.001

As anticipated, MK-801, NGP1-01 and memantine showed significant inhibitory activity (figure 4.1) of 97.47%, 57.20% and 57.90%, respectively. MK-801 is a known uncompetitive NMDA receptor antagonist with high affinity for the PCP binding site located within the channel (Black *et al.*, 1996). Antagonist such as MK-801 is trapped in the receptor channel and recovery for this trap-blocked state is generally slow thus producing a very long duration of action (Geldenhuys *et al.*, 2007). This accounts for the high inhibitory activity when compared to both memantine and NGP1-01, polycyclic cage molecules. Although memantine and

NGP1-01 are potent NMDA receptor blockers, affinities toward the receptor channel are considered low due to the faster rate of blocking (Hao *et al.*, 2008). The inhibitory effect of NGP1-01 was slightly less than memantine.

The synthesised compounds (**1-10**), evaluated at 100 μM , were subjected to the same treatment as the control (DMSO only) and the reference compounds. Of the 10 compounds, only compound **2**, **3** and **7** showed significant NMDA inhibitory activity ($p < 0.05$) of 78.00%, 96.07% and 100%, respectively when compared to the control (figure 4.2). The remaining compounds (**1**, **4**, **5**, **6**, **8**, **9** and **10**) showed weak to moderate NMDA inhibitory activity in the range between 0.33% and 48.33%.

Compound **1** (33.33%) showed moderate inhibitory activity at 100 μM . However, significant increase in NMDA receptor inhibition was observed with compound **2** (78.00%) and **3** (96.07%). The inhibitory activity of compound **2** exceeded that of the reference compounds, memantine and NGP1-01, while compound **3** showed inhibition similar to MK-801. The increased inhibitory activity of compound **2** compared to compound **1** suggests that the reduction of the C=C bond in the cyclohexene aromatic ring improved interaction with the NMDA receptor channel. It can be argued that the presence of the C=C bond offers rigidity to the open polycyclic cage (compound **1**; Ito *et al.*, 2007; Etkorn *et al.*, 2009) thus restricting movement that enable it to conform to the receptor pocket which would be required to effectively antagonise the NMDA receptor ion channel. Further reduction of one of the carbonyl moieties to a hydroxyl moiety (compound **3**) resulted in a significant increase in NMDA antagonism similar to MK-801. The increased activity can be attributed to improved hydrogen bonding interaction with the NMDA receptor pocket mediated by the hydroxyl group (Nagata *et al.*, 1995; Gitto *et al.*, 2014). However, a weaker inhibitory activity was observed with the more conformational restricted polycyclic cage molecule (compound **4**). The increased lipophilicity incurred and/or halo-substitution (Br) at position C-10 may also have contributed to the reduced inhibitory activity.

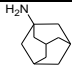
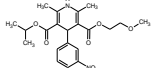
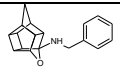
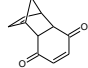
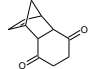
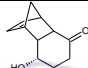
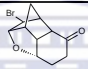
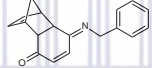
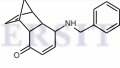
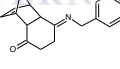
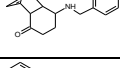
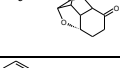
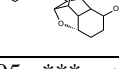
Of the novel tricycloundecyl amine and imine derivatives, only compound **7** (100%) showed significant NMDA inhibitory activity. The activity observed exceeded the reference compounds. However, the activity of compound **7** needs to be tested at lower concentrations to proof that its activity is in the same range as MK-801. This would eliminate false positive NMDA receptor inhibitory activity. It should be noted that compound **7** is a benzylimine derivative of compound **2**, therefore the

improved activity was expected as suggested by Geldenhuys *et al.* 2007. It is thus suggested that the benzyl ring improves the NMDA receptor interaction and therefore increases NMDA antagonism for this group of compounds. It can be argued that the benzyl ring undergoes a π - π type aromatic interaction with (an) aromatic acid(s) located at the entrance of the NMDA receptor channel. Such interaction would allow the molecule to be anchored in such a way that the cage can descend into the channel lumen and enable optimal NMDA inhibitory activity (Geldenhuys *et al.*, 2007). Unfortunately, the reduction of the C=N (compound **7**) bond to C-N (compound **8**) abolished the inhibitory activity and it is suggested that the drastic reduced activity observed with compound **8** was due to: (1) uncontrolled flexibility that is beyond acceptable NMDA receptor conformation, and (2) steric hindrance offered by the receptor channels. Compound **5** (0.33%), **6** (10.53%), **9** (38.20%) and **10** (33.33%) showed weak to moderate NMDA inhibition.

4.3.2: VGCC calcium flux inhibition

Tricycloundecane derivatives were evaluated for VGCC inhibition by measuring calcium influx into murine synaptoneurosome using the fluorescent technique as described. The ratiometric fluorescent indicator, Fura-2 AM, was used to monitor the change in intracellular calcium ion concentration after depolarisation of the VGCC with a high KCl (140 mM) concentration solution. The ratio of the calcium bound and unbound fluorescent intensities of test compounds, relative to a control (100% influx), gives an estimate of the degree of inhibition produced by the reference compounds and the synthesised (**1-10**) compounds. In this study, the reference compounds were nimodipine, amantadine and NGP1-01. Nimodipine is a commercially available dihydropyridine *l*-type calcium channel blocker used to treat vascular disorders. When compared to other calcium blockers, it passes the blood brain barrier more readily and binds specifically with high affinity to *l*-type calcium channels in the brain functionally antagonising steady state calcium load upon long or weak depolarization. Thus, nimodipine is a good candidate to evaluate the neuroprotection offered by VGCC antagonism (Marchetti & Usai, 1996; Bailey *et al.*, 2013). NGP1-01 and its derivatives have been shown to block VGCC and offer neuroprotection to neurons in the brain. Although amantadine and its derivatives have neuroprotective properties, they only inhibit NMDA receptors but not VGCC.

Table 4.2: Calcium influx inhibition (VGCC) by tested compounds.

Compound	Structure	Calcium flux inhibition (100 μ M) (%)
^e Control		0
Amantadine		2.57
Nimodipine		90.19 ^{***}
NGP1-01		25.63 ^{**}
1		11.97
2		0.67
3		3.50
4		3.00
5		1.90
6		34.03 [*]
7		38.07 ^{**}
8		6.67
9		14.33
10		40.33 [*]

^eControl = DMSO only * $p < 0.1$ ** $p < 0.05$ *** $p < 0.001$

The results in table 4.2 show the average inhibition of three experiments on different synaptoneurosomal preparations at 100 μ M. From the calcium flux data (figure 4.3), nimodipine showed very high VGCC inhibition indicated by little or no increase in fluorescence ratio after depolarisation. Nimodipine exhibited statistically significant VGCC inhibitory activity in synaptoneurosomes at a concentration of 100 μ M (90.19%) when compared to the KCl control treated synaptoneurosomes.

At the same concentration, compounds **6** (34.03%), **7** (38.07%), and **10** (40.33%) exhibited better VGCC inhibitions than NGP1-01 (25.63%) with significant

activity ($p < 0.05$) when compared to the control (DMSO). Compound **1**, **2**, **3**, **4**, **5**, **8** and **9** exhibited weak calcium antagonism between 1.90% and 14.33%. Although some of the synthesised compounds showed significant activity, none had inhibitory activity compared to nimodipine.

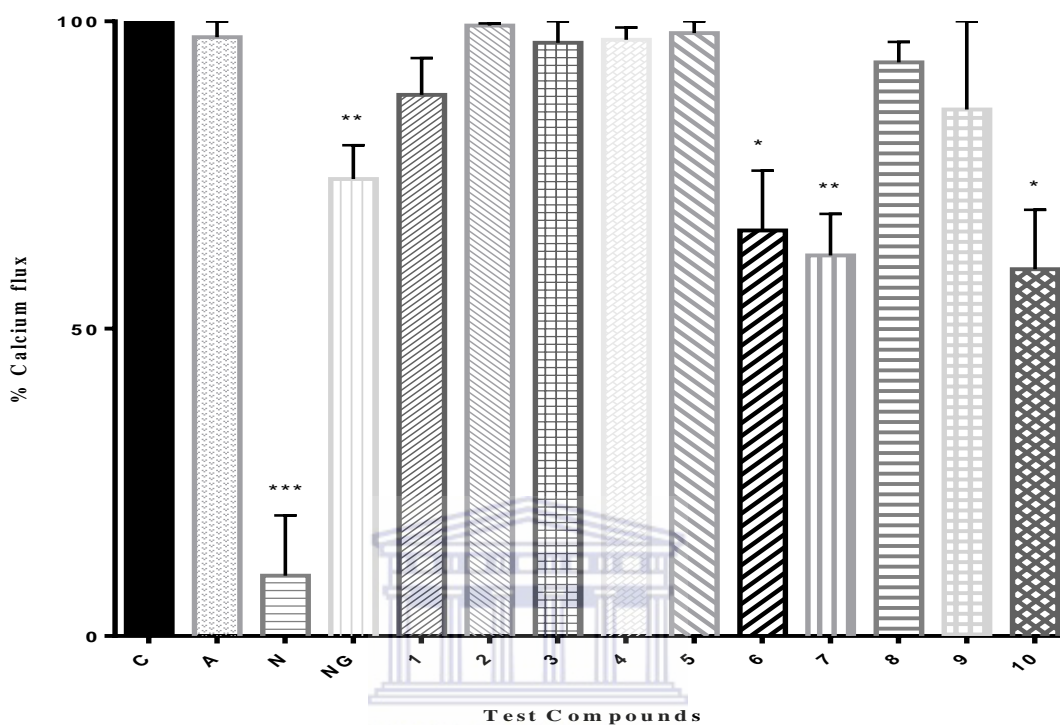


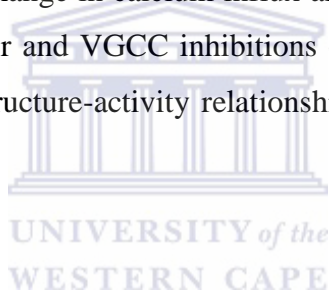
Figure 4.3: Screening of test compounds (100 μ M, $n = 9$) for inhibition of VGCC-mediated calcium flux in murine synaptoneuroosomes. Each bar denotes mean percentage of the control values \pm SEM. Abbreviations are: Control (C), amantadine (A), nimodipine (N) and NGP1-01 (NG). Statistical analysis was performed on raw data. The asterisks indicate significance of inhibitory effect of test compounds [(*) $p < 0.1$. (**) $p < 0.05$. (***) $p < 0.001$] when compared to the control (100%).

There was no or little activity observed with the basic polycyclic structures (**1-4**) while some of the novel polycyclic amine and imine compounds (**6**, **7** and **10**) showed significant VGCC inhibitory activity. This suggests the importance of benzylamine and benzylimine group for activity. Of the novel polycyclic amines evaluated, compound **6**, **7** and **10** showed improved activities when compared to NGP1-01, an established VGCC blockers with neuroprotective properties. An increased activity was observed when the carbonyl group of compound **9** was reduced to a hydroxyl group (**10**). It can be argued that the presence of the hydroxyl group provides better interaction with the binding sites of the voltage-gated calcium channels. The influence of the unsaturated (C=C and C=N) bonds were noticeable

from the comparison of compounds **5**, **6**, **7** and **8**. Compound **6** and **7** showed significant VGCC activity that exceeded the activity of NGP1-01. It can be argued that the reduction of one of the unsaturated bonds of compound **5**, as seen in compound **6**, offers flexibility to the structures and thus a better fit in the channel-binding site. The reduction of compound of the imine in **7** to the amine, as demonstrated in compound **8**, reduced VGCC activity. This is possibly due to a change in the orientation of compound **8** into a configuration unsuitable for VGCC activity.

4.4: Conclusion

The procedure developed to evaluate the synthesised compounds, with reference to literature, was able to indicate potential NMDA receptor and VGCC inhibitory activities for the test compounds when compared to known active reference standards. This procedure, using the fluorescent ratiometric calcium indicator, Fura-2 AM, monitored the relative change in calcium influx affected by the test compounds. The potential NMDA receptor and VGCC inhibitions of the synthesised compounds were established and their structure-activity relationships discussed using the newly developed method.



CHAPTER FIVE

Conclusion

5.1: General

The progression of neurodegenerative disorders are mediated by various degenerative processes. This has been the major challenge for the treatment thereof. The challenges lie not only in the multi-interrelated degenerative processes, but also the development of drug-like molecules that halt degenerative processes or facilitate neuronal regeneration. There is thus a need for neuroprotective agents with multifunctional activity with the potential to cure these disorders. Although several mechanisms have been proposed and structures designed, a standard mechanism for neuroprotection has not been established and no single agent has yet been successful in clinical trials. Of the known mechanisms, excitotoxic effects *via* disruption in calcium homeostasis on neuronal cells are prominent. The increase in intracellular calcium, or excessive accumulation thereof in neuronal cells, results in cellular dysfunction and subsequently neuronal cell death. Two major pathways, namely the VGCC and NMDA receptors, have been demonstrated in the literature to be responsible for this excessive calcium influx and ultimately excitotoxicity. The activation can either be direct or *via* coupled-protein activation. Targeting these pathways could be of therapeutic value in the design and development of molecular functionalities with dual- or multi-functional activities that attenuate the degenerative process. Although inhibiting these channels and receptors could prove valuable, it is important to maintain calcium-mediated physiological functions. With this in mind, we embarked on synthesising several open cages and rearranged polycyclic moieties structurally similar to NGP1-01, a known NMDA receptor and VGCC blocker, and evaluated their inhibitory potential on these channels.

5.2: Chemistry

Open polycyclic compounds (**1-8**) and endocyclic ether structures (**9-10**) with a number of distinct functionalities were successfully synthesised (figure 5.1). The lead molecule, an *endo* form of tricycloundeca-4,9-diene-3,6-dione (**1**), has high symmetry that allows for facile selective reactions at one or both carbonyl groups by means of classical and non-classical reagents (Ito *et al.*, 2007). The lead molecule was synthesised using the cycloaddition reaction described by Ito *et al.* (2007). This procedure yielded compound **1** as the *endo* isomer after recrystallisation from hexane

to produce pure yellow crystals (86%). In the presence of zinc and glacial acetic acid, the lead molecule was selectively reduced to yield **2** (50.3%). Compound **2** was further reduced with NaBH_4 at the carbonyl group present in position 3 and compound **3** was obtained in 82.7% yield. The treatment of **3** with *N*-bromosuccinimide resulted in a closed ring bromoether derivative (**4**) in substantial yield (94.4%). The structures of these compounds (**1**, **2**, **3** and **4**) were confirmed on the basis of their respective NMR and IR spectra and served as precursors for the novel tricycloundecane derivatives.

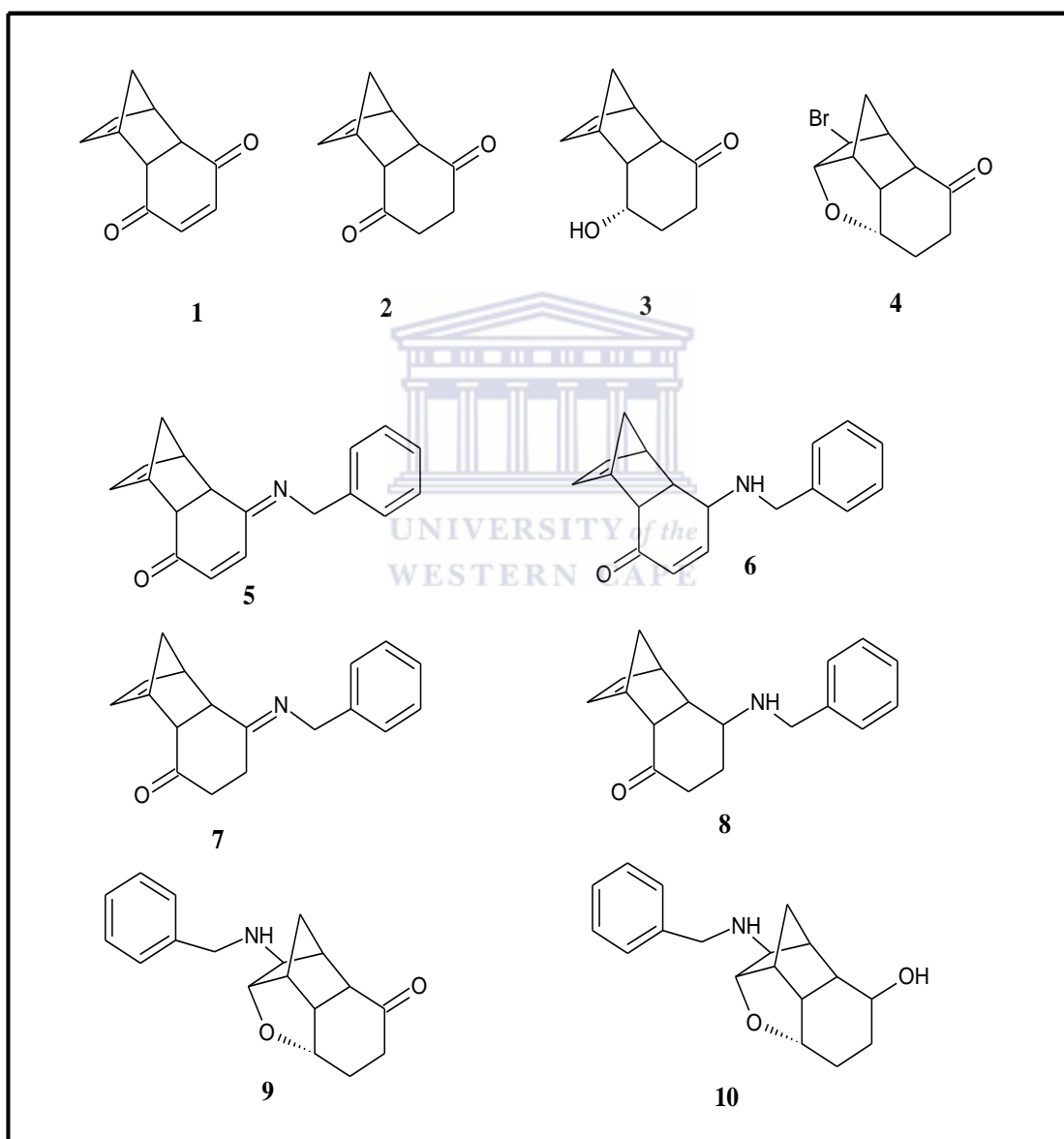


Figure 5.1: Structures of tricycloundecane derivatives (**1-10**).

Novel compounds (**5** and **7**) were obtained through amination of the precursors with an equal molar amount of benzylamine in THF. The selective protonation, at 0 °C, of one of the carbonyl groups (**1** and **2**) made the structures prone to nucleophilic

attack by the free electron pair on the nitrogen of the primary amine found in benzylamine. The nucleophilic attack resulted in the formation of carbinolamine intermediates which was dehydrated under Dean-Stark conditions to obtain the imines **5** (4.6%) and **7** (4.1%), respectively. The reduction of compound **5** and **7** using NaBH₄ as a reducing agent yielded compound **6** (82%) and **8** (1.9%), respectively. The formation of compound **9** (34.1%) required the use microwave irradiation at 150 °C, 150 W and 200 psi. Under these extreme conditions, the bromide group of compound **4**, as opposed to the carbonyl group, reacted with the primary amine on the benzylamine to yield the desired compound (**9**). This suggest that compound **4** might have a configuration that shielded the carbonyl group, thus minimising interaction at this site and facilitating S_N2 nucleophilic substitution at the bromide group. Compound **10** (30%) was obtained by the reduction of the carbonyl group of **9** using NaBH₄. The spectra from MS, IR and NMR were used to confirm these novel polycyclic cage-like molecules.

5.3: Biological activity

In this study, the NMDA receptor and VGCC inhibitory activities of the successfully synthesised polycyclic cage molecules were evaluated using a fluorescent ratiometric calcium indicating technique. In the NMDA/glycine-mediated calcium influx assay, significant inhibitory activities compared to NGP1-01 and memantine were recorded for compound **2** and **3**. Interestingly, the benzylimine derivative (**7**) of compound **2** demonstrated the highest inhibitory activity. Compound **7** showed inhibitory activity in the same range as MK-801, a known potent NMDA receptor antagonist. The NMDA receptor inhibitory activities of the remaining compounds (**1**, **4**, **5**, **6**, **8**, **9** and **10**) were in the low to moderate range. These activities suggested and supported the important role of hydrogen bond and hydrophobic interactions at the NMDA receptor site as reported in the literature (Leeson *et al.*, 1990; Kroemer *et al.*, 1998; Gitto *et al.*, 2014). It was also evident that structural modifications significantly influenced the activities of this group of compounds. A significant increase in activity was noted from compound **2** to **3** and the activity dramatically improved by formation of the benzylimine derivative (**7**). However, reduction of the imine to an amine abolished NMDA receptor inhibitory activity. In the KCl-mediated calcium influx assay which was used to demonstrate VGCC inhibitory activity, low activities were observed with compound **1**, **2**, **3**, **4**, **5**, **8** and **9**. Significant inhibitory activities were recorded for compound **6**, **7** and **10**. The increased activities exceeded that of NGP1-

01, but none matched the activity of nimodipine. The reduction of compound **9** to an alcohol derivative (**10**) resulted in a significant increase in VGCC inhibitory activity. The increased hydrophilicity of **10** appeared to offer better interaction with VGCC and enhanced inhibitory activity. Significant increase in VGCC inhibitory activities were also observed following the conversion of the benzylimine (**5**) to benzylamine (**6**). The formation of **6** offered less rigidity to the cage-like molecule and improved the activity thereof. The activity of **7** diminished after reduction to its amine (**8**).

This study confirms the possibility of VGCC inhibition (**6** and **10**), NMDA receptors inhibition (**2** and **3**) and dual-inhibition (**7**) for the respective compounds. Compound **6**, **7** and **10** were the novel tricycloundecane derivatives while structure **2** and **3** were previously described (Ito *et al.*, 2007) but their NMDA receptor and/or VGCC activities were not explored. Mono-inhibition (NMDA receptor or VGCC) or dual-inhibition (NMDA receptor and VGCC) have been proven to attenuate calcium influx through these major pathways. This offers protection to neuronal cells where death is caused by excessive calcium influx mediated by over-activation of NMDA receptor channels and VGCC. We have thus established that open and endocyclic ether containing polycyclic cage derivatives, structurally similar to NGP1-01 and MK-801, exhibit potential neuroprotective properties by inhibition of NMDA receptors and/or VGCC. These polycyclic cage-like molecules could be further explored or used as lead structures for the development of compounds that may be potential treatment options for neurodegenerative disorders mediated by excitotoxicity.

5.4: Conclusion and further recommendations

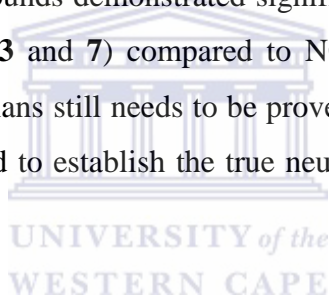
A series of tricycloundecane derivatives were successfully synthesised and their potential inhibitory activities on NMDA receptors and VGCC were demonstrated. The tricycloundecane derivatives (compound **2**, **3**, **6**, **7** and **10**) can thus be considered as potential neuroprotective agents, a notion supported by the results, and may serve as new lead polycyclic cages for the development of active pharmaceutical agents.

From the results obtained, it is recommended that a more comprehensive series be synthesised to increase our understanding of the structure-activity relationships and mechanism of interaction with the putative binding sites of this group of compounds. Further multifunctional neuroprotective activity of these compounds is also yet to be confirmed and future investigation on the sigma receptor

could provide valuable information to establish the potential of these compounds as neuroprotective agents with a broad-spectrum of activities for the treatment of neurodegenerative disorders. Blood-brain permeability studies, kinetic studies and cytotoxicity assays of these compounds are also recommended.

The biological assay described has demonstrated potential neuroprotective properties of the synthesised compound *via* NMDA receptor and VGCC antagonism thus it is a useful tool for preliminary calcium flux inhibitory screening of prospective lead structures. Albeit, it did not provide information about the true blocking actions, bindings, or affinities of the synthesised compounds to the receptors and channels. Electrophysiological studies are required to further elaborate on the mechanism of action of the tricycloundecane derivatives. Further development of these structures should also be conducted to elaborate on their true potential NMDA receptor and VGCC inhibitions and neuroprotective abilities.

Although these compounds demonstrated significant VGCC activity (**6**, **7** and **10**) and NMDA activity (**2**, **3** and **7**) compared to NGP1-01 and memantine, their clinical use and safety in humans still needs to be proven. Further *in vitro* and *in vivo* studies are thus recommended to establish the true neuroprotective potential of these polycyclic molecules.



References

- Aarts, M.M. & Tymianski, M. (2003)** Novel treatment of excitotoxicity: targeted disruption of intracellular signalling from glutamate receptors. *Biochemical Pharmacology*, **66**, 877-886.
- Abdel-Hamid, K.M. & Baimbridge, K.G. (1997)** The effects of artificial calcium buffers on calcium responses and glutamate-mediated excitotoxicity in cultured hippocampal neurons. *Neuroscience*, **81(3)**, 673-687.
- Arikkath, J., Felix, R., Ahern, C., Chen, C., Mori, Y., Song, I., Shin, H., Coronado, R. & Campbell, K. (2002)** Molecular characterisation of a two-domain form of the neuronal voltage-gated P/Q-type calcium channel $\alpha_{12.1}$ subunit. *FEBS Letters*, **532**, 300-308.
- Arikkath, J. & Campbell K. (2003)** Auxiliary subunits: essential components of the voltage calcium channel complex. *Current Opinion in Neurobiology*, **13**, 298-307.
- Artal-Sanz, M. & Tavernarakis, N. (2005)** Proteolytic mechanisms in necrotic cell death and neurodegeneration. *FEBS Letters*, **579**, 3287-3296.
- Bailey, J, Hutsell, B. & Newland, M. (2013)** Dietary nimodipine delays the onset of methylmercury neurotoxicity in mice. *Neurotoxicology*, **37**, 108-117.
- Bains, J. & Shaw, C. (1997)** Neurodegenerative disorders in humans: the role of glutathione in oxidative stress-mediated neuronal death. *Brain research reviews*, **25**, 335-358.
- Barber, S., Mead, R. & Shaw, P. (2006)** Oxidative stress in ALS: A mechanism of neurodegeneration and a therapeutic target. *Biochimica et Biophysica Acta*, **1762**, 1051-1067.
- Barlow, B.K., Cory-Slechta D.A., Richfield, E.K. & Thiruchelvam, M. (2007)** The gestational environment and Parkinson's disease: evidence for neurodevelopmental origins of a neurodegenerative disorders. *Reproductive Toxicology*, **23 (3)**, 457-470.

- Betzen, C., White, R., Zehendner, C., Pietrowski, E., Bender, B., Luhmann, H. & Kuhlmann, C. (2009)** Oxidative stress upregulates the NMDA receptor on cerebrovascular endothelium. *Free Radical Biology & Medicine*, **47**, 1212-1220.
- Bigge, C. (1999)** Ionotropic glutamate receptors. *Current Opinion in Chemical Biology*, **3**, 441-447.
- Black, M., Lanthorn, T., Small, D., Mealing, G., Lam, V. & Morley, P. (1996)** Study of potency, kinetics of block and toxicity of NMDA receptor antagonists using fura-2. *European Journal of Pharmacology*, **317**, 377-381.
- Block, M. & Hong, J. (2005)** Microglia and inflammation-mediated neurodegeneration: Multiple triggers with a common mechanism. *Progress in Neurobiology*, **76**, 77-98.
- Bonneau, B., Prudent, J., Popgeorgiev, N., Gillet, G. (2013)** Non-apoptotic roles of Bcl-2 family: The calcium connection. *Biochimica et Biophysica Acta*, **1833** (7), 1755-1765.
- Bordi, F. & Ugolini, A. (1999)** Group I metabotropic glutamate receptors: implications for brain diseases. *Progress in Neurobiology*, **59**, 55-79.
- Bozark, S., Kelly, R., Kramer, B., Matoba, Y., Marsh, J. & Reers, M. (1990)** In situ calibration of fura-2 and BCECF fluorescence in adult rat ventricular myocytes. *The American Journal of Physiological Society*, **259**, H973-H981.
- Buraei, Z. & Yang, J. (2013)** Structure and function of the β subunit of voltage-gated Ca^{2+} channels. *Biochimica et Biophysica Acta*, **1828**, 1530-1540.
- Calabrese, V., Scapagnini, G., Giuffrida Stella, A.M., Bates, T.E. & Clark, J.B. (2001)** Mitochondrial Involvement in Brain Function and Dysfunction: Relevance to Aging, Neurodegenerative Disorders and Longevity. *Neurochemical Research*, **26** (6), 739-764.
- Calon, F. & Cole, G. (2007)** Neuroprotective action of omega-3 polyunsaturated fatty acids against neurodegenerative diseases: Evidence from animal studies. *Prostaglandins, Leukotrienes and Essential Fatty acids*, **77**, 287-293.

Caraci, F., Battaglia, G., Sortino, Maria A., Spampinato, S., Molinaro, G., Copani, A., Nicoletti, F. & Bruno, V. (2012) Metabotropic glutamate receptors in neurodegeneration/neuroprotection: Still a hot topic? *Neurochemistry International*, **61** (4), 559-565.

Catterall, W. (2010) Voltage-gated calcium channels. **In Bradshaw, R. & Dennis, E. Ed. Chapter 112:** Handbook of cell signalling, Three-volume set, 2nd edition, Elsevier Inc., Washington, 897-909.

Catterall, W. (2011) Voltage-gated calcium channels. *Cold Spring Harbor Perspectives in Biology*, **3**, 1-23.

Celsi, F., Pizzo, P., Brini, M., Leo, S., Fotino, C., Pinton, P. & Rizzuto, R. (2009) Mitochondria, calcium and cell death: A deadly triad in neurodegeneration. *Biochimica et Biophysica Acta*, **1787**, 335-344.

Chen, B. & Roche, K. (2007) Regulation of NMDA receptors by phosphorylation. *Neuropharmacology*, **53**, 362-368.

Chen, H.S. & Lipton, S.A. (2006) The chemical biology of clinically tolerated NMDA receptor antagonists. *Journal of Neurochemistry*, **97** (6), 1611-1626.

Choe, W., Messinger, R., Leach, E., Eckle, V., Obradovic, A., Salajegheh, R., Jevtovic-Todorovic, V. & Todorovic, S. (2011) TTA-P2 is a potent and selective blocker of T-Type calcium channels in rat sensory neurons and a novel antinociceptive agent. *Molecular Pharmacology*, **80** (5), 900-910.

Choi, D., Koh, J. & Peters, S. (1988) Pharmacology of glutamate neurotoxicity in cortical cell culture: Attenuation by NMDA antagonist. *The Journal of Neuroscience*, **8** (1), 185-196.

Christel, C. & Lee, A. (2012) Ca²⁺-dependent modulation of voltage-gated Ca²⁺ channels. *Biochimica et Biophysica Acta*, **1820**, 1243-1252.

Chung, K.K.K. & David, K.K. (2010) Emerging roles of nitric oxide in neurodegeneration. *Nitric Oxide*, **22** (4), 290-295.

- Connor, B. & Dragunow, M. (1998)** The role of neuronal growth factors in neurodegenerative disorders of the human brain. *Brain Research Reviews*, **27**, 1-39.
- Conte Camerino, D., Tricarico, D. & Desaphy, J. (2007)** Ion channel pharmacology. *The Journal of the American Society for Experimental Neurotherapeutics*, **4**, 184-198.
- Cookson, R., Crundwell, E., Hill, R. & Hudec, J. (1964)** Photochemical cyclisation of Diels-Alder Adducts. *Journal of the Chemical Society*, 3062-3075.
- Costa, B.M., Irvine, M.W., Fang, G., Eaves, R.J., Mayo-Martin, M.B., Laube, B., Jane, D.E. & Monaghan, D.T. (2011)** Structure-activity relationships for allosteric NMDA receptor inhibitors based on 2-naphthoic acid. *Neuropharmacology*, **62**, 1730-1736.
- Crews, F.T., Steck, J.C., Chandler, J.L., Yu Jiang, C. & Day, A., (1998)** Ethanol, Stroke, Brain Damage, and Excitotoxicity. *Pharmacology Biochemistry and Behavior*, **59** (4), 981-991.
- Crouch, P.J., Harding, S.E., White, A.R., Camakaris, J., Bush, A.I. & Masters, C.L. (2008)** Mechanisms of $A\beta$ mediated neurodegeneration in Alzheimer's disease. *The International Journal of Biochemistry & Cell Biology*, **40**, 181-198.
- Cull-Candy, S.G., Brickley, S.G., Misra, C., Feldmeyer, D., Momiyama, A. & Farrant, M. (1998)** NMDA receptor diversity in the cerebellum: identification of subunits contributing to functional receptors. *Neuropharmacology*, **37**, 1369-1380.
- Davies, A., Hendrich, J., Tran Van Minh, A., Wratten, J., Douglas, L. & Dolphin, A. (2007)** Functional biology of the $\alpha 2\delta$ subunits of voltage-gated calcium channels. *Trends in Pharmacological Sciences*, **28** (5), 220-228.
- De Palma, C., Falcone, S., Panzeri, C., Radice, S., Bassi, M. & Clementi, E. (2008)** Endothelial nitric oxide synthase overexpression by neuronal cells in neurodegeneration: a link between inflammation and neuroprotection. *Journal of Neurochemistry*, **106**, 193-204.

- Diels, O. & Alder, K. (1928)** Synthesen in der hydroaromatischen reihe. Justus Liebigs Annalen der Chemie, **460 (1)**, 98-122.
- Di Liberto, V., Bonomo, A., Frinchi, M., Belluardo, N., & Mudò, G. (2010)** Group II metabotropic glutamate receptor activation by agonist ly379268 treatment increases the expression of brain derived neurotrophic factor in the mouse brain. Neuroscience, **165**, 863-873.
- Di Matteo, V., Pierucci, M., Di Giovanni, G. & Esposito, E. (2007)** Prevention and Therapy of Neurodegenerative Disorders: Role of Nutritional Antioxidants. In **Qureshi, Ali G., Parvez, Hassan S. ed.** Oxidative Stress and Neurodegenerative Disorders. Elsevier B.V, 621-661.
- Doble, A. (1999)** The Role of Excitotoxicity in Neurodegenerative Disease: Implications for Therapy. Pharmacology & Therapeutics, **81 (3)**, 163-221.
- Emard J., Thoueez, J. & Gauvreau, D. (1995)** Neurodegenerative diseases and risk factors: A literature review. Social Science & Medicine, **40 (6)**, 847-858.
- Eriksen, J.L., Zehr, C. & Lewis J. (2008)** Biologic models of neurodegenerative disorders. In Duyckaerts C. Litvan, I. Handbook of Clinical Neurology, 3rd series, **89**, 173-188.
- Etzkorn, M., Amado-Sierra, M., Smeltz, S. & Gerken, M. (2009)** Diels-Alder reactivity of anti-tricyclo[4.2.1.1.2,5]deca-3,7-diene derivatives. Tetrahedron Letters, **50**, 2991-2993.
- Fan, M.M.Y. & Raymond, L.A. (2007)** *N*-Methyl-D-aspartate (NMDA) receptor function and excitotoxicity in Huntington's disease. Progress in neurobiology, **81**, 272-293.
- Farooqui, T. & Farooqui, A.A. (2009)** Aging: An important factor for the pathogenesis of neurodegenerative diseases. Mechanism of Ageing and Development, **130 (4)**, 203-215.

- Ferdek, P., Gerasimenko, J., Peng, S., Tepikin, A., Petersen, O. & Gerasimenko, O. (2012)** A novel role for Bcl-2 in regulation of cellular calcium extrusion. *Current Biology*, **22**, 1241-1246.
- Fontaine, B., Plassart-Schiess, E. & Nicole, S. (1997)** Diseases caused by voltage-gated ion channels. *Molecular Aspects of Medicine*, **18**, 415-463.
- Fratiglioni, L. & Qui, C. (2009)** Prevention of common neurodegenerative disorders in the elderly. *Experimental Gerontology*, **44**, 46-50.
- Galpern, W.R. & Cudkowicz, M.E. (2007)** Coenzyme Q treatment of neurodegenerative diseases of aging. *Mitochondrion*, **7**, 146-153.
- Gardoni, F. & Di Luca, M. (2006)** New target for pharmacological intervention in the glutamatergic synapse. *European Journal of Pharmacology*, **545** (1), 2-10.
- Gascon, S., Sobrado, M., Roda, J.M., Rodriguez-Pena, A. & Diaz-Guerra, M. (2008)** Excitotoxicity and focal cerebral ischemia induce truncation of the NR2A and NR2B subunits of the NMDA receptor and cleavage of the scaffolding protein PSD-95. *Molecular Psychiatry*, **13**, 99-114.
- Gee, K., Archer, E., Lapham, L., Leonard, M. Zhou, Z., Bingham, J. & Diwu, Z. (2000)** New ratiometric fluorescent calcium indicators with moderately attenuated binding affinities. *Biochemistry & Medicinal Chemistry Letters*, **10** (14), 1515-1518.
- Geldenhuis, W.J., Malan, S.F., Murugesan T., Van der Schyf, C.J. & Bloomquist, J.R. (2004)** Synthesis and biological evaluation of pentacyclo[5.4.0.0^{2,6}.0^{3,10}.0^{5,9}]undecane derivatives as potential therapeutic agents in Parkinson's disease. *Bioorganic & Medicinal Chemistry*, **12**, 1799-1806.
- Geldenhuis, W.J., Malan, S.F., Bloomquist, J.R. & Van der Schyf, C.J. (2007)** Structure-activity relationships of pentacycloundecylamines at the N-methyl-D-aspartate receptor. *Bioorganic & Medicinal Chemistry*, **15** (3), 1525-1532.
- Geldenhuis, W.J., Bezuidenhout, L. & Dluzen, D.E. (2009)** Effects of a novel dopamine uptake inhibitor upon extracellular dopamine from superfused murine striatal tissue. *European journal of pharmacology*, **619**, 38-43.

Geldenhuys, W.J., Youdim, M.B.H., Carroll, R.T. & Van der Schyf, C.J. (2011) The emergence of designed multiple ligands for neurodegenerative disorders. *Progress in Neurobiology*, **94**, 347-359.

Gilgun-Sherki, Y., Melamed, E. & Offen, D. (2001) Oxidative stress induced-neurodegenerative diseases: the need for antioxidants that penetrate the blood brain barrier. *Neuropharmacology*, **40** (8), 959-975.

Gitto, R., De Luca, L., Ferro, S., Russo, E., De Sarro, G., Chisari, M., Ciranna, L., Alvarez-Builla, J., Alajarin, R., Buemi, M.R. & Chimirri, A. (2014) Synthesis, modelling and biological characterisation of 3-substituted-1H-indoles as ligands of GluN2B-containing *N*-methyl-D-aspartate receptors. *Bioorganic & Medicinal Chemistry*, **22** (3), 1040-1048.

Gonsette, R.E. (2008) Neurodegeneration in multiple sclerosis: The role of oxidative stress and excitotoxicity. *Journal of the Neurological Sciences*, **274**, 48-53.

Greenwood, S.M. & Connolly, C.N. (2007) Dendritic and mitochondrial changes during glutamate excitotoxicity. *Neuropharmacology*, **53**, 891-898.

Grobler, E., Grobler, A., Van der Schyf, C.J. & Malan, S.F. (2006) Effect of polycyclic cage amines on the transmembrane potential of neuronal cells. *Bioorganic & Medicinal Chemistry*, **14**, 1176-1181.

Grosskreutz, J., Van Den Bosch, L. & Keller, B. (2010) Calcium dysregulation in amyotrophic lateral sclerosis. *Cell Calcium*, **47**, 165-174.

Haddad, John J. (2005) *N*-methyl-D-aspartate (NMDA) and the regulation of mitogen-activated protein kinase (MAPK) signalling pathways: A revolving neurochemical axis for therapeutic intervention? *Progress in Neurobiology*, **77**, 252-282.

Hao, J. Mdzinarishvili, A., Abbruscato, T.J., Klein, J., Geldenhuys, W.J., Van der Schyf, C. J. & Bickel, U. (2008) Neuroprotection in mice by NGP1-01 after transient focal brain ischemia. *Brain Research*, **1196**, 113-120.

- He, L., Zhang, Y., Chen, Y., Yamada, Y. & Yang, J. (2007)** Functional modularity of the β -subunit of voltage-gated Ca^{2+} channels. *Biophysical Journal*, **93**, 834-845.
- Hedegaard, M., Hansen, K.B., Andersen, K.T., Bräuner-Osborne, H. & Traynelis, S.F. (2012)** Molecular pharmacology of human NMDA receptors. *Neurochemistry International*, **61** (4), 601-609.
- Hildebrand, M., Smith, P., Bladen, C., Eduljee, C., Xie, J., Chen, L., Fee-Maki, M., Doering, C., Mezeyova, J., Zhu, Y., Belardetti, F., Pajouhesh, H., Parker, D., Americ, S., Parmar, M., Porreca, F., Tringham, E., Zamponi, G. & Snutch, T. (2012)** A novel slow-inactivation-specific ion channel modulator attenuates neuropathic pain. *Pain*, **152**, 833-843.
- Hogg, R.C., Buisson, B. & Bertrand, D. (2005)** Allosteric modulation of ligand-gated ion channels. *Biochemical Pharmacology*, **70**, 1267-1276.
- Hu, Z., Yu, L. & Yu, Z. (2005)** Theoretical analysis of ratiometric fluorescent indicators caused biased estimates of intracellular free calcium concentrations. *Journal of Photochemistry and Photobiology B: Biology*, **78** (3), 179-187.
- Hurley, M. & Dexter, D. (2012)** Voltage-gated calcium channels and Parkinson's disease. *Pharmacology & Therapeutics*, **133**, 324-333.
- Ito, F.M., Petroni, J.M., de Lima, D.P., Beatriz, A., Marques, M.R., de Moraes, M.O., Costa-Lotufo, L.V., Montenegro, R.C, Magalhaes, H.I.F, do O Pessoa, C. (2007)** Synthesis and biological evaluation of rigid polycyclic derivatives of the Diels-Alder Adduct tricyclo[6.2.1.0^{2,7}]undeca-4,9-diene-3,6-dione. *Molecules*, **12**, 271-282.
- Jarvis, S. & Zamponi, G. (2007)** Trafficking and regulation of neuronal voltage-gated calcium channels. *Current Opinion in Cell Biology*, **19**, 474-482.
- Jellinger, K.A. (2007)** Advance in our understanding of neurodegeneration. In Parvez, S.H. ed. *Oxidative stress and neurodegenerative disorders*, 1st edition, Elsevier, United Kingdom, 1.
- Jensen, M., Sukumaran, M., Johnson, C., Greger, I. & Neuweiler, H. (2011)** Intrinsic motions in the N-terminal domain of an ionotropic glutamate receptor

detected by fluorescence correlation spectroscopy. *Journal of Molecular Biology*, **414** (1), 96-105.

Johnson, J.W. & Kotermanski, S.E. (2006) Mechanism of action of memantine. *Current Opinion in pharmacology*, **6**, 61-67.

Joubert J., van Dyk, S., Green, I.R. & Malan, S.F. (2011) Synthesis, evaluation and application of polycyclic fluorescent analogues as *N*-methyl-D-aspartate receptor and voltage gated calcium channel ligands. *European Journal of Medicinal Chemistry*, **46**, 5010-5020.

Kabanov, A.V. & Gendelman, H.E. (2007) Nanomedicine in the diagnosis and therapy of neurodegenerative disorders. *Progress Polymer Science*, **32** (8-9), 1054-1082.

Kaul, M. & Lipton, S.A. (2000) The NMDA Receptor - Its Role in Neuronal Apoptosis and HIV-Associated Dementia. *NeuroAids*, **3** (6). Available at <http://aidsscience.com/neuroaids/zones/articles/2000/11/NMDA/index.asp>: accessed on 13 June 2012.

Kennedy, G.J. (2007) From symptom palliation to disease modification: Implications for dementia care. *Primary Psychiatry*, **14** (11) 30-34.

Kiss, L., Cheng, G., Bednar, B., Bednar, R.A., Bennett, P.B., Kane, S.A., McIntyre, C.J., McCauley, J.A. & Koblan, K.S. (2005) In vitro characterization of novel NR2B selective NMDA receptor antagonists. *Neurochemistry International*, **46**, 453-464.

Krantic, S., Mechawar, N., Reix, S. & Quirion, R. (2005) Molecular basis of programmed cell death involved in neurodegeneration. *TRENDS in Neurosciences*, **28** (12), 670-676.

Kroemer, R.T., Koutsilieri, E., Hecht, P., Liedl, Klaus R., Riederer, P. & Kornhuber, J. (1998) Quantitative Analysis of the Structural Requirements for Blockade of the *N*-Methyl-D-aspartate Receptor at the Phencyclidine Binding Site. *Journal of Medicinal Chemistry*, **41** (3), 393-400.

REFERENCES

- Kukkonen, J. (2009)** An easy ratiometric compensation for the extracellular Ca²⁺ indicator-caused fluorescence artifact. *Analytical Biochemistry*, **390** (2), 212-214.
- Landrigan, P.J., Sonawane, B., Butler, R.N., Trasande, L., Callan, R. & Droller, D. (2005)** Early Environmental Origins of Neurodegenerative Disease in Later Life. *Environmental Health Perspectives*, **113** (9), 1230-1233.
- Lau, A. & Tymianski, M. (2010)** Glutamate receptors, neurotoxicity and neurodegeneration. *European Journal of Physiology*, **460**, 525-542.
- Lee, S. & Kim, M. (2006)** Aging and neurodegeneration: Molecular mechanisms of neuronal loss in Huntington's disease. *Mechanisms of Ageing and Development*, **127** (5), 432-435.
- Leeson, P.D., Carling, R.W., James, K., Smith, J.D., Moore, K.W., Wong, E.H.F. & Bake, R. (1990)** Role of Hydrogen Bonding in Ligand Interaction with the *N*-Methyl-D-aspartate Receptor Ion Channel. *Journal of Medicinal Chemistry*, **33** (5), 1296-1305.
- Le Feuvre, R., Brough, D. & Rothwell, N. (2002)** Extracellular ATP and P2X7 receptors in neurodegeneration. *European Journal of Pharmacology*, **447**, 261-269.
- Leist, M. & Nicotera, P. (1998)** Apoptosis, excitotoxicity, and neuropathology. *Experimental Cell Research*, **239**, 183-201.
- Li, Y. & Han, T. (2008)** Glycine modulates synaptic NR2A- and NR2B-containing NMDA receptor-mediated responses in the rat visual cortex. *Brain Research*, **1190**, 49-55.
- Lipton, S.A. (2004)** Failures and successes in NMDA receptor antagonists: molecular basis for the use of open-channel blockers like memantine in the treatment of acute and chronic neurologic insult. *The American Society for Experimental NeuroTherapeutics*, **1**, 101-110.
- Lipton, S.A. (2007)** Pathologically-activated therapeutics for neuroprotection: mechanism of NMDA receptor block by memantine and S-nitrosylation. *Current Drug Targets*, **8** (5), 621-632.

- Lobo, V., Patil, A., Phatak, A. & Chandra, N. (2010)** Free radicals, antioxidants and functional foods: Impact on human health. *Pharmacognosy Review*, **4** (8), 117-126.
- Lockman, J., Geldenhuys, W., Jones-Higgins, M., Patrick, J., Allen, D. & Van der Schyf, C. (2012)** NGP1-01, a multi-targeted polycyclic cage amine, attenuates brain endothelial cell death in iron overload conditions. *Brain Research*, **1489**, 133-139.
- Loscher, W. & Schmidt, D. (2006)** New horizons in the development of antiepileptic drugs: Innovative strategies. *Epilepsy Research*, **69** (3), 183-272.
- Losi, G., Lanza, M., Makovec, F., Artusi, R., Caseli, G. & Puia, G. (2006)** Functional in vitro characterization of CR 3394: A novel voltage dependent *N*-methyl-D-aspartate (NMDA) receptor antagonist. *Neuropharmacology*, **50**, 277-285.
- Love, S. (2003)** Apoptosis and brain ischaemia. *Progress in Neuro-Psychopharmacology & Biological Psychiatry*, **27**, 267-282.
- Lukic-Panin, V., Kamiya, T., Zhang, H., Hayashi, T., Tsuchiya, A., Sehara, Y., Deguchi, K., Yamashita, T. & Abe, K. (2007)** Prevention of neuronal damage by calcium channel blockers with antioxidative effects after transient focal ischemia in rats. *Brain Research*, **1176**, 143-150.
- Malan, S.F., Van der Walt, J.J. & Van der Schyf, C.J. (2000)** Structure-activity relationships of polycyclic aromatic amines with calcium channel blocking activity. *Arch Pharm (Weinheim)*, **333** (1), 10-16.
- Mandolesi, G., Cesa, R., Autuori, E. & Strata, P. (2009)** An orphan ionotropic glutamate receptor: The $\delta 2$ subunit. *Neuroscience*, **158** (1), 67-77.
- Marambaud, P., Dreses-Werringloer, U. & Vingtdeux, V. (2009)** Calcium signaling in neurodegeneration. *Molecular Neurodegeneration*, **4**: 20. Available at <http://www.molecularneurodegeneration.com/content/4/1/20>: accessed on 20 June 2012.

- Marchetti, C. & Usai, C. (1996)** High affinity block by nimodipine of the internal calcium elevation in chronically depolarised rat cerebellar granule neuron. *Neuroscience Letters*, **207** (2), 77-80.
- Martin, L., Al-Abdulla, N., Brambrink, A., Kirsch, J., Sieber, F. & Portera-Cailliau, C. (1998)** Neurodegeneration in excitotoxicity, global cerebral ischemia, and target deprivation: A perspective on the contributions of apoptosis and necrosis. *Brain Research Bulletin*, **46** (4), 281-309.
- Mayer, M.L. (2005)** Glutamate receptor ion channels. *Current Opinion in Neurobiology*, **15**, 282-288.
- Mayer, M.L. (2011)** Structure and mechanism of glutamate receptor ion channel assembly, activation and modulation. *Current Opinion in Neurobiology*, **21**, 283-290.
- Mayeux, R. (2003)** Epidemiology of neurodegeneration. *Annual Review of Neuroscience*, **26**, 81-104.
- McDonough, S. (2007)** Gating modifier toxins of voltage-gated calcium channels. *Toxicon*, **49**, 202-212.
- Mdzinarishvili, A., Geldenhuys, W.J., Abbruscato, T.J., Bickel, U., Klein, J. & Van der Schyf, C.J. (2005)** NGP1-01, a lipophilic polycyclic cage amine, is neuroprotective in focal ischemia. *Neuroscience Letters*, **383**, 49-53.
- Mehta, A., Prabhakar, M., Kumar, P., Deshmukh, R. & Sharma P. (2013)** Excitotoxicity: Bridge to various triggers in neurodegenerative disorders. *European Journal of Pharmacology*, **698** (1-3), 6-18.
- Milatovic, D., Zaja-Milatovic, S., Gupta, R.C., Yu, Y. & Aschner, M. (2009)** Oxidative damage and neurodegeneration in manganese-induced neurotoxicity. *Toxicology and Applied Pharmacology*, **240**, 219-225.
- Monaghan, D.T., Irvine, M.W., Costa, B.M., Fang, G. & Jane, D.E. (2012)** Pharmacological modulation of NMDA receptor activity and the advent of negative and positive allosteric modulators. *Neurochemistry International*, **61** (4), 581-592.

- Moreira, P., Zhu, X., Wang, X., Lee, H., Nunomura, A., Petersen, R., Perry, G. & Smith, M. (2012)** Mitochondria: A therapeutic target in neurodegeneration. *Biochimica et Biophysica Acta*, **1802** (1), 212-220.
- Morton, R., Norlin, S., Vollmer, C. & Valenzuela, C. (2013)** Characterisation of *L*-type voltage-gated Ca²⁺ channel expression and function in developing Ca3 pyramidal neurons. *Neuroscience*, **238**, 59-70.
- Nagata, R., Ae, N. & Tanno, N. (1995)** Structure-activity relationships of tricyclic quinoxalinediones as potent antagonists for the glycine binding site of the NMDA receptor 1. *Bioorganic & Medicinal Chemistry Letters*, **5** (14), 1527-1532.
- Neher, E. (1995)** The use of Fura-2 for estimating Ca buffers and Ca fluxes. *Neuropharmacology*, **34** (11), 1423-1442.
- Nicholls, D.G. & Budd, S.L. (1998)** Mitochondria and neuronal glutamate excitotoxicity. *Biochimica et Biophysica Acta*, **1366**, 97-112.
- Nicoletti, F., Bruno, V., Catania, M.V., Battaglia, G., Copani, A., Barbagallo, G., Cena, V., Sanchez-Prieto J., Spano, P.F. & Pizzi, M. (1999)** Group-I metabotropic glutamate receptors: hypotheses to explain their dual role in neurotoxicity and neuroprotection. *Neuropharmacology*, **38**, 1477-1484.
- Nyiredy, S.Z., Erdelmeier, C.A.J., Meier, B. and Sticher, O. (1985)** 'Prisma': ein model zur optimierung der mobile phase für die Dünnschichtchromatographie, vorgestellt anhand verschiedener naturstofftrennungen. *Planta medica*, 241-246.
- O'Brien, R.J., Lau, L. & Haganir, R.L. (1998)** Molecular mechanisms of glutamate receptor clustering at excitatory synapses. *Current Opinion in Neurobiology*, **8**, 364-369.
- Parsons, C.G., Danysz, W. & Quack, G. (1999)** Memantine is a clinically well tolerated *N*-methyl-D-aspartate (NMDA) receptor antagonist-a review of preclinical data. *Neuropharmacology*, **38**, 735-767.
- Pellegrini-Giampietro, D.E., Peruginelli, F., Meli, E., Cozzi, A., Albani-Torregrossa, S., Pellicciari, R. & Moroni, F. (1999)** Protection with metabotropic

glutamate I receptor antagonists in models of ischemic neuronal death: time-course and mechanisms. *Neuropharmacology*, **38**, 1607-1619.

Prins, L.H.A., du Preez, J.L., van Dyk, S. & Malan, S.F. (2009) Polycyclic cage structures as carrier molecules for neuroprotective non-steroidal anti-inflammatory drugs. *European Journal of Medicinal Chemistry*, **44**, 2577-2582.

Puyal, J., Ginet, V. & Clarke P. (2013) Multiple interacting cell death mechanisms in the mediation of excitotoxicity and ischemic brain damage: A challenge for neuroprotection. *Progress in Neurobiology*, **105**, 24-48.

Qian A. & Johnson, J.W. (2002) Channel gating of NMDA receptors. *Physiology & Behavior*, **77**, 577-582.

Qiu, S., Li, X. & Zhuo, M. (2011) Post-translational modification of NMDA receptor GluN2B subunit and its roles in chronic pain and memory. *Seminars in Cell & Developmental Biology*, **22**, 521-529.

Qureshi, I.A. & Mehler, M.F. (2013) Epigenetic mechanisms governing the process of neurodegeneration. *Molecular Aspects of Medicine*, **34** (4), 875-882.

Qureshi, G.A., Baig, S., Sarwar, M. & Parvez, S.H. (2004) Neurotoxicity, Oxidative stress and cerebrovascular disorders. *Neurotoxicology*, **25**, 121-138.

Raffray, M. & Cohen, G.M. (1997) Apoptosis and Necrosis in Toxicology: A Continuum or Distinct Modes of Cell Death? *Pharmacology & Therapeutics*, **75** (3), 153-177.

Ricciarelli, R., Argellati, F., Pronzato, M.A. & Domenicotti, C. (2007) Vitamin E and neurodegenerative diseases. *Molecular Aspects of Medicine*, **28**, 591-606.

Rodriguez, M.J., Bernal, F., Andres, N., Malpesa, Y. & Mahy, N. (2000) Excitatory amino acids and neurodegeneration: A hypothetical role of calcium precipitation. *International Journal of Development Neuroscience*, **18** (2-3), 299-307.

Salles, R.C., Lacerda Jr, V., Barbosa, L.R., Ito, F.M., de Lima, D.P., dos Santos, R.B. Greco, S.J., Neto, A.C., de Castro, E.V.R. & Beatriz, A. (2012) GIAO chemical shifts calculations of some polycyclic cage compounds: Unambiguous

assignment of NMR signals and stereoisomers. *Journal of Molecular Structure*, **1007**, 191-195.

Sas K., Robotka, H., Toldi, J. & Vécsei, L. (2007) Mitochondria, metabolic disturbances, oxidative stress and the kynurenine system, with focus on neurodegenerative disorders. *Journal of the Neurological Sciences*, **257**, 221-239.

Schmechel, D.E., Browndyke, J. & Ghio, A. (2006) Strategies for dissecting genetic-environmental interactions in neurodegenerative disorders. *NeuroToxicology*, **27**, 637-657.

Scott, V., Vortherms, T., Niforatos, W., Swensen, A., Neelands, T., Milicic, I., Banfor, P. King, A., Zhong, C., Simler G., Zhan, C., Bratcher, N., Boyce-Rustay, J., Zhu, C., Bhatia, P., Doherty, G., Mack, H., Stewart, A. & Jarvis, M. (2012) A-1048400 is a novel, orally active, state-dependent neuronal calcium channel blocker that produces dose-dependent antinociception without altering hemodynamic function in rats. *Biochemical Pharmacology*, **83**, 406-418.

Snutch, T., Sutton, K. & Zamponi, G. (2001) Voltage-dependent calcium channels – beyond dihydropyridine antagonists. *Current Opinion in Pharmacology*, **1**, 11-16.

Snutch, T. (2009) Voltage-gated calcium channels. *Encyclopaedia of Neuroscience*, Elsevier Ltd, Canada, 427-441.

Soltseva, E., Bukanova, J., Marchenka, E. & Skrebitsky, V. (2007) Donepezil is a strong antagonist of voltage-gated calcium and potassium channels in molluscan neurons. *Comparative Biochemistry and Physiology, Part C* **144**, 319-326.

Sonkusare, S., Kaul, C. & Ramarao, P. (2005) Dementia of Alzheimer's disease and other neurodegenerative disorders-memantine, a new hope. *Pharmacological Research*, **51 (1)**, 1-17.

Stawski, P., Janovjak, H. & Trauner, D. (2010) Pharmacology of ionotropic glutamate receptors: A structural perspective. *Bioorganic & Medicinal Chemistry*, **18 (22)**, 7759-7772.

- Stewart, V.C. & Heales, S.J.R. (2003)** Nitric oxide-induced mitochondrial dysfunction: implications for neurodegeneration. *Free Radical Biology & Medicine*, **34** (3), 287-303.
- Stone, T.W. & Addae, J.I. (2002)** The pharmacological manipulation of glutamate receptors and neuroprotection. *European Journal of Pharmacology*, **447**, 285-296.
- Stout, A., Reynolds, I. (1999)** High-affinity calcium indicators underestimate increases in intracellular calcium concentrations associated with excitotoxic glutamate stimulations. *Neuroscience*, **89** (1), 91-100.
- Takahashi, M. & Ogura, A. (1983)** Dihydropyridines as potent calcium channel blockers in neuronal cells. *FEBS Letters*, **152** (2), 191-194.
- Tichelaar, W., Safferling, M., Keinanen, K., Stark, H. & Madden, D. (2004)** The three-dimensional structure of an ionotropic glutamate receptor reveals a dimer-of-dimers assembly. *Journal of Molecular Biology*, **344** (2), 435-442.
- Triggle, D. (1999)** The pharmacology of ion channels: with particular reference to voltage-gated Ca²⁺ channels. *European Journal of Pharmacology*, **375**, 311-325.
- Van Damme, P., Van Den Bosch, L. & Robberecht, W. (2003)** Excitotoxicity and oxidative stress in pathogenesis of Amyotrophic lateral sclerosis/motor neuron disease. *Blue Books of Practical Neurology*, **20**, 259-284.
- Van Den Bosch, L., Van Damme, P., Bogaert, E. & Robberecht, W. (2006)** The role of excitotoxicity in the pathogenesis of amyotrophic lateral sclerosis. *Biochimica et Biophysica Acta*, **1762** (11-12), 1068-1082.
- Van Der Schyf, C.J. & Geldenhuys, W.J. (2009)** Polycyclic Compounds: Ideal Drug Scaffolds for the Design of Multiple Mechanism Drugs? *Journal of the American Society for Experimental NeuroTherapeutics*, **6** (1), 175-186.
- Van Der Schyf, C.J. & Youdim, M.B.H. (2009)** Multifunctional drugs as neurotherapeutics. *Neurotherapeutics*, **6** (1), 1-3.
- Varming, T., Christophersen, P., Moller, A., Peters, D., Axelsson, O. & Nielsen, E. (1996)** Synthesis and biological activity of the neuronal calcium channel blockers

REFERENCES

2-amino-1-(2,5-dimethoxyphenyl)-5-trifluoromethyl benzimidazole (NS-649). *Bioorganic & Medicinal Chemistry Letters*, **6** (3), 245-248.

Waldmeier, P.C. (2003) Prospects for antiapoptotic drug therapy of neurodegenerative diseases. *Progress in Neuro-Psychopharmacology & Biological Psychiatry*, **27**, 303-321.

Walker, F.O. (2007) Huntington's disease. *Lancet*, **369**, 218-228.

Wang, Y., Pettus, M., Gao, D., Phillips, C. & Bowersox, S. (2000) Effects of intrathecal administration of ziconotide, a selective neuronal *N*-type calcium channel blocker, on mechanical allodynia and heat hyperalgesia in a rat model of postoperative pain. *Pain*, **84**, 151-158.

Wenk, G.L. (2007) Neurodegenerative diseases and memory: a treatment approach. In: *Neurobiology of Learning and Memory*, second edition, Elsevier Inc., 519-539.

Witte, M., Geurts, J., de Vries, H., van der Valk, P. & van Horsen, J. (2010) Mitochondrial dysfunction: A potential link between neuroinflammation and neurodegeneration? *Mitochondrion*, **10**, 411-418.

Wollmuth, L.P. & Sobolevsky, A.I. (2004) Structure and gating of the glutamate receptor ion channel. *TRENDS in Neurosciences*, **27** (6), 321-328.

Wong, E., Yu, W., Yap, W., Venkatesh, B. & Soong, T. (2006) Comparative genomics of the human and fugu voltage-gated calcium channel $\alpha 1$ -subunit gene family reveals greater diversity in fugu. *Gene*, **366**, 117-127.

Wooten, G.F., Currie, L.J., Bovbjerg, V.E., Lee, J.K. & Patrie, J. (2004) Are men at greater risk for Parkinson's disease than women? *Journal of Neurology, Neurosurgery & Psychiatry*, **75**, 637-639.

Yanamadala, V. & Friedlander, R.M. (2009) Complement in neuroprotection and neurodegeneration. *Trends in Molecular Medicine*, **16** (2), 69-76.

Youdim, M.B.H. (2010) Why Do We Need Multifunctional Neuroprotective and Neurorestorative Drugs for Parkinson's and Alzheimer's Diseases as Disease Modifying Agents. *Experimental Neurobiology*, **19**, 1-14.

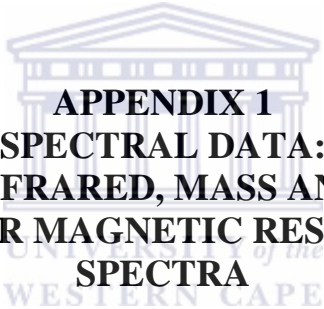
Zamponi, G., Feng, Z., Zhang, L., Pajouhesh, H., Ding, Y., Belardetti, F., Pajouhesh, H., Dolphin, D., Mitscher, L. & Snutch, T. (2009) Scaffold-based design and synthesis of potent *N*-type calcium channel blockers. *Bioorganic & Medicinal Chemistry Letters*, **19**, 6467-6472.

Related reference websites:

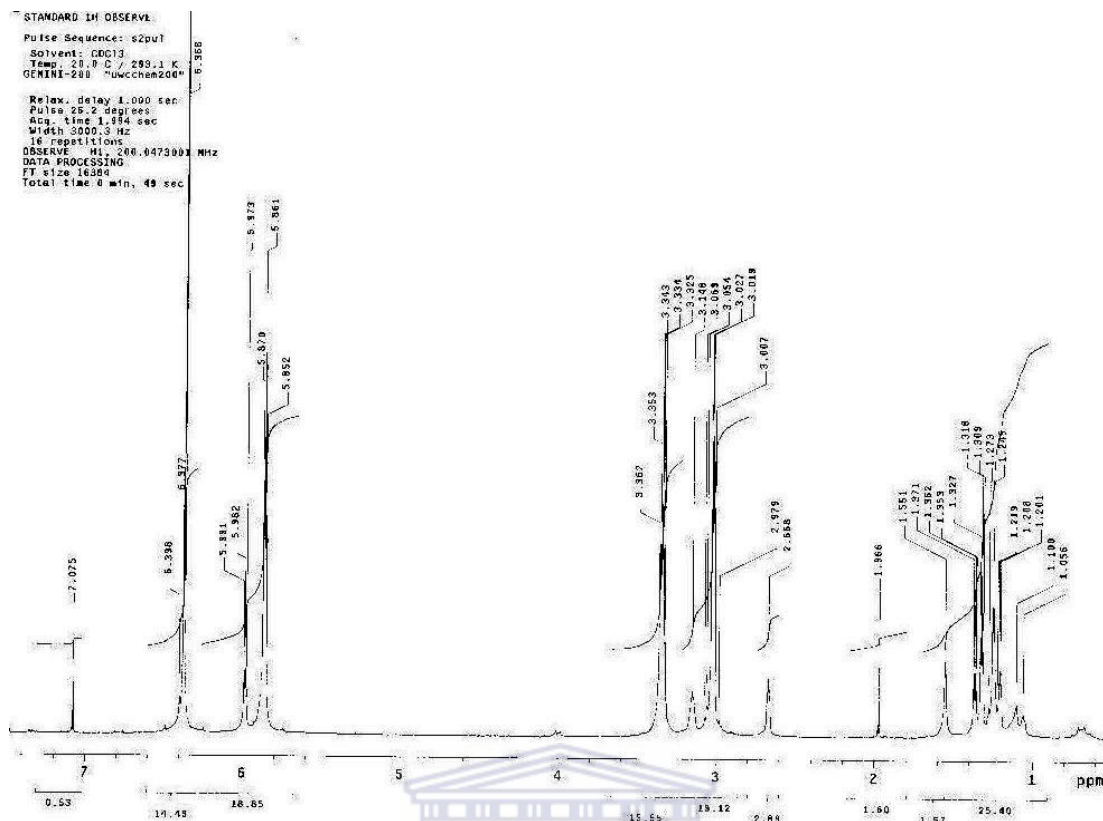
Sigma-Aldrich. Mitochondria in apoptosis. Available at <http://www.sigmaaldrich.com/life-science/cell-biology/learning-center/pathway-slides-and/mitochondria-in-apoptosis.html>: accessed on **24 June 2012**.

Wikispaces. Amino acids. Available at <http://appsyctextbk.wikispaces.com/Amino+Acids>: accessed on **20 August 2013**.





APPENDIX 1
SPECTRAL DATA:
INFRARED, MASS AND
NUCLEAR MAGNETIC RESONANCE
SPECTRA

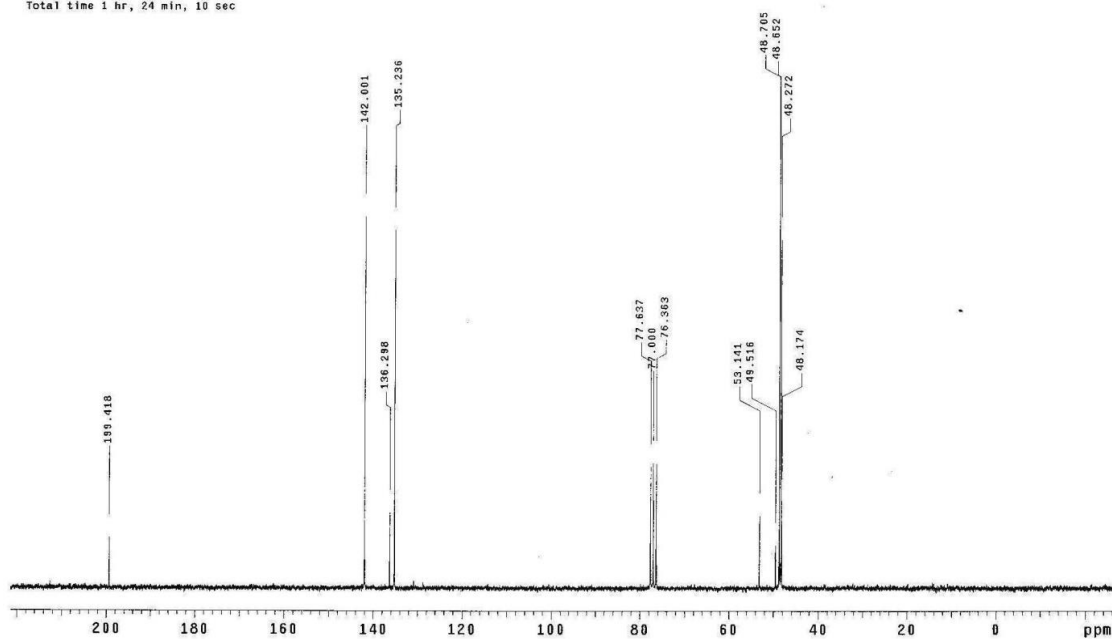


Spectrum 1: ^1H NMR of tricyclo[6.2.1.0^{2,7}]undeca-4,9-diene-3,6-dione (1).

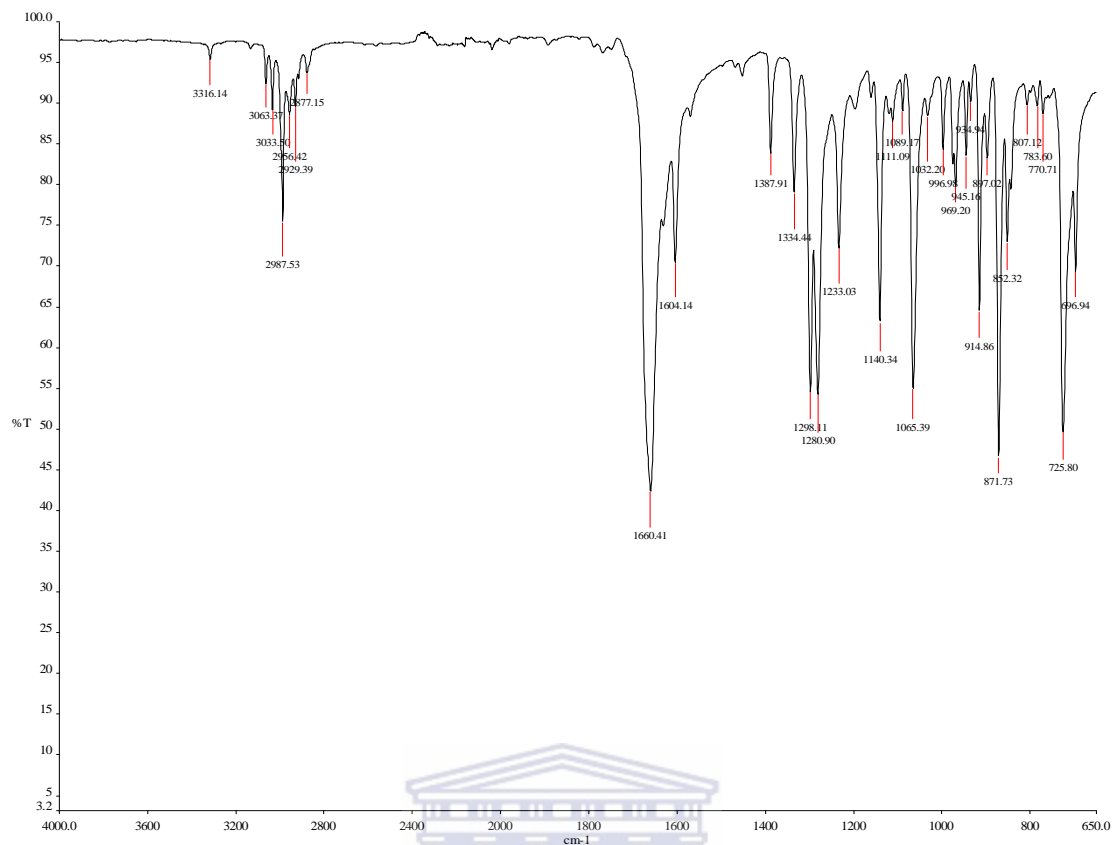
13C OBSERVE

Pulse Sequence: s2pu1
 Solvent: CDCl3
 Temp: 20.0 C / 293.1 K
 GEMINI-200 "uwcchem200"

Pulse 62.5 degrees
 Acq. time 1.498 sec
 Width 12500.0 Hz
 3000 repetitions
 OBSERVE C13, 50.3019150 MHz
 DECOUPLE H1, 200.0482640 MHz
 Power 30 dB
 continuously on
 WALTZ-16 modulated
 DATA PROCESSING
 Line broadening 1.0 Hz
 FT size 65536
 Total time 1 hr, 24 min, 10 sec



Spectrum 2: ^{13}C NMR of tricyclo[6.2.1.0^{2,7}]undeca-4,9-diene-3,6-dione (1).



Spectrum 3: Infrared of tricyclo[6.2.1.0^{2,7}]undeca-4,9-diene-3,6-dione (**1**).

COMP2 FR2 AY0 proton in cdc13 23-10-2012

Pulse Sequence: s2pu1

Solvent: CDCl3

Temp. 20.0 C / 293.1 K

GEMINI-200 "uwchem200"

Relax. delay 1.000 sec

Pulse 26.2 degrees

Acq. time 1.884 sec

Width 3000.3 Hz

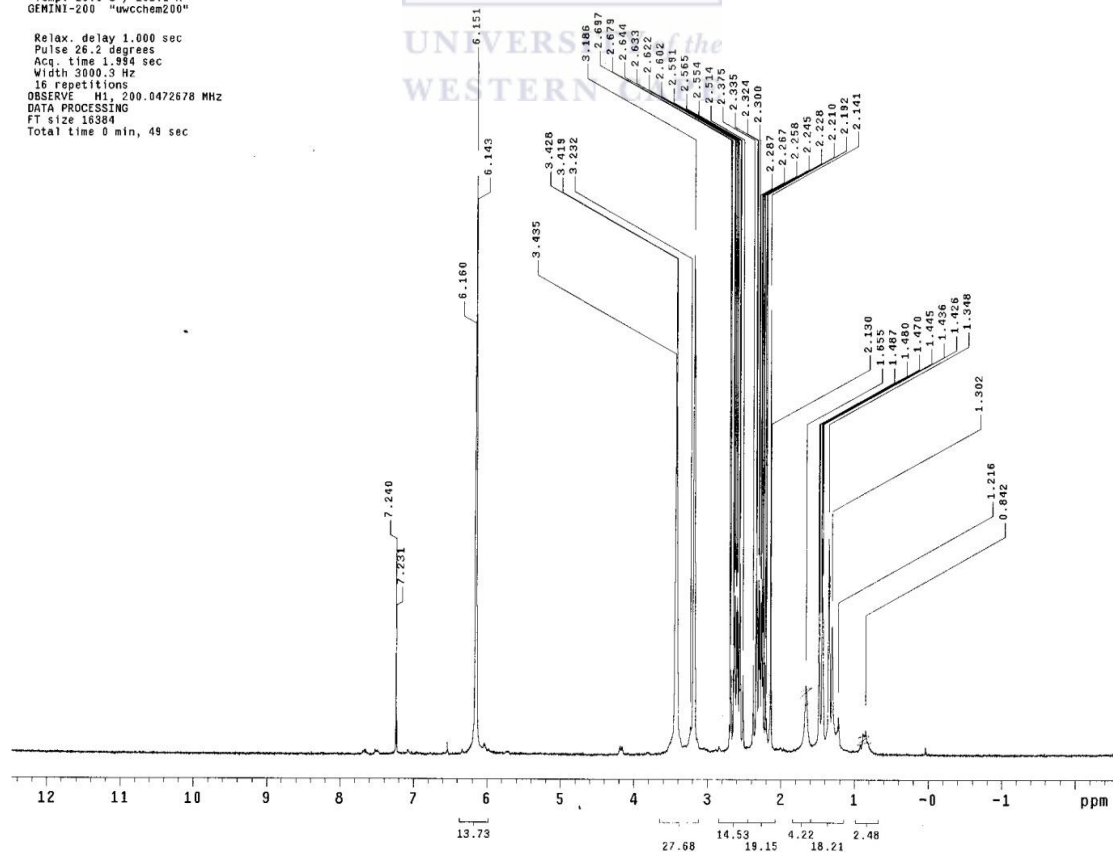
16 repetitions

OBSERVE H1, 200.0472678 MHz

DATA PROCESSING

FT size 16384

Total time 0 min, 48 sec

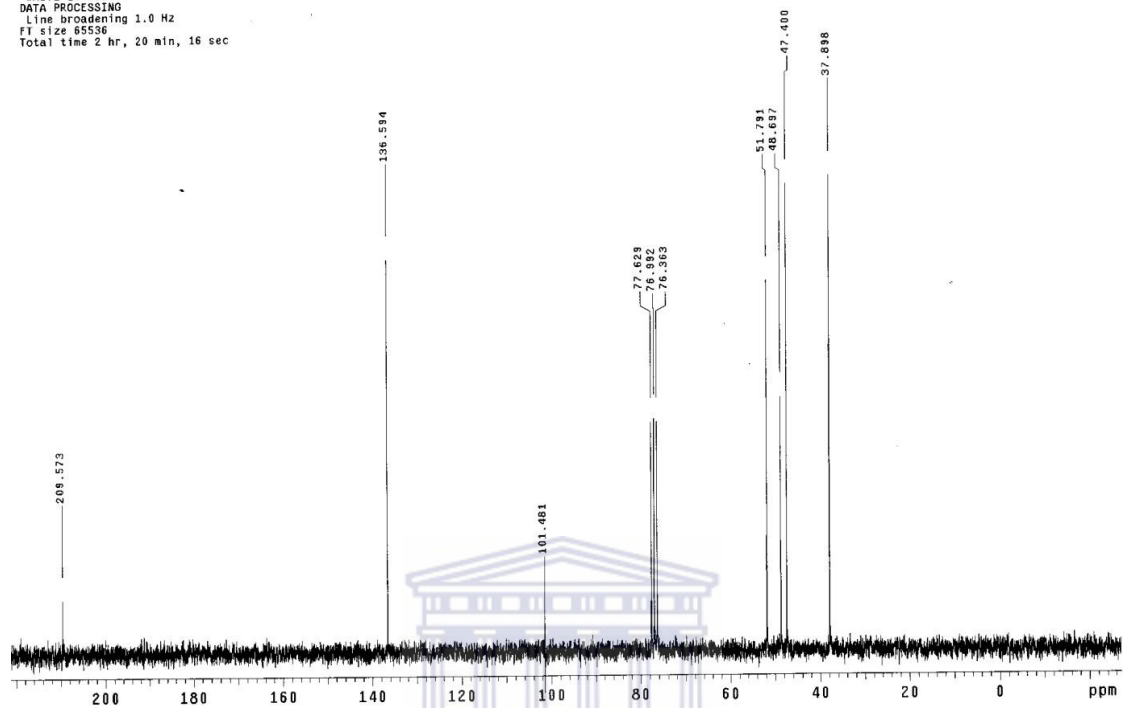


Spectrum 4: ¹H NMR of tricyclo[6.2.1.0^{2,7}]undec-9-ene-3,6-dione (**2**).

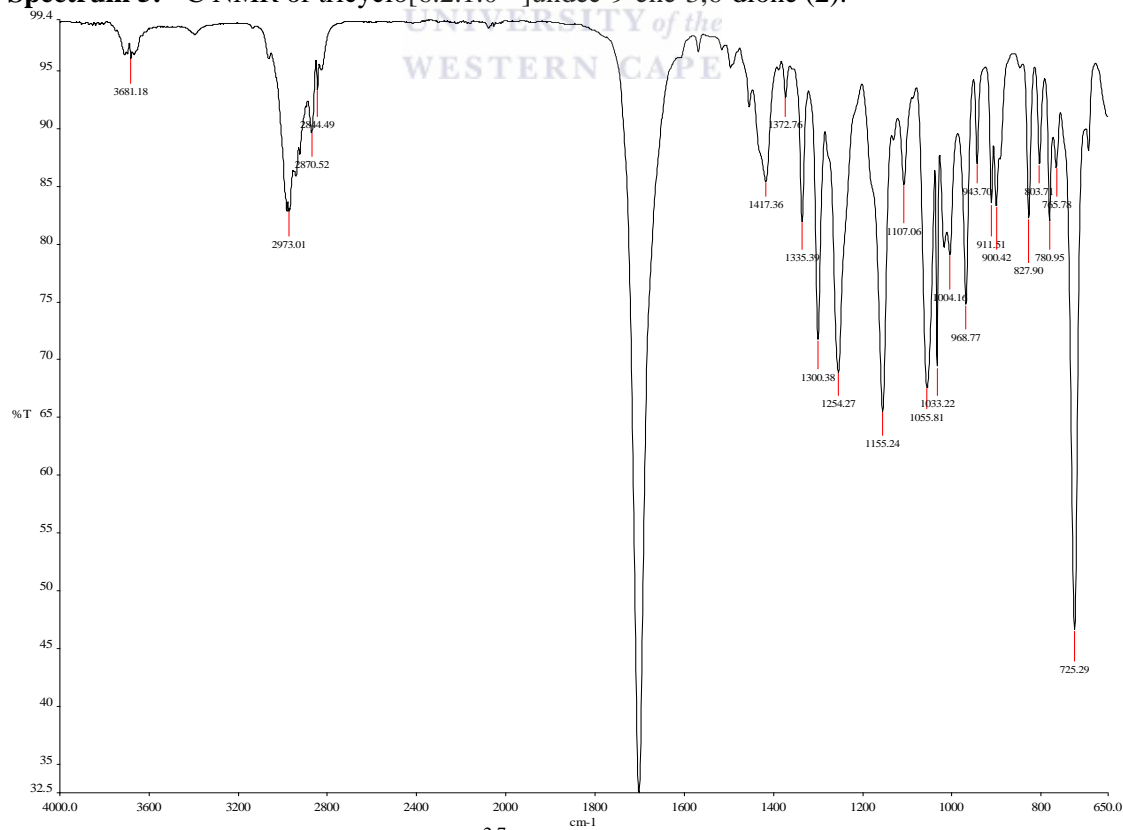
COMP2 FR2 AYO C13 1n cdc13 23-10-2012

Pulse Sequence: s2pu1
 Solvent: CDC13
 Temp: 20.0 C / 293.1 K
 GEMINI-200 "uwchem200"

Pulse 62.9 degrees
 Acq. time 1.498 sec
 Width 12500.0 Hz
 592 repetitions
 OBSERVE C13, 50.3019146 MHz
 DECOUPLE H1, 200.0482640 MHz
 Power 30 dB
 continuously on
 WALTZ-16 modulated
 DATA PROCESSING
 Line broadening 1.0 Hz
 FI size 65536
 Total time 2 hr, 20 min, 16 sec



Spectrum 5: ¹³C NMR of tricyclo[6.2.1.0^{2,7}]undec-9-ene-3,6-dione (2).

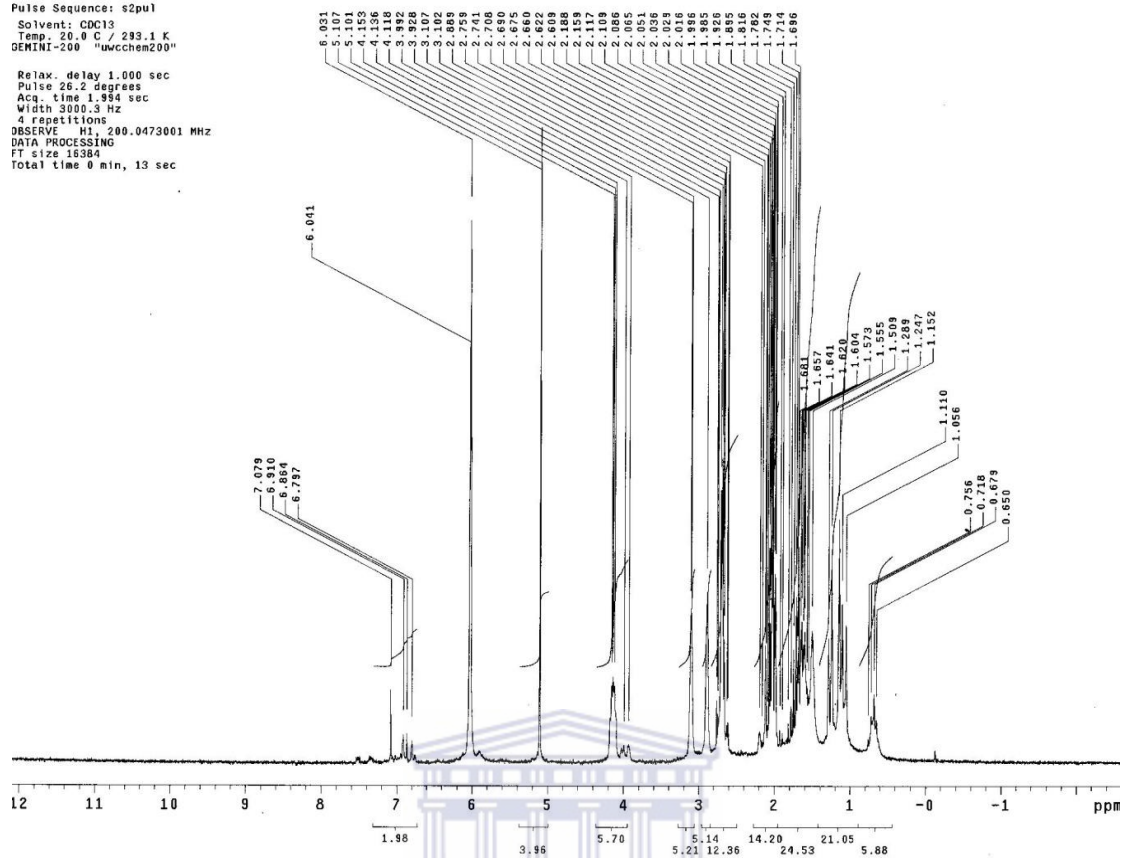


Spectrum 6: Infrared of tricyclo[6.2.1.0^{2,7}]undec-9-ene-3,6-dione (2).

comp3 fr2 AY0 proton in cdc13

Pulse Sequence: s2pul
 Solvent: CDCl3
 Temp: 20.0 C / 293.1 K
 GEMINI-200 "uwchem200"

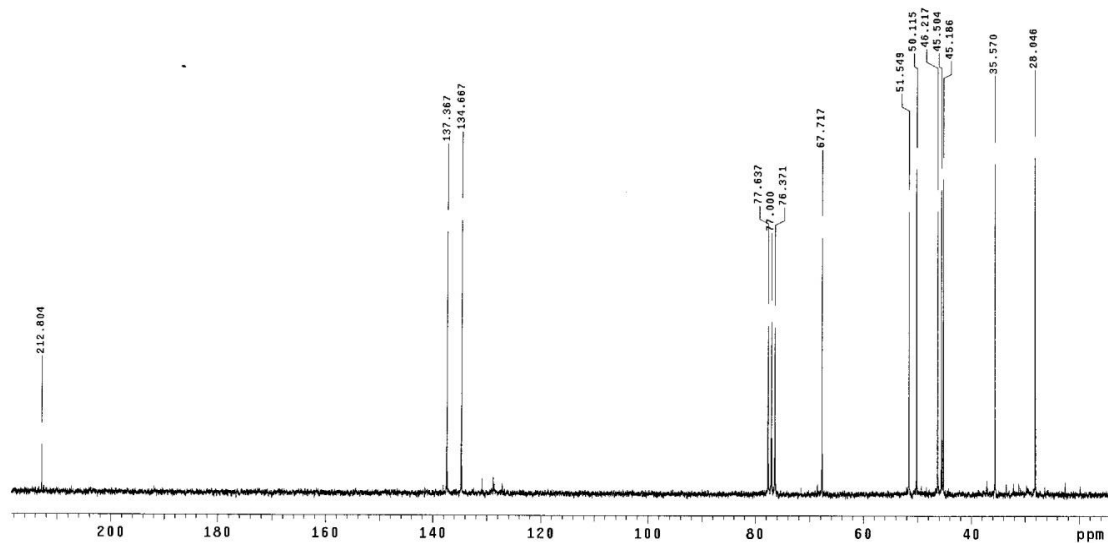
Relax. delay 1.000 sec
 Pulse 26.2 degrees
 Acq. time 1.994 sec
 Width 3000.3 Hz
 4 repetitions
 OBSERVE H1, 200.0473001 MHz
 DATA PROCESSING
 FT size 13384
 Total time 0 min, 13 sec

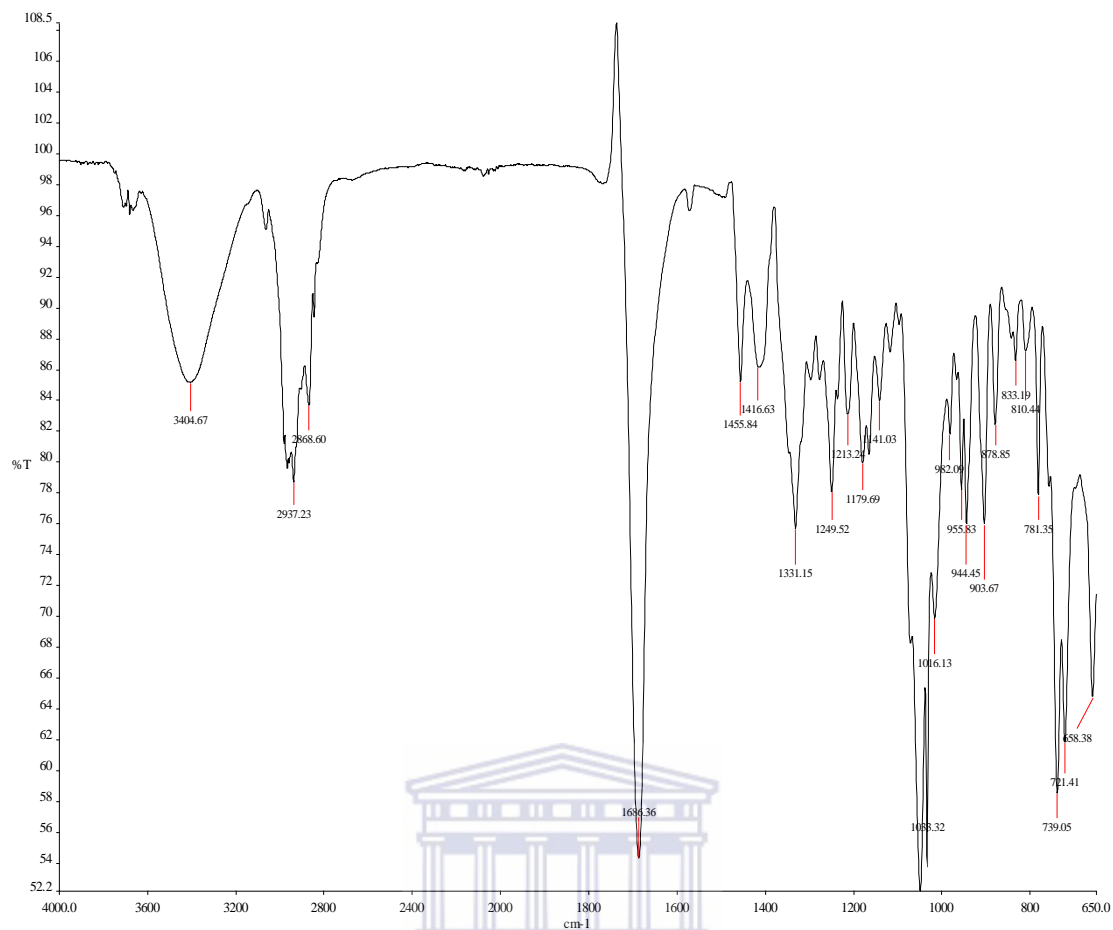
Spectrum 7: ^1H NMR of 6-hydroxytricyclo[6.2.1.0^{2,7}]undec-9-en-3-one (**3**).

Comp9 1n cdc13 4-03-2013

Pulse Sequence: s2pul
 Solvent: CDCl3
 Temp: 20.0 C / 293.1 K
 GEMINI-200 "uwchem200"

Pulse 62.3 degrees
 Acq. time 1.458 sec
 Width 12500.0 Hz
 4484 repetitions
 OBSERVE C13, 50.3018142 MHz
 DECOUPLE H1, 200.0482840 MHz
 Power 30 dB
 continuously on
 WALTZ-16 modulated
 DATA PROCESSING
 Line broadening 1.0 Hz
 FT size 65536
 Total time 4 hr, 40 min, 29 sec

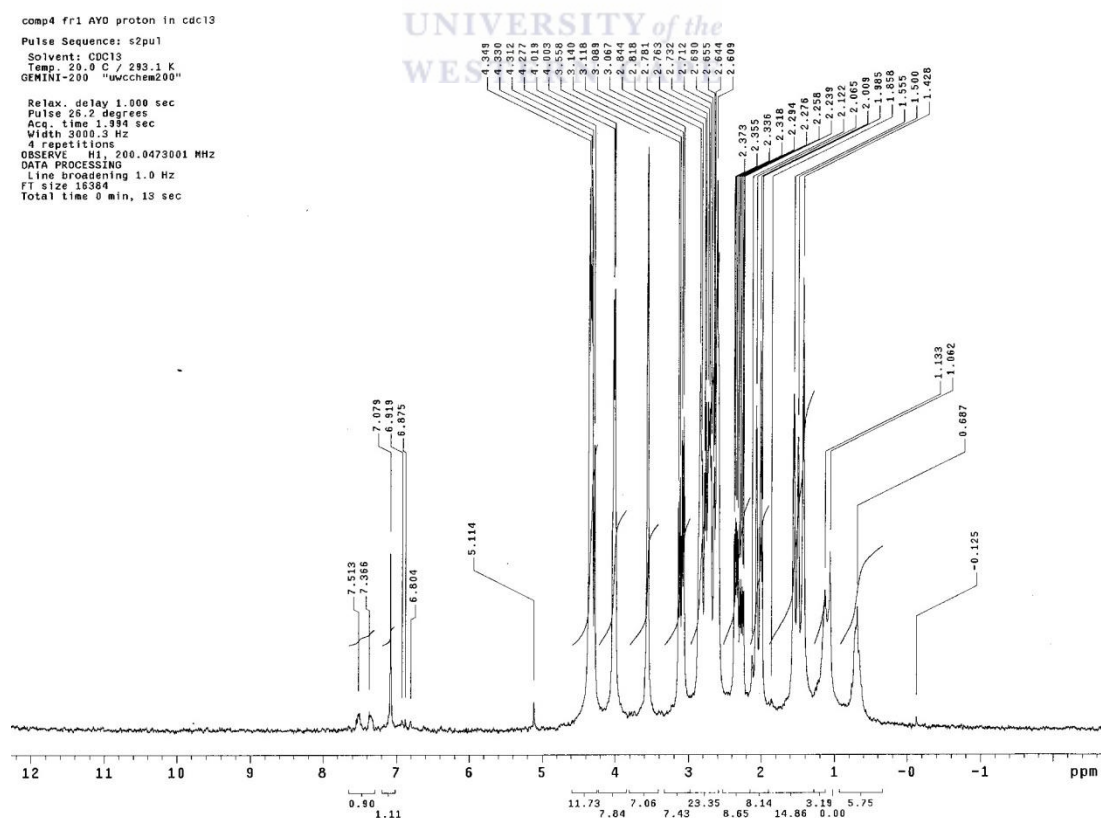
Spectrum 8: ^{13}C NMR of 6-hydroxytricyclo[6.2.1.0^{2,7}]undec-9-en-3-one (**3**).



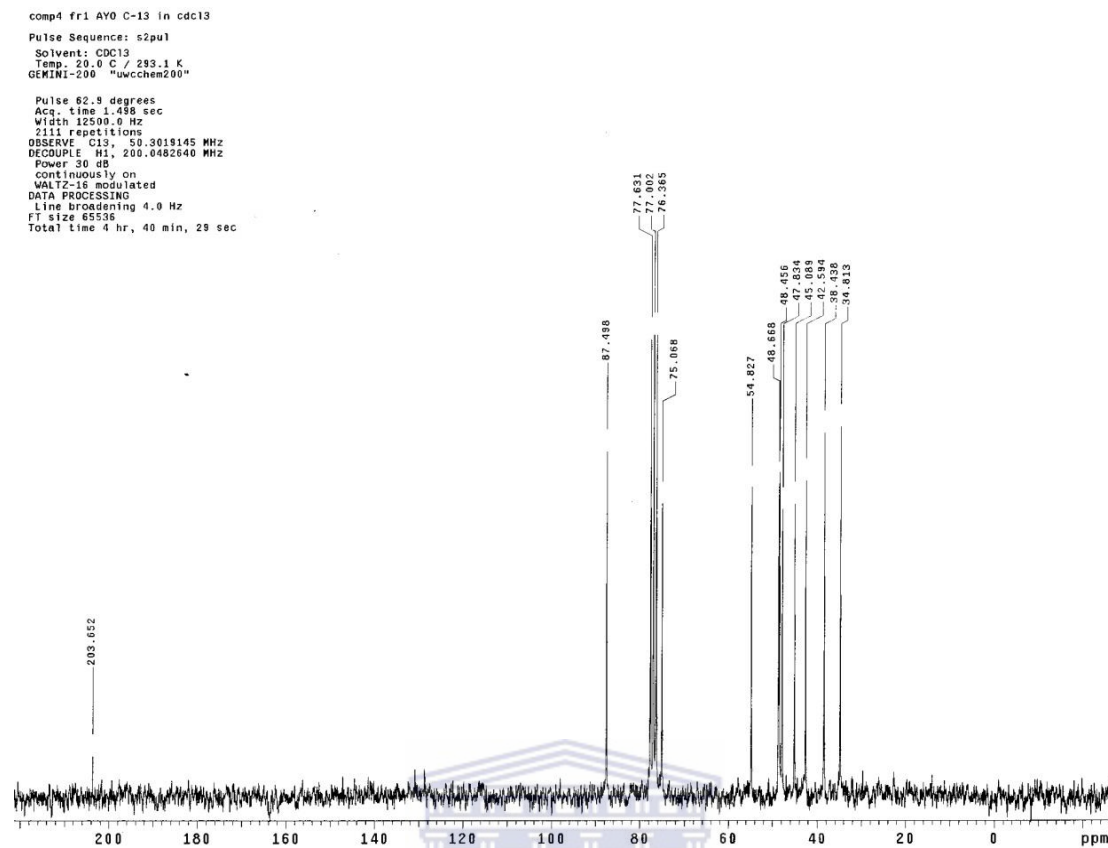
Spectrum 9: Infrared spectrum of 6-hydroxytricyclo[6.2.1.0^{2,7}]undec-9-en-3-one (**3**).

comp4 fr1 AYD proton in cdc13
 Pulse Sequence: s2pu1
 Solvent: CDCl3
 Temp. 20.0 C / 293.1 K
 GEMINI-200 "uwcchem200"

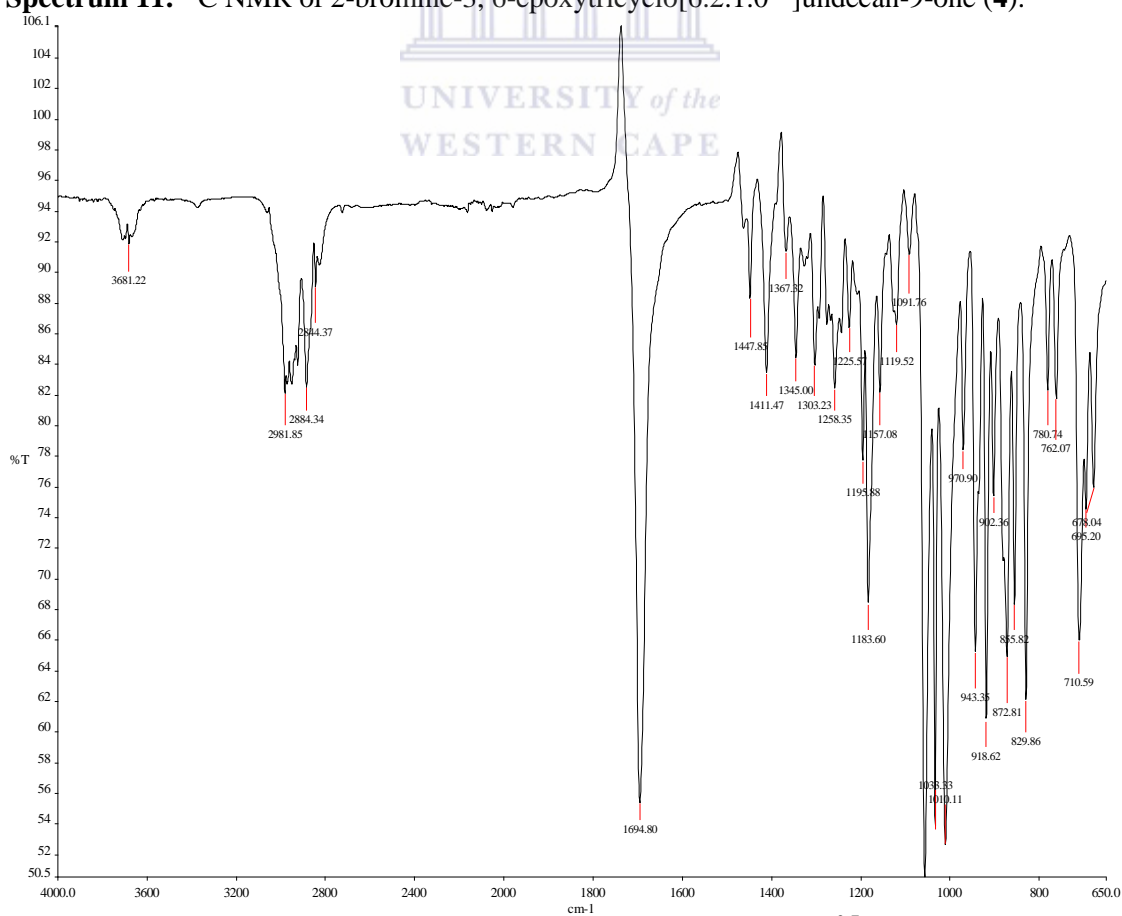
Relax. delay 1.000 sec
 Pulse 26.2 degrees
 Acq. time 1.384 sec
 Width 2000.3 Hz
 4 repetitions
 OBSERVE: H1, 200.0473001 MHz
 DATA PROCESSING
 Line broadening 1.0 Hz
 FT size 15384
 Total time 0 min, 13 sec



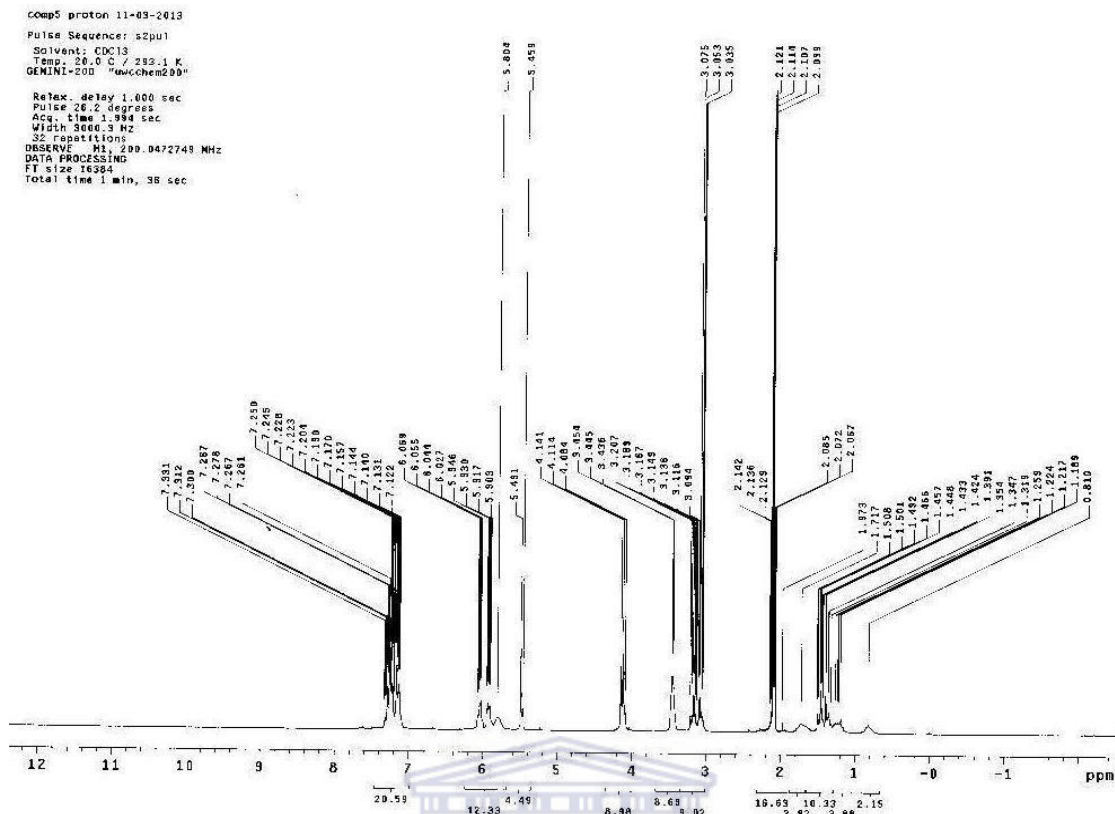
Spectrum 10: ¹H NMR of 2-bromine-3, 6-epoxytricyclo[6.2.1.0^{2,7}]undecan-9-one (**4**).



Spectrum 11: ^{13}C NMR of 2-bromine-3, 6-epoxytricyclo[6.2.1.0^{2,7}]undecan-9-one (**4**).



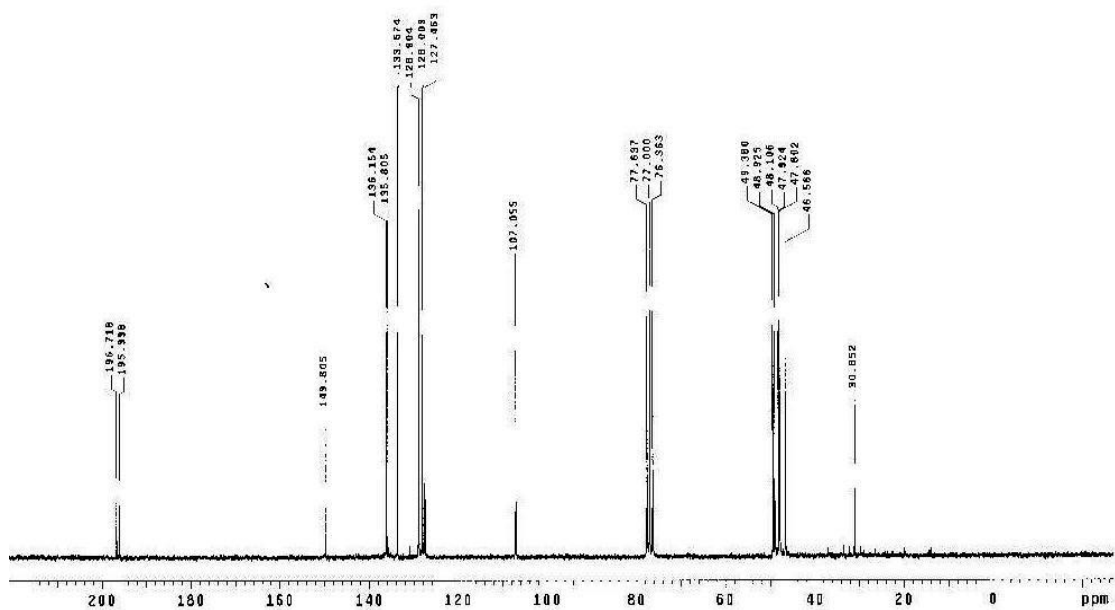
Spectrum 12: Infrared spectrum 2-bromine-3, 6-epoxytricyclo[6.2.1.0^{2,7}]undecan-9-one (**4**).



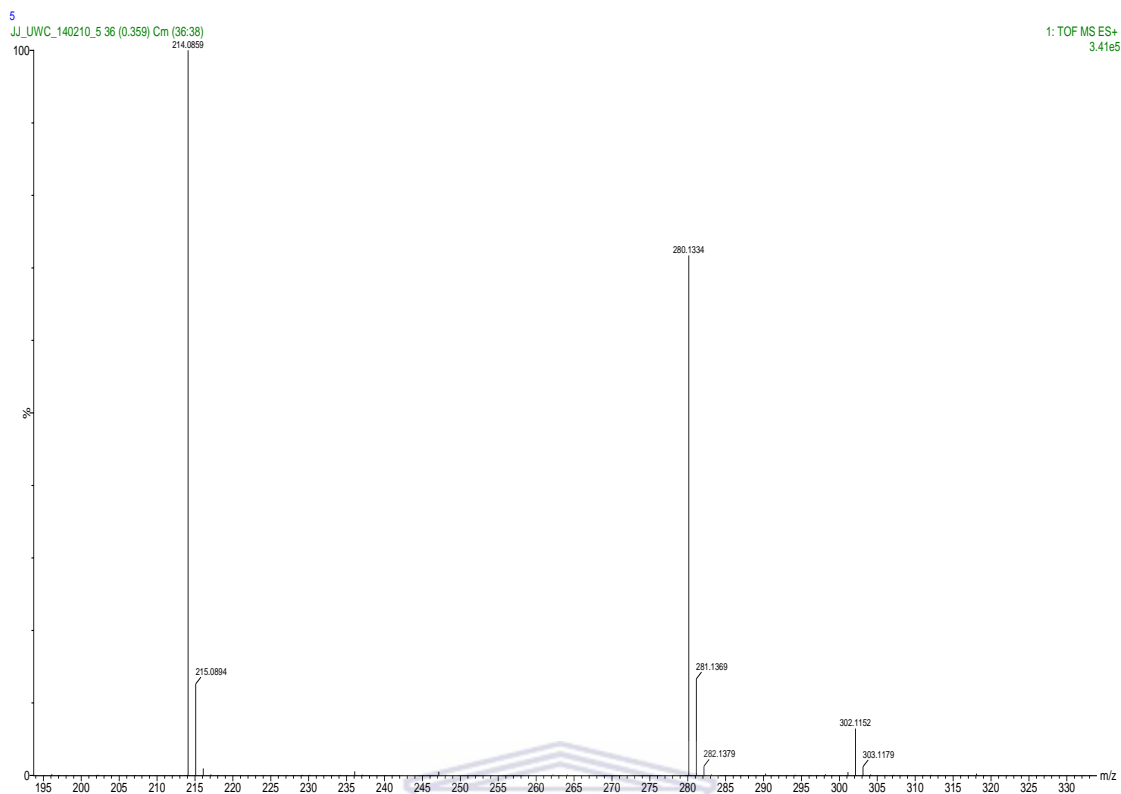
Spectrum 13: ^1H NMR of 3-(benzylimino)tricyclo[6.2.1.0^{2,7}]undeca-4,9-dien-6-one (5).

Martin-comp-15X
Pulse Sequence: s2pu1
Solvent: CDCl3
Temp. 20.0 C / 293.1 K
GEMINI-200 "nuovochem200"

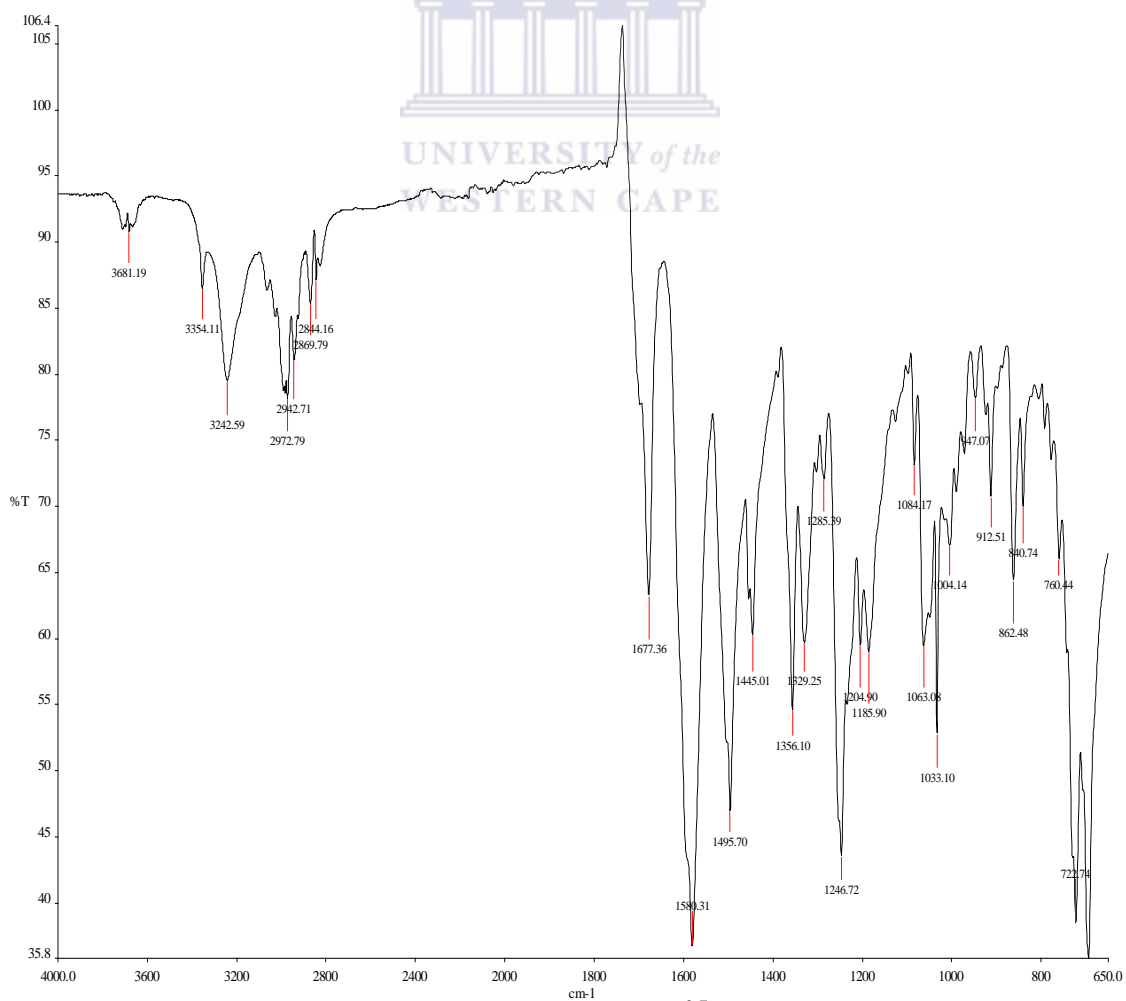
Pulse 52.9 degrees
Acq. time 1.488 sec
Width 12500.0 Hz
23588 repetitions
OBSERVE C13, 50.3019138 MHz
DECOUPLE W1, 299.0462640 MHz
Power 30 dB
continuously on
WALTZ-16 modulated
DATA PROCESSING
Line broadening 1.0 Hz
F1 size 65536
Total time 14 hr, 1 min, 29 sec



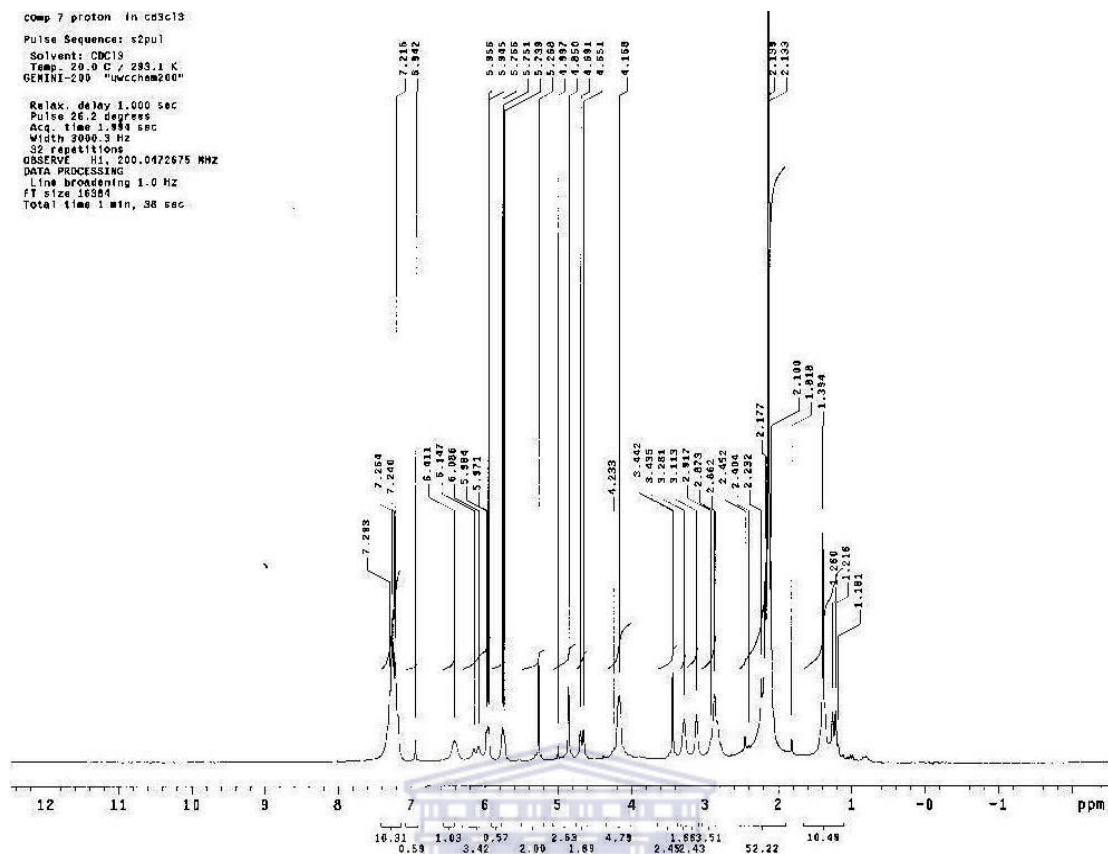
Spectrum 14: ^{13}C NMR of 3-(benzylimino)tricyclo[6.2.1.0^{2,7}]undeca-4,9-dien-6-one (5).



Spectrum 15: MS of 3-(benzylimino)tricyclo[6.2.1.0^{2,7}]undeca-4,9-dien-6-one (**5**).



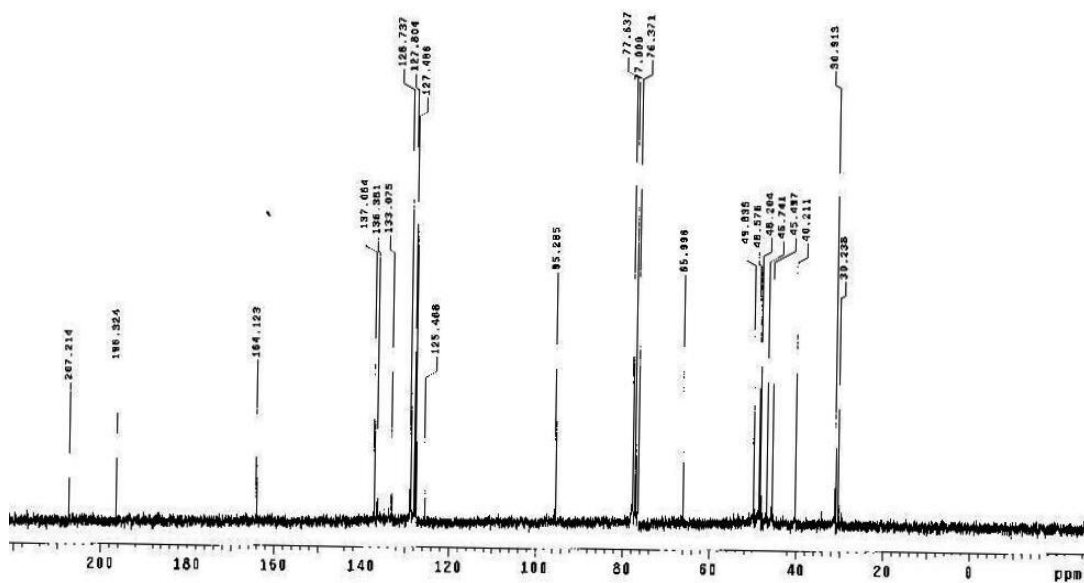
Spectrum 16: infrared of 3-(benzylimino)tricyclo[6.2.1.0^{2,7}]undeca-4,9-dien-6-one (**5**).



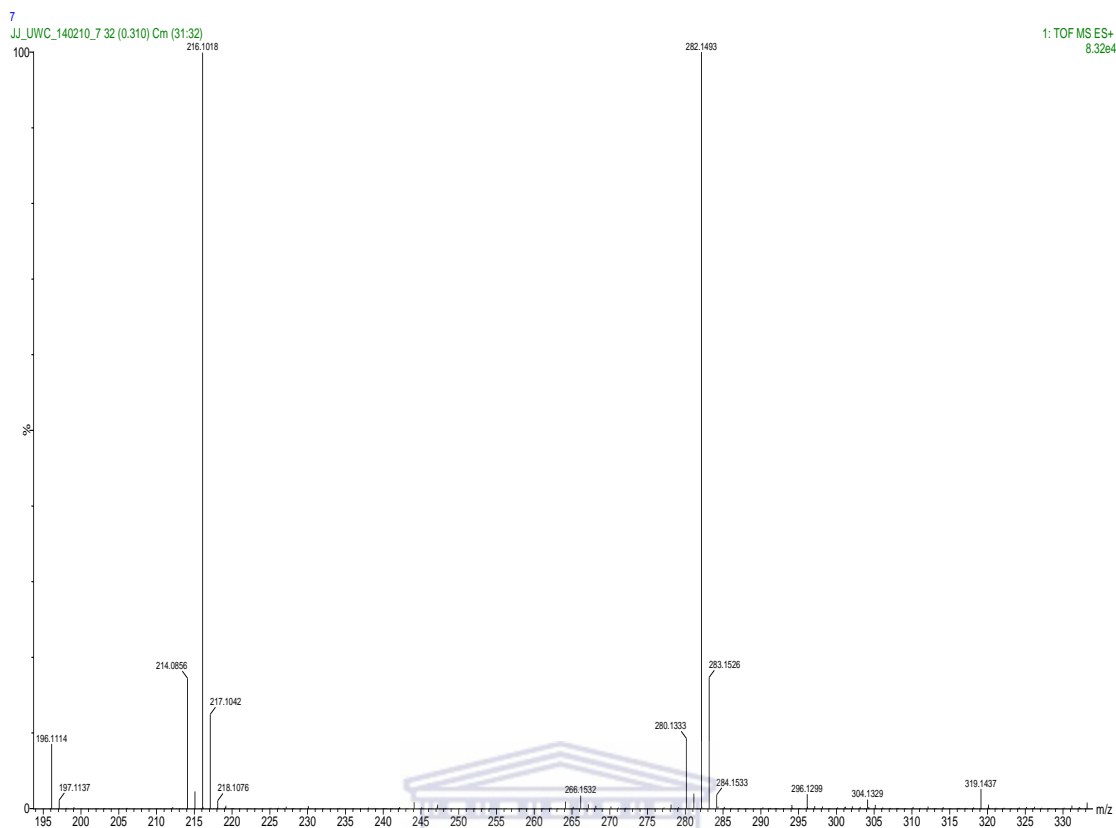
Spectrum 17: ^1H NMR of 3-(benzylamino)tricyclo[6.2.1.0^{2,7}]undeca-4,9-dien-6-one (**6**).

comp-7 C13 in cdv13
Pulse Sequence: s2pu1
Solvent: CDCl3
Temp: 20.0 C / 283.1 K
GENIINI-200 "uvchem200"

Pulse 62.9 degree
Acq. time 1.588 sec
Width 12500.0 Hz
5853 repetitions
OBSERVE C13, 30.3048150 MHz
DECOUPLE H1, 200.0482640 MHz
Power 30 dB
continuously on
WALTZ-16 modulated
DATA PROCESSING
Line broadening 1.0 Hz
FT size 65536
Total time 4 hr, 40 min, 28 sec



Spectrum 18: ^{13}C NMR of 3-(benzylamino)tricyclo[6.2.1.0^{2,7}]undeca-4,9-dien-6-one (**6**).



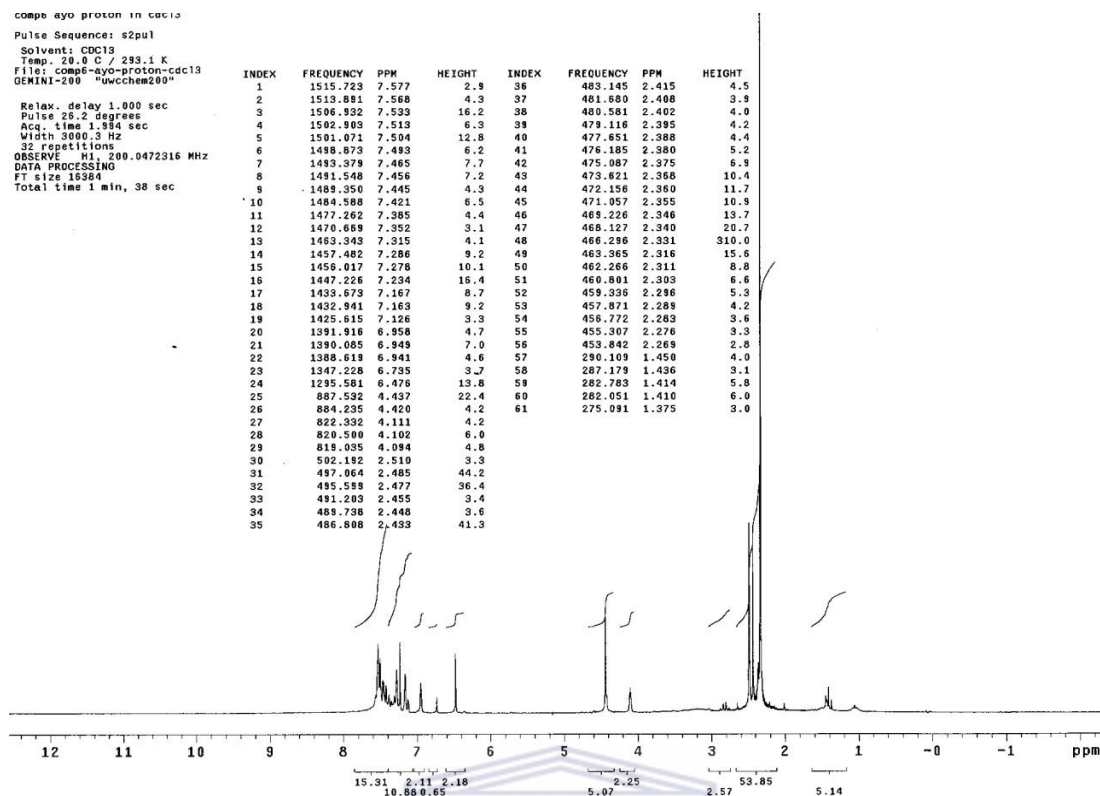
Spectrum 19: MS of 3-(benzylamino)tricyclo[6.2.1.0^{2,7}]undeca-4,9-dien-6-one (**6**).



Spectrum 20: Infrared spectrum of 3-(benzylamino)tricyclo[6.2.1.0^{2,7}]undeca-4,9-dien-6-one (**6**).

comp5 ayo proton in cdc13
 Pulse Sequence: s2pul
 Solvent: CDC13
 Temp: 20.0 C / 293.1 K
 File: comp5-ayo-proton-cdc13
 GEMINI-200 "uwchem200"

INDEX	FREQUENCY PPM	HEIGHT	INDEX	FREQUENCY PPM	HEIGHT	
1	1515.723	7.577	2.9	36	483.145 2.415	4.5
2	1513.881	7.568	4.3	37	481.600 2.408	3.9
3	1506.932	7.533	16.2	38	480.581 2.402	4.0
4	1502.869	7.513	6.3	39	479.116 2.395	4.2
5	1501.071	7.504	12.8	40	477.651 2.388	4.4
6	1498.873	7.483	6.2	41	476.185 2.380	5.2
7	1493.379	7.465	7.7	42	475.087 2.375	6.9
8	1491.548	7.456	7.2	43	473.621 2.368	10.4
9	1489.350	7.445	4.3	44	472.156 2.360	11.7
10	1484.588	7.421	6.5	45	471.057 2.355	16.5
11	1477.262	7.385	4.4	46	469.226 2.346	13.7
12	1470.689	7.352	3.1	47	468.127 2.340	20.7
13	1463.343	7.315	4.1	48	466.296 2.331	310.0
14	1457.482	7.286	9.2	49	463.965 2.316	15.6
15	1456.017	7.278	10.1	50	462.266 2.311	8.8
16	1447.226	7.234	16.4	51	460.801 2.303	6.6
17	1433.673	7.167	8.7	52	459.336 2.296	5.3
18	1432.941	7.163	9.2	53	457.871 2.289	4.2
19	1425.615	7.126	3.3	54	456.772 2.283	3.6
20	1391.916	6.958	4.7	55	455.307 2.276	3.3
21	1390.085	6.949	7.0	56	453.842 2.269	2.8
22	1388.619	6.941	4.6	57	290.109 1.450	4.0
23	1347.228	6.795	3.7	58	287.179 1.436	3.1
24	1295.581	6.476	13.8	59	282.783 1.414	5.8
25	887.532	4.437	22.4	60	282.051 1.410	6.0
26	884.235	4.420	4.2	61	275.091 1.375	3.0
27	822.332	4.111	4.2			
28	820.500	4.102	6.0			
29	819.035	4.094	4.8			
30	502.182	2.510	3.3			
31	497.064	2.485	44.2			
32	495.599	2.477	36.4			
33	491.203	2.455	3.4			
34	489.738	2.448	3.6			
35	486.808	2.433	41.3			

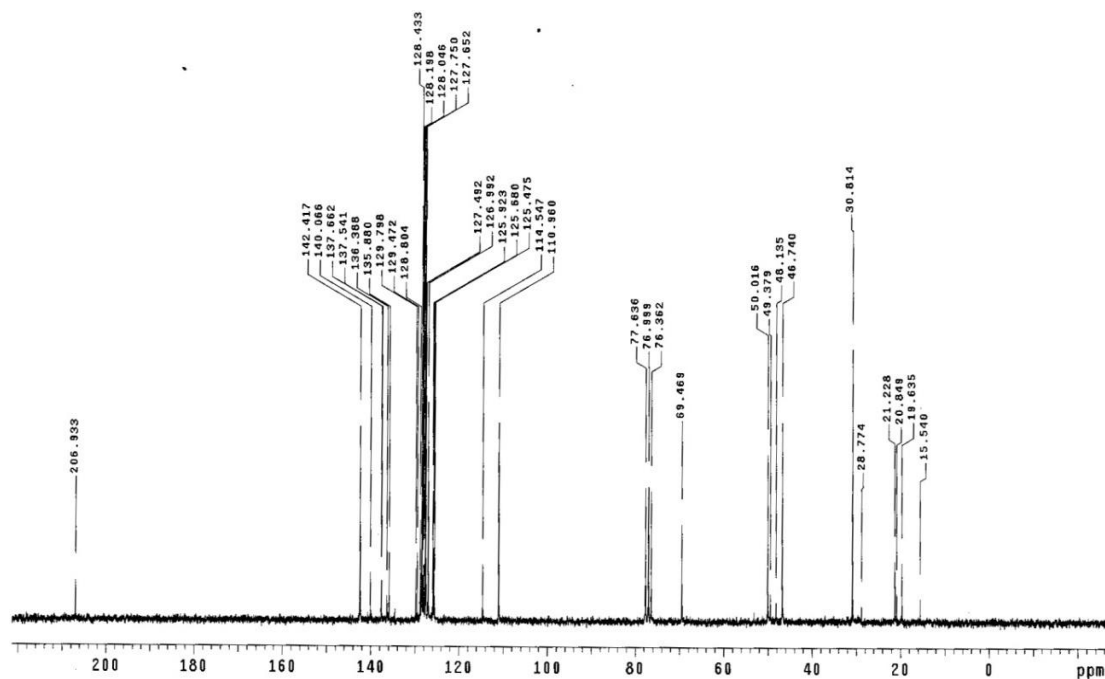


Spectrum 21: ^1H NMR of 3-(benzylimino)tricyclo[6.2.1.0^{2,7}]undec-9-en-6-one (7).

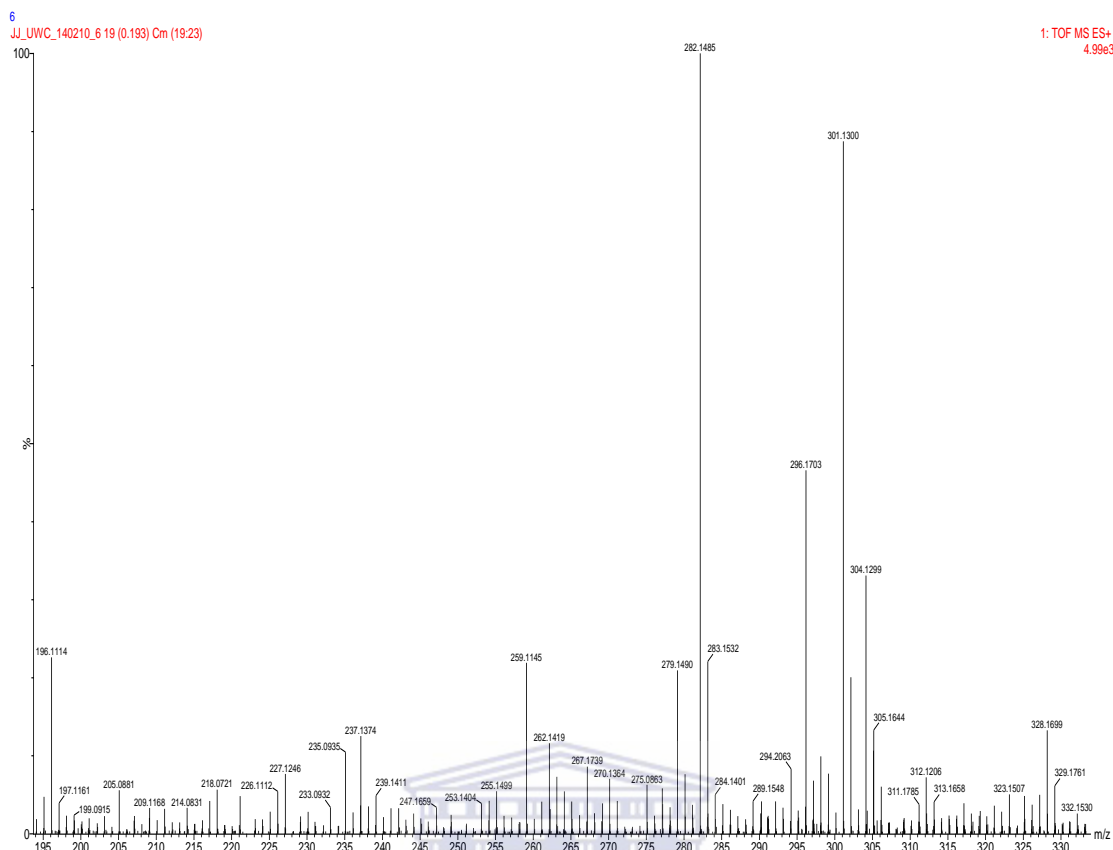
comp5 ayo C13 in cdc13
 Pulse Sequence: s2pul
 Solvent: CDC13
 Temp: 20.0 C / 293.1 K
 GEMINI-200 "uwchem200"

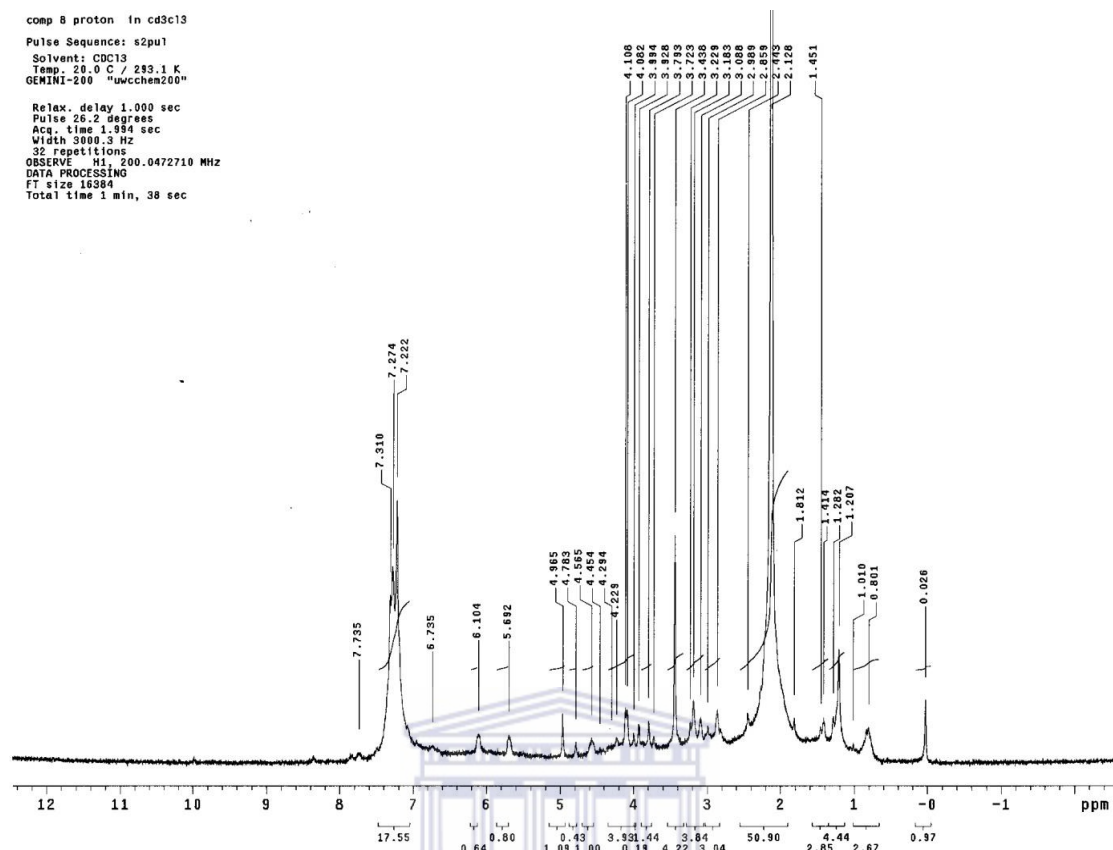
Pulse 62.9 degrees
 Acq. time 1.438 sec
 Width 12500.0 Hz
 2182 repetitions
 OBSERVE C13, 50.3019184 MHz
 DECOUPLE H1, 200.0482640 MHz
 Power 30 dB
 continuously on
 WALTZ-16 modulated
 DATA PROCESSING
 Line broadening 1.0 Hz
 FT size 65536
 Total time 4 hr, 40 min, 28 sec

UNIVERSITY of the
 WESTERN CAPE

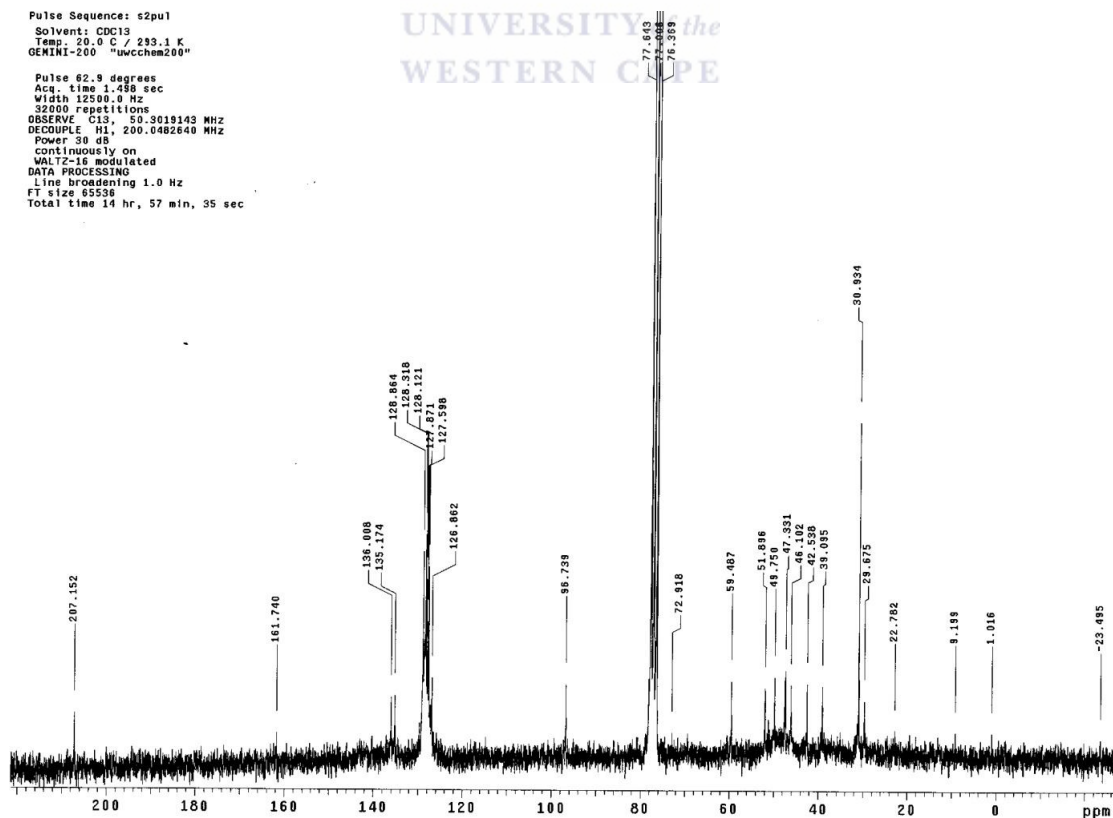


Spectrum 22: ^{13}C NMR of 3-(benzylimino)tricyclo[6.2.1.0^{2,7}]undec-9-en-6-one (7).

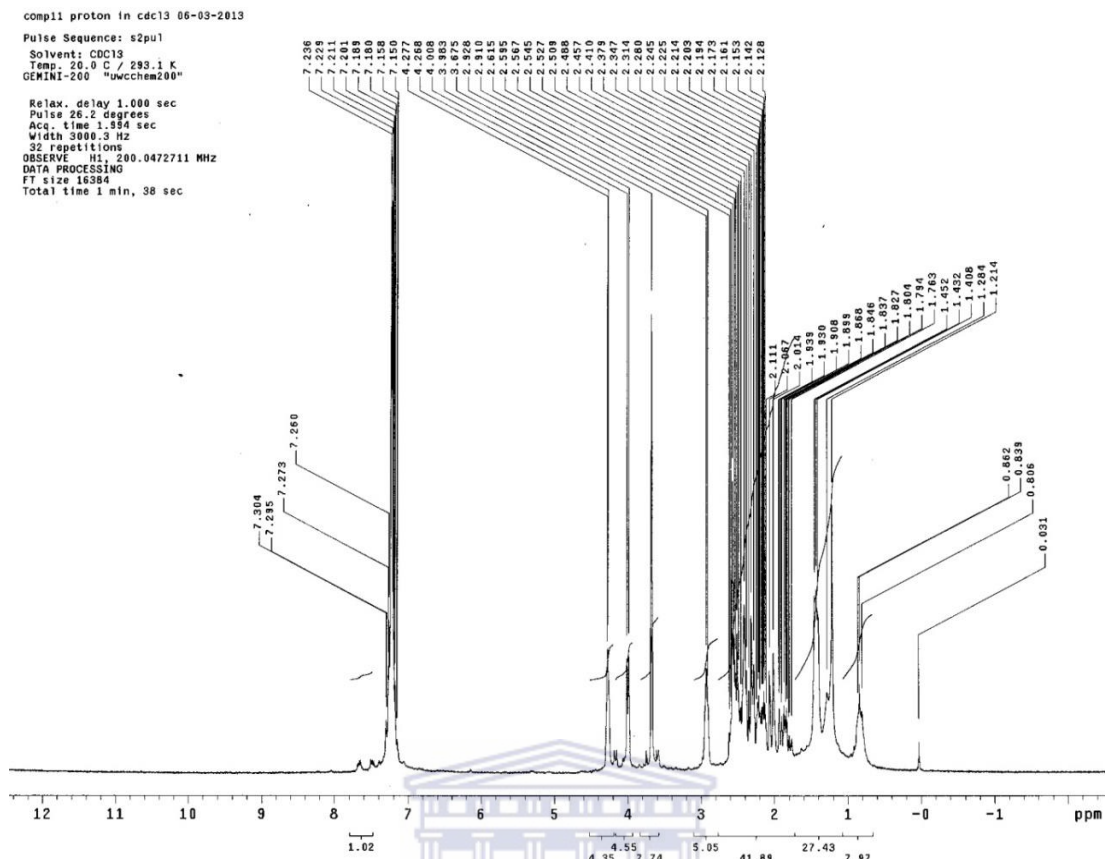




Spectrum 25: ^1H NMR of Impure 3-(benzylamino)tricyclo[6.2.1.0^{2,7}]undec-9-en-6-one (**8**).



Spectrum 26: ^{13}C NMR of Impure 3-(benzylamino)tricyclo[6.2.1.0^{2,7}]undec-9-en-6-one (**8**).



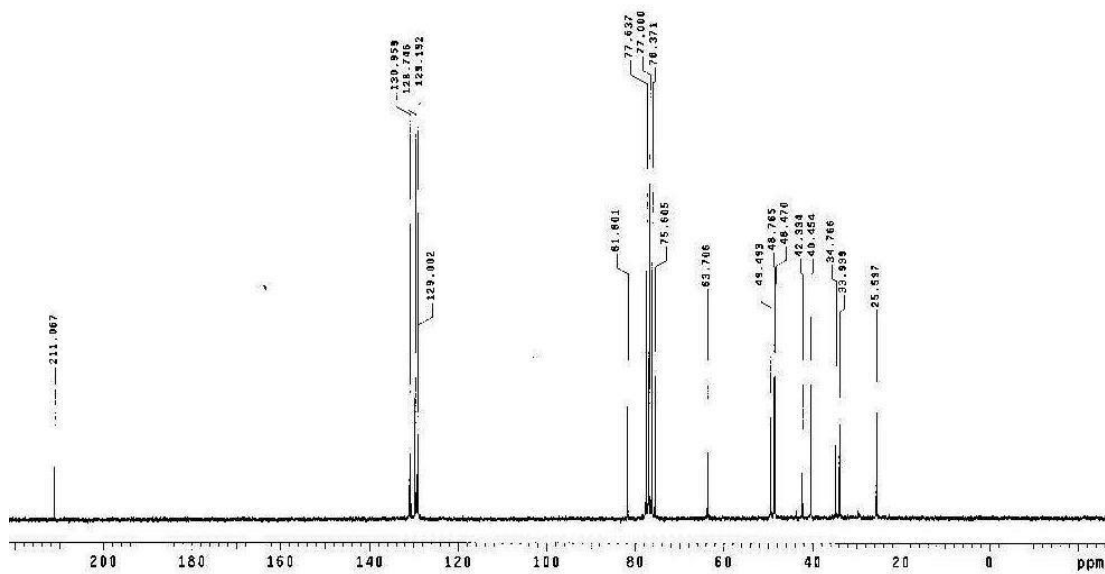
Spectrum 25: ^1H NMR of 10-(benzylamino)-6,9-epoxytricyclo[6.2.1.0^{2,7}]undecan-3-one (9).

ayodej1-no2 - comp 11

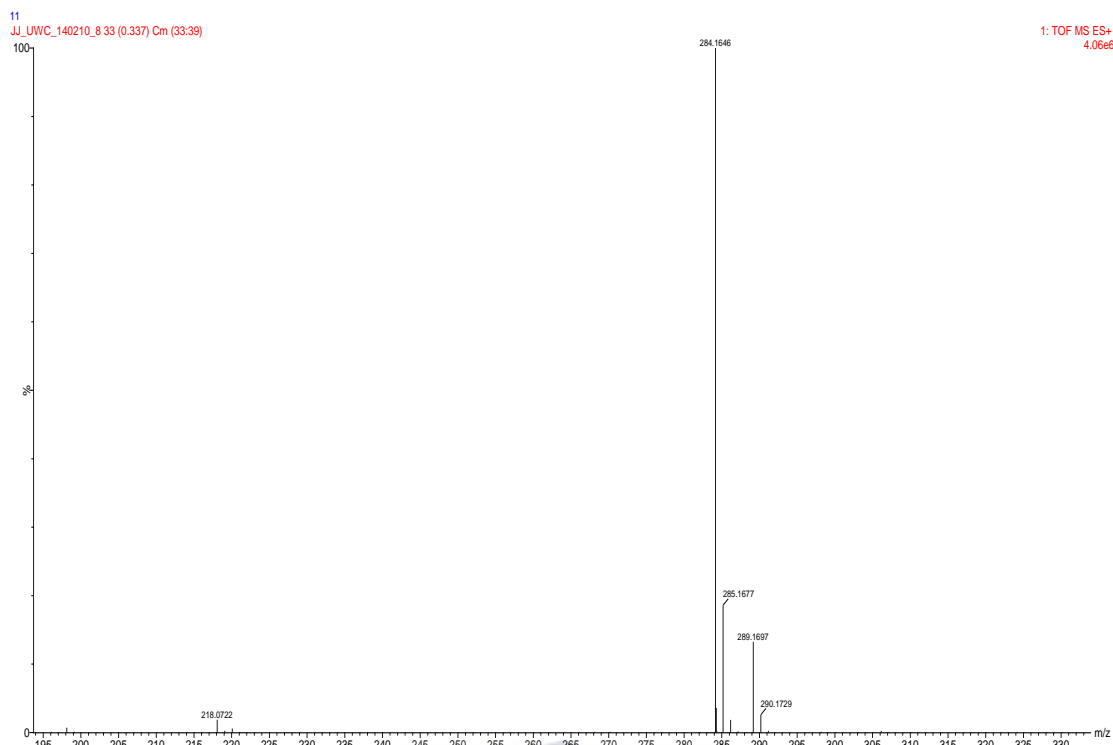
Pulse Sequence: s2pu1
 Solvent: CDC13
 Temp: 20.0 C / 293.1 K
 GEMINI-200 "uwchem200"

Pulse 52.9 degrees
 Acq. time 1.456 sec
 Width 12500.0 Hz
 32000 repetitions
 OBSERVE C13, 50.3015146 MHz
 DECOUPLE H1, 200.9452640 MHz
 Power 30 dB
 continuously on
 WALTZ-16 modulated
 DATA PROCESSING
 Line broadening 1.0 Hz
 FT size 65536
 Total time 14 hr, 57 min, 35 sec

UNIVERSITY of the
WESTERN CAPE



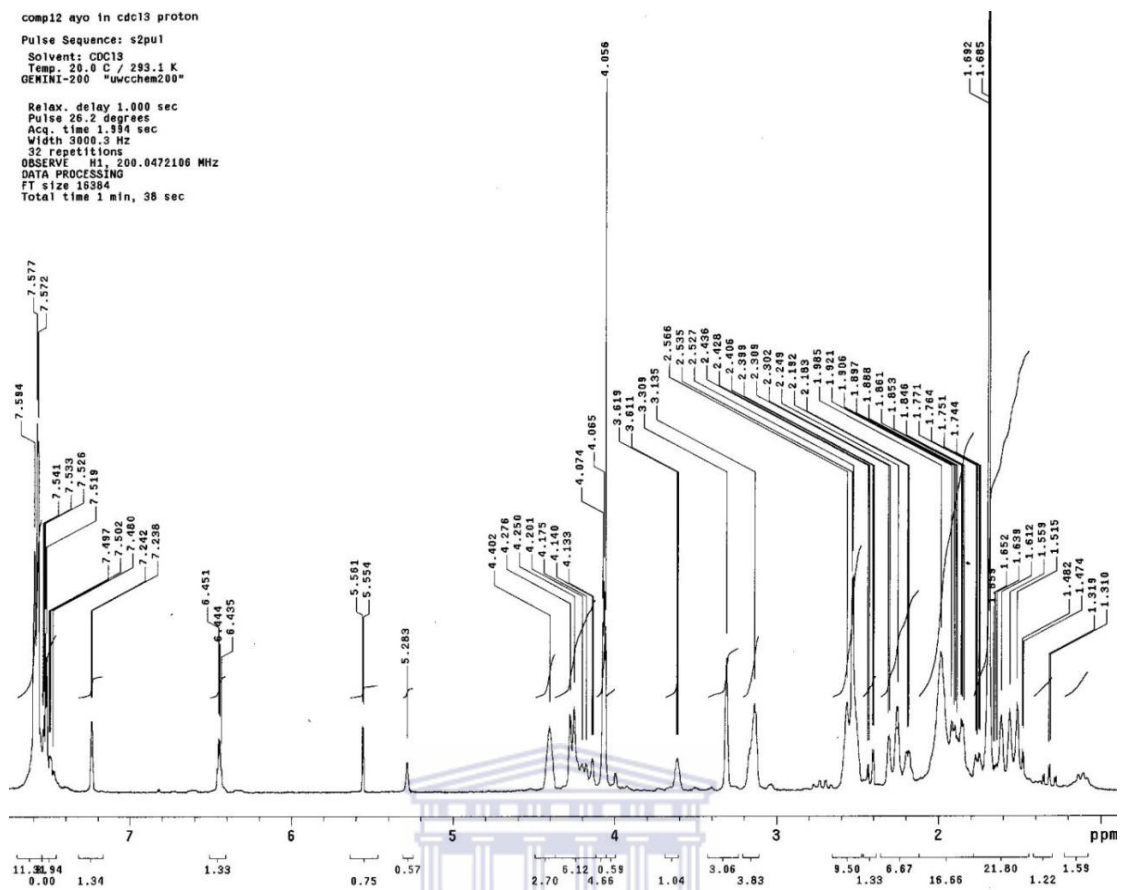
Spectrum 26: ^{13}C NMR of 10-(benzylamino)-6,9-epoxytricyclo[6.2.1.0^{2,7}]undecan-3-one (9).



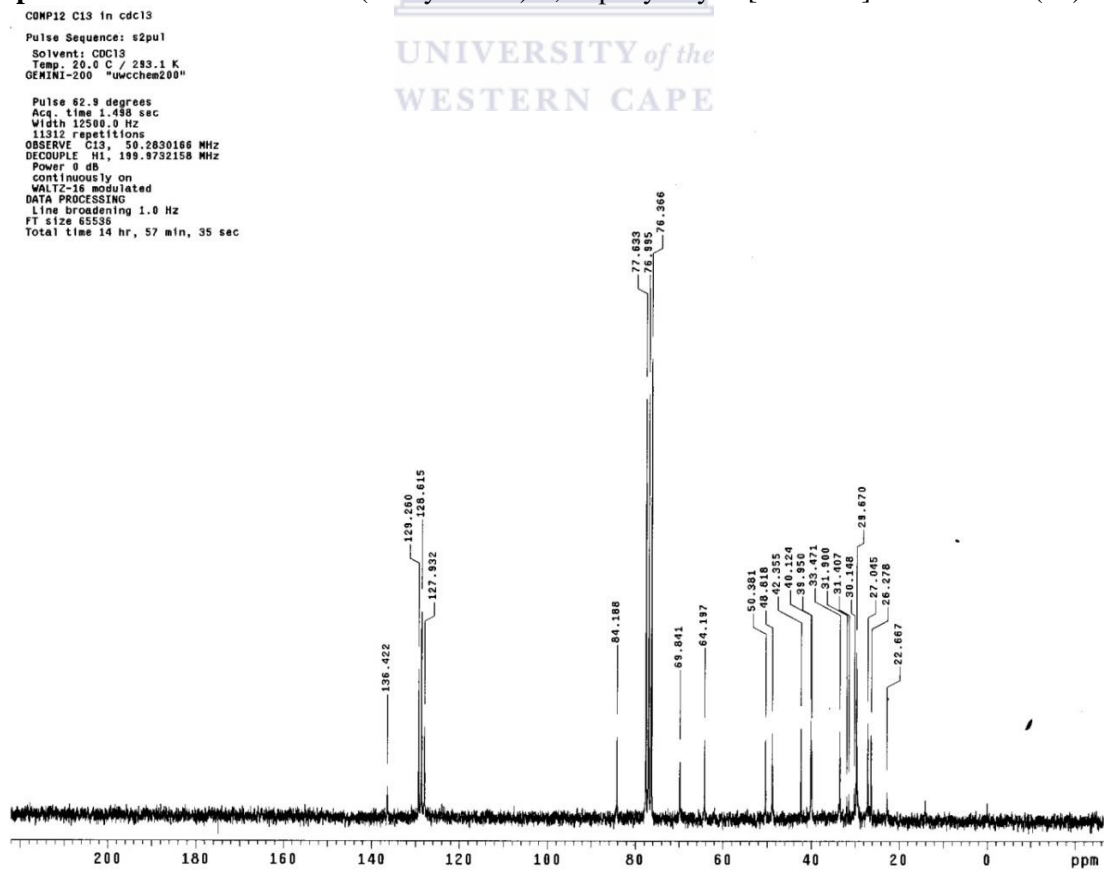
Spectrum 27: MS of 10-(benzylamino)-6,9-epoxytricyclo[6.2.1.0^{2,7}]undecan-3-one (**9**).



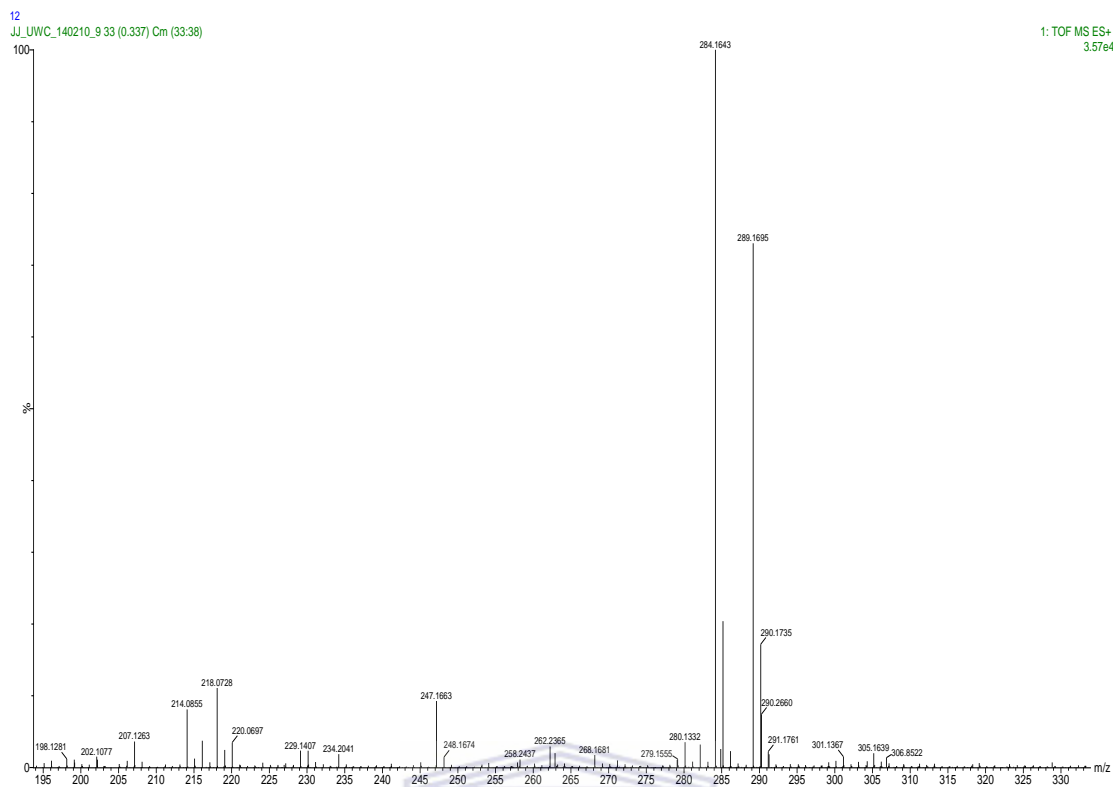
Spectrum 28: Infrared spectrum of 10-(benzylamino)-6,9-epoxytricyclo[6.2.1.0^{2,7}]undecan-3-one (**9**).



Spectrum 29: ^1H NMR of 10-(benzylamino)-6,9-epoxytricyclo[6.2.1.0^{2,7}]undecan-3-ol (**10**).



Spectrum 30: ^{13}C NMR of 10-(benzylamino)-6,9-epoxytricyclo[6.2.1.0^{2,7}]undecan-3-ol (**10**).



Spectrum 31: MS of 10-(benzylamino)-6,9-epoxytricyclo[6.2.1.0^{2,7}]undecan-3-ol (**10**).



Spectrum 32: Infrared spectrum of 10-(benzylamino)-6,9-epoxytricyclo[6.2.1.0^{2,7}]undecan-3-ol (**10**).